AN EXPERIMENT STUDY OF WATER-ASSISTED INJECTION MOLDING OF PLASTIC TUBES WITH DIFFERENT CORNER ANGLE

TIWAGORN PUDPONG

A THESIS SUBMITTED IN PARTIAL FULFILLMENT
OF THE REQUIREMENT FOR THE DEGREE OF
MASTER OF ENGINEERING IN AUTOMOTIVE ENGINEERING
(INTERNATIONAL PROGRAM)
INTERNATIONAL COLLEGE
KING MONGKUT'S INSTITUTE OF TECHNOLOGY LADKRABANG
2011

KMITL-2011-IC-M-004-017

AN EXPERIMENT STUDY
OF WATER-ASSISTED INJECTION MOLDING
OF PLASTIC TUBES WITH DIFFERENT CORNER ANGLE

TIWAGORN PUDPONG

A THESIS SUBMITTED IN PARTIAL FULFILLMENT

OF THE REQUIREMENT FOR THE DEGREE OF

MASTER OF ENGINEERING IN AUTOMOTIVE ENGINEERING

(INTERNATIONAL PROGRAM)

INTERNATIONAL COLLEGE

KING MONGKUT'S INSTITUTE OF TECHNOLOGY LADKRABANG

2011

KMITL-2011-IC-M-004-017

TOPIC OF THESIS	AN EXPERIMENT STUDY OF WATER-ASSISTED INJECTION MOLDING OF PLASTIC TUBES WITH DIFFERENT CORNER ANGLE
NAME OF STUDENT	TIWAGORN PUDPONG
STUDENT CODE	50061918
DEGREE	MASTER DEGREE OF ENGINEERING
MAJOR	AUTOMOTIVE ENGINEERING
ADVISOR	ASST. PROF. DR. SURAT AREERAT
CO-ADVISOR	DR. WUTTIPONG RUNGSEESANTIVANON
CO-ADVISOR	PROF. DR.ISAO SATOH
CO-ADVISOR	ASSOC.PROF. DR.TAKUSHI SAITO

ABSTRACT

Water-Assisted Injection Molding (WAIM) is convenient and effective technique in production with lower overall costs and less assembly time. The basic requirement of molding plastic tubets is that uniform wall thickness should be obtained along the tubes. The non-uniform sections are always problematic, mostly found at the sharp corners. WAIM technology in the plastic industry is not widely used due to problem in adjustment of injection parameters, complication of design, and the construction of water-assisted injection molding equipments.

This researched has imitated the model of fuild line in engine compartment for this experiment to study about the condition affecting to residual wall thickness (RWT) at the sharp corner. The polypropylene (PP) is used as samples. The condition as started as follows: melt temperature, mold temperature, water delay time, water holding time and water holding pressure are studied to find the effects on inner and outer residual wall thickness. Moreover the sharp corner angles sectional are seven geometries and veries 15 degree from straight tube till 90 degree. The result of the conditions can be analyzed to find out their relationships of inner and outer residual wall thickness. The analysis shows that the straight tube was more uniform residual wall thickness than the curve tube. The experiment result suggest that water injection delay time and water pressure were the major parameter affecting the hollowed core ratio of all molded tubes, while the percentage different of inner and outer wall thickness were mainly influenced by the melt temperature.

ACKNOWLEDGMENTS

I would like to express my sincere gratitude to Dr.SuratAreeratand Dr.Wuttipong Rungseesuntivanon, Prof. Isao Satoh and Assoc.Prof. Dr.Takushi Saito for their helpful guidance, suggestion, and encouragement throughout this study.

Special thanks go to Mr. DumrongThanomjit for refine mold used in this research. Also, Mr. KraiSompongnawakitand Mr. YuttanaKositsagulfor his assistance for usage of the water injection unitfor their help during the experimentsat any time I need and I am would like to thank the National Metal and Materials Technology Center (MTEC) for usage of facilities. Furthermore, I am really thanked to CH.Radiators and CH.Industry Companies for providing financial support from research fund.

I am grateful to National Science and Technology Development Agency (NSTDA), which provided the full scholarship for studying in the master program.

Moreover, my sincere thanks go to all my teachers, colleagues and others whose names are not mentioned here, for their helps and kindness.

Eventually, I would like to use this opportunity to express my profound thanks to my beloved parents for their moral support and understanding.

Tiwagorn Pudpong

CONTENTS

Page

CONTENTS (CONT.)

Page

CONTENTS (CONT.)

Page

CONTENTS (CONT.)

CONTENTS (CONT.)

Page

CONTENTS (CONT.)

LIST OF TABLES

LIST OF TABLES (CONT.)

Table Page

LIST OF TABLES (CONT.)

Table Page

LIST OF TABLES (CONT.)

Table Page

LIST OF TABLES (CONT.)

Table Page

LIST OF FIGURE

Figure Page

LIST OF FIGURE (CONT.)

Figure Page

LIST OF FIGURE (CONT.)

Figure Page

LIST OF FIGURE (CONT.)

Figure Page

LIST OF FIGURE (CONT.)

Figure Page

LIST OF FIGURE (CONT.)

Figure Page

LIST OF FIGURE (CONT.)

Figure Page

LIST OF FIGURE (CONT.)

NOMENCLATURE

Acronym

ABS	=	Acrylonitrile - Butadiene – Styrene
ASTM	=	American Society for Testing and Materials
GAIM	=	Gas-Assisted Injection Molding
GF	=	Glass Fiber
GIT	=	Gas assisted Injection Technique
HIPS	=	High Impact Polystyrene
IM	=	Injection Molding
MFI	=	Melt Flow Index
PA	=	Polyamide
PE	=	Poly Ethylene
PP	=	Poly Propylene
RWT	=	Residual Wall Thickness
WAIM	=	Water-Assisted Injection Molding
WIT	=	Water assisted Injection Technique

Symbols

η	=	Shear viscosity
$\dot{\gamma}$	=	shear rate
τ	=	shear stress

NOMENCLATURE (CONT.)

Symbols

v	=	velocity
m	=	flow exponent
n	=	viscosity exponent
Φ	=	fluidity
k	=	consistency factor
θ	=	sharp corner angle

CHAPTER 1

INTRODUCTION

1.1 Background

Today plastics materials play a key role in automotive industry. The automobile ducts are normally made of metal and require several production steps [1]. Therefore, the cost of production is very high. A large number of rod-shaped parts integrated into other function parts are found in automobiles, especially in the engine compartment.

There are a number of methods for processing the automobile ducts. Typical metal-based automobile duct structures are composed of small individual parts requiring several secondary assembly operations. On the other hand, the plastic duct structures can be easily consolidates into one component. Plastics ducts eliminate several secondary operations that metal ducts usually require such as welding, finishing, painting and coating because metal is vulnerable to corrosion. Moreover, the automobile plastic ducts can be also molded by using three-dimensional blow molding process. Therefore, the cost of production is very high.

A novel water assisted injection molding (WAIM) technology [2] has been expanding its applications in recent years and used for the production of tube parts, bent parts, flats parts with struts, and complex parts consisting of both thin and thick sections [3]. Compared with the conventional injection molding, WAIM can substantially reduce material cost, clamp tonnage, and cycle time. Product quality can be improved by reducing sink marks, residual stress, distortion, and warpage that are normally encountered in conventional injection molding. It also allows more freedom in design and manufacture of plastics parts [4-5].

Water-assisted injection molded parts can be either short-shot molded or overflow molded. In a short-shot water-assisted injection molding, the mold cavity is partially filled with the polymer melt followed by the injection of water into the core of the polymer melt. A schematic diagram of the short-shot water-assisted injection molding is shown in Figure 1 (a). One of the limitations of short-shot water-assisted injection molded parts is the switchover mark on the surface of molded products and provide smoother inner surfaces in Class A [6]. The overflow process attempts to eliminate the switchover mark from the final product by moving the position of the melt front at the end of filling outside of the product "envelope". Melt is short shot injected up to the end of the product envelope where an overflow cavity at the end of flow accepts the melt displaced by the water injection [7]. The process sequence is the same as for short shot. Figure 1b schematically shows the overflow (without shut-off) water-assisted. Water-assisted injection molding is taking hollow-part injection molding into region where gas-assisted has never been before. It was first use in fluid-transport applications where it proved able to provide smoother inner walls than gas.

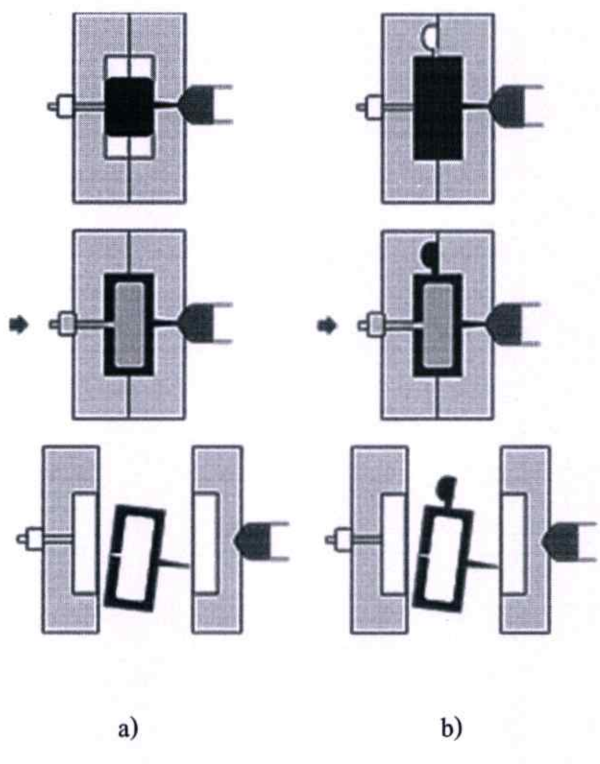

Figure 1 Schematic of (a) short-short and (b) overflow (without shut-off) water-assisted injection molding

Despite all the advantages associated with water-assisted injection molding, several key problems have never been systematically investigate. One of them is the thickness distribution in molded plastic tubes. Liu and Hsieh [8] and Liu and Lin [9] respectively studied the gas-assisted and water-assisted injection molding of curved tube and report that the residual wall thickness is not uniform at transitions. The residual wall thickness around dimensional transitions is a critical factor determining the wall thickness near dimensional curved sections is greatly needed.quality of such tube. Another common feature of tubes is the presence of curved sections. The mechanism involved and its relation to processing conditions about this non-uniformity have not been fully investigated. To enhance the technology of water-assisted molding of tubes-shaped parts, systematic study of the residual wall thickness near dimensional curved sections is greatly needed.

1.2 Objectives

1.2.1 To investigate the distribution of the residual wall thickness in curved sections and its relation to material properties and processing conditions.

1.2.2 To investigate effect of sharp corners with different angles to the residual wall thickness.

1.2.3 To investigate the effect of processing parameter on the internal surface, external surface and evaluation of the structure in the cross-section of water-assisted injection molded parts

1.3 Scope

1.3.1 Design mold for automobile ducts with different sharp corner angle geometries obtained by changing the moving-half inserts.

1.3.2 The material used in this study is Polypropylene(PP) grade HP400K, HP400M and HP550R are produced by HMC Polymers Company.

1.3.3 Study on the effects of material properties and process variables : melt temperature, mold temperature, water delay time, water hold time, water holding pressure and sharp corner angle geometries in water-assisted injection molding.

1.3.4 Measurement the Residual Wall Thickness (inner and outer corner) at sharp corner and Comparison.

1.3.5 Measurement the internal surface roughness, external surface quality and observe for structure in the cross-section of water-assisted injection molded parts by Microstopic.

1.3.6 Measurement the deflection resistance of water assisted injection molded parts.

1.4 Methodology of the Study

1.4.1 Study method of water-assisted injection molding.

1.4.2 Study processing parameter water-assisted injection molding.

1.4.3 Construct the water-assisted injection mold.

1.4.4 Review of relevant literature.

1.4.5 Comparison of the results of experimental data using statistical methods.

1.4.6 Conclude the results and write a report

1.5 Outcome of the Study

1.5.1 Results from this study would indicate parameters in water-assisted injection molding, in order to improve the quality of parts in plastic injection process.

1.5.2 Results from this study can be used as a guideline in design process and the construction of water-assisted injection mold.

CHAPTER 2

LITERATURE REVIEW

2.1 Flow properties of polymer melts.

The flow process in plastics processing of injection molding involve mainly shear of the melt. Shear flow occurs because of plastics melts adhere to the surface of the tooling being used to shape them (Stoke's adhesion, wall adhesion). This can be illustrated in simplified form quite well with the two-plate model (Figure 2.1). When one plate is moved relative to the other, the liquid layers in between slide correspondingly and the melt is sheared. A volume element of fluid is deformed as shown in Figure 2.2.

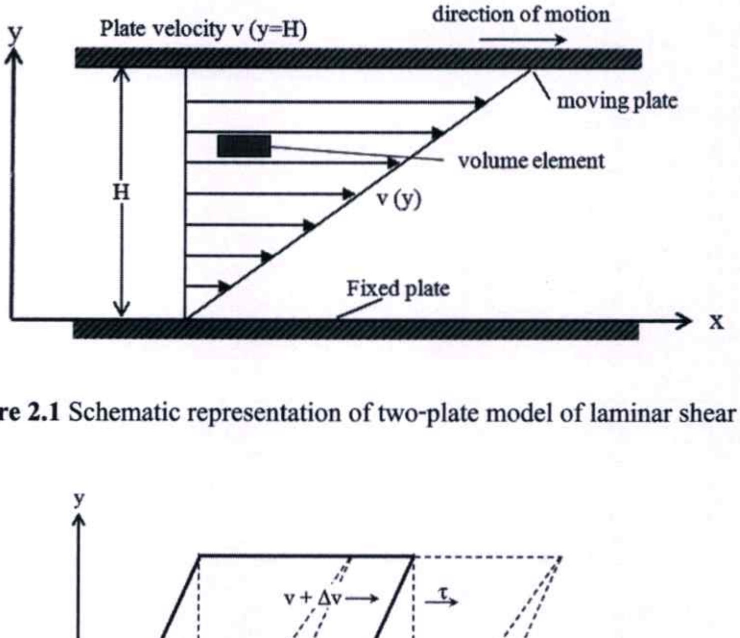

Figure 2.1 Schematic representation of two-plate model of laminar shear flow

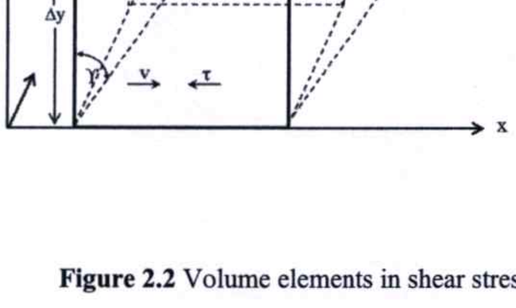

Figure 2.2 Volume elements in shear stress

The shear rate is calculated from the difference in velocity between the upper and the lower side of the volume element in relation to its thickness.

$$\dot{\gamma} = \frac{\Delta v}{\Delta y} \tag{2.1}$$

Where $\dot{\gamma}$ is the shear rate, v is the velocity, and y is the distance between the plates.

2.1.1 Newtonian and Non-Newtonian fluids.

Shear stress, τ, is the shearing force necessary to deform the material divided by the area of the volume element. In the simplest case of a Newtonian fluid, the shear stress is proportional to the shear rate. Thus,

$$\tau = \eta \cdot \dot{\gamma} \tag{2.2}$$

The proportionality factor η is called the dynamic *shear viscosity,* or only the *viscosity* for short. It has the dimension Pa s (Pascal seconds). This shear viscosity represents a criterion for the flow resistance in the shear in the sheared liquid (Figure 2.3). The higher the viscosity, the higher is the level of shear stress that has to exert at the shear rate.

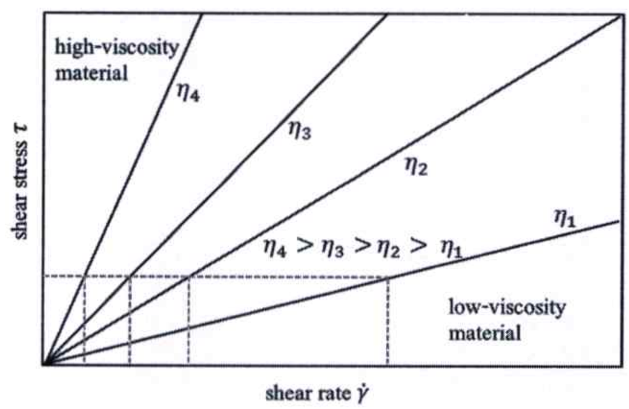

Figure 2.3 Shear stress as a function of shear rate for Newtonian liquids

In contrast, plastics melt generally exhibit non-Newtonian behavior. Their viscosity is not constant, but rather a function of the shear rate. In analogy to the relationship valid for

Newtonian fluids, the flow law is written:

$$\tau = \eta(\dot{\gamma}) \cdot \dot{\gamma} \tag{2.3}$$

or

$$\eta(\dot{\gamma}) = \tau/\dot{\gamma} \neq \text{const.} \tag{2.4}$$

Liquids that behave in accordance with Equation (2.3) and (2.4) are called non-Newtonian fluids.

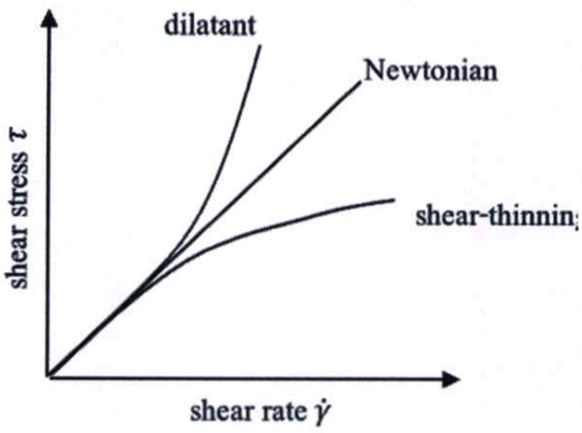

Figure 2.4 Newtonian, shear-thinning and dilatant flow behaviors

For an ideal viscous liquid, the Newtonian liquid, the viscosity (the slope of the graph) is constant as shown in Figure 2.4 deviations from a constant viscosity are possible. In certain cases, viscosity may increase as shear rate rises. As a result, a higher shear stress (compared to Newtonian flow) must be used. This flow behavior is called *dilatant*. The more usual behavior in polymers is for viscosity to decrease with increasing shear rate, so that stress increases less rapidly as shear rate rise. This effect is called *shear thinning*. An explanation of shear thinning is that macromolecules become less entangled and more oriented. When thus oriented, the molecules can be more easily displaced while forces are acting, as occurs during flow.

Molten plastics behave in a shear-thinning way only a certain range of shear rate. Frequently polymer exhibit Newtonian flow behavior at extremely low shear rates as shown in Figure 2.5 [10]. Shear thinning behavior is obtained at higher shear rates. Note that viscosity versus shear rate is usually shown on a log-log graph to cover the wide range of values.

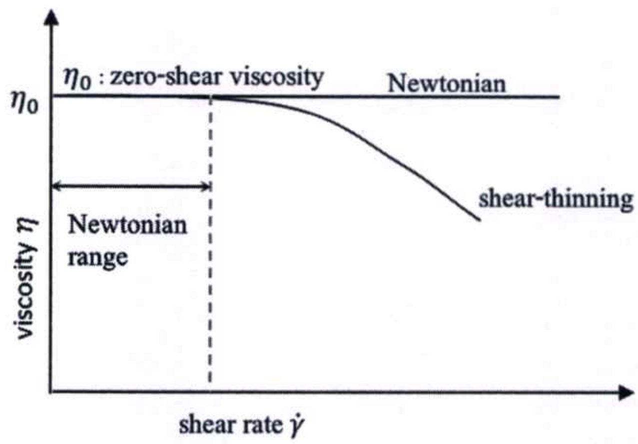

Figure 2.5 Viscosity versus shear rate for Newtonian and shear thinning fluids

2.1.2 Mathematical approximation of rheological behavior

If the flow curves of different polymers are presented in a log-log graph, curve are obtained that consist of two approximately liner sections and a transition region (Figure 2.5). In many case, one operating in only one of two regions, so that to mathematically describe this section of curve a function of the form

$$\dot{\gamma} = \Phi \cdot \tau^m \tag{2.5}$$

Equation (2.5) represents the so-called *Ostwald and de Waele Power Law* with two parameter flow exponent m and fluidity Φ. The flow exponent m characterizes the flow properties of a material and its deviation from Newtonian behavior. It follows that:

$$m = \frac{\Delta\,(\log \dot{\gamma})}{\Delta\,(\log \tau)} \tag{2.6}$$

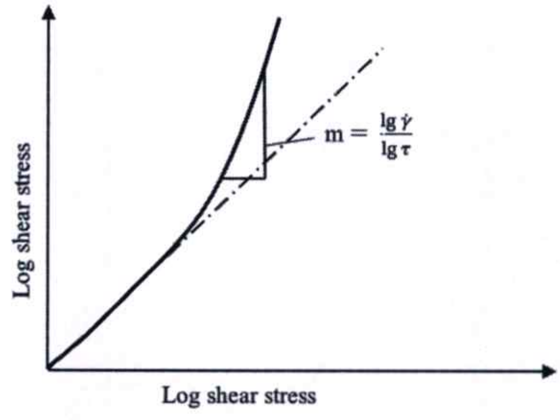

(a)

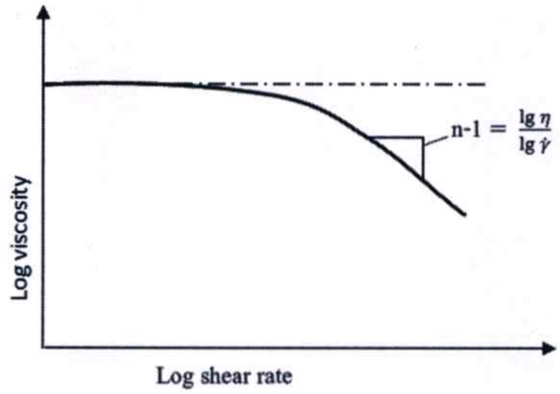

(b)

Figure 2.6 Description of the flow and velocity curves with aid of the power law

where m is the slope of the flow curve in the region of interest when plotted in a log-log diagram as shown in Figure 2.5 (a) and the viscosity is represented by

$$\eta = \Phi^{-1} \cdot \tau^{1-m} \tag{2.7}$$

$$= \Phi^{-1/m} \cdot \dot{\gamma}_{1/m^{-1}}$$

with

$$k = \Phi^{-1/m}$$

and

$$n = \frac{1}{m}$$

the following is obtained for the usual representation of the viscosity function:

$$\eta = k \cdot \dot{\gamma}^{1-m} \tag{2.8}$$

The factor k is called the consistency factor. It represents the viscosity at a shear rate of γ =1 s^{-1}. The viscosity exponent n is equal to 1 for Newtonian behavior and is < 1 for most polymers. It describes the slope of the viscosity curve as shown in Figure 2.6.

2.2 Introduction of Water-Assisted Injection Molding (WAIM)

2.2.1 Introduction and development.

The Principle of WAIM is similar to sandwich injection molding technique, except that, instead of injecting a second polymer material as the core component, a process medium is employed. In gas-assisted injection molding (GAIM), normally nitrogen is employed as the process medium. In the case of the water assisted injection technique (WIT), a fluid is injected precisely into the melt, so that the molten core of the developing part is displaced and a hollow section is formed. The fluid injection technique offers considerable potential to produce high-quality lightweight plastic parts in short cycle times. Thus, significant advantages can be achieved compared to products, which are manufactured traditionally using metals or conventional injection molding. Some of the advantages of WAIM are listed below: [2-6, 8-12]

• Cutting production costs by:

- Reduction of cooling and therefore cycle time

- Savings in material and weight

- Integration of process steps

- Reduction of clamping forces

• Increasing quality by:

- Reduction of sink marks, more uniform shrinkage, and reduced warpage

- Enhancement of weight-specific mechanical properties

• Simplification of part and mold construction by increasing design options

Obviously, not all advantages can be obtained at once for any specific part, and certain efforts need to be made towards stable WAIM processing. For each application, costs and benefits have to be evaluated at the earliest possible step of product development. Alternative manufacturing methods should be taken into account. However, in many cases, the additional efforts associated with the application of PIT are justified by the resulting benefits in terms of lower manufacturing costs and increased product quality. Drawbacks of the fluid injection technique typically include:

• Additional costs (investment, operation and maintenance costs for WAIM-equipment)

• Increased complexity of the processes and systems

• Increased demands for operational personnel (specialized knowledge of WAIM)

During the last two decades, GAIM has been well established as a special injection molding process for thermoplastics and has become recently develop technique. However, GAIM is accompanied by different limitations, for instance the marginal heat transfer towards the gas, the eventual foaming of the inner melt layer, as well as limited part diameters among others. Depending on the polymer and part geometry, WAIM offers the following significant advantages when directly compared to GAIM for certain applications:

• A reduction of cycle times of up to 70%

• Slightly lower residual wall thicknesses

• Better concentricity of the hollow sections in redirection

Water-assisted injection molding (WAIM) appears at the beginning of the 70s but its real development started at the Institut fur Kunststoffverarbeitung (IKV) Aachen, Germany in 1998.[10] WAIM are a specialty newest way of injection molding process to mold hollow or partly hollow parts, closely related to Gas assisted injection molding (GAIM) [11,28]. But WAIM has some advantages over GAIM. This is because water is incompressible, inexpensive, readily available, and a more effective coolant. The thermal conductivity of water is 40 times and water's heat capacity greater than gas.[6]

First industrial of WAIM the component of shopping cart (Figure 2.7) at Fakuma 2000. WAIM used for basket rim and side panel. There are two companies cooperated with IKV to present the result, namely, A schulman GmbH, Kerpen (Germany), and SULO plast. GmbH & Co .KG, Herford (Germany). The project started in 1998. It used Schulman's PP and PME's WIT technology to mold a part with three water channels from 20 to 60 mm of diameter and 800 to 1500 mm long. The PP trolley had previously been molded with gas-assist in 280 sec, while WAIM took just 68 sec or shorter than 4 times.[4]

Figure 2.7 Prototype shopping cart

2.2.2 Water-Assisted Injection Molding Process

Water assisted injection molding (WAIM) is the special technique for producing parts with hollow core. The process consists of two components that are water and plastics.

2.2.3 Process Sequence

The sequence of the WAIM process is largely similar to gas-assisted injection molding.[14,15] A schematic diagram of water-assisted injection molding is illustrated in Figure 2.8 and Figure 2.9 shows the generalized process cycle for the water injection technique. The first step of the process is the injection of a short (partial) or full shot of melt into the closed cavity Generally, after a short time delay, the still molten core of the pre-molding is displaced by a fluid and moved towards unfilled areas of the mold and opened sections of the cavity or even backwards into the plasticizing unit. For every process variant, the backpressure is applied by the injected fluid. Therefore, in contrast to conventional injection. gate sealing point. As soon as the part is dimensionally stable, the water is retrieved. Each process variant

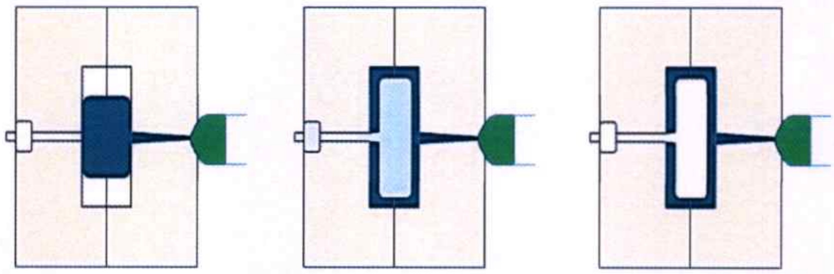

Figure 2.8 Schematic of the water-assisted injection molding process

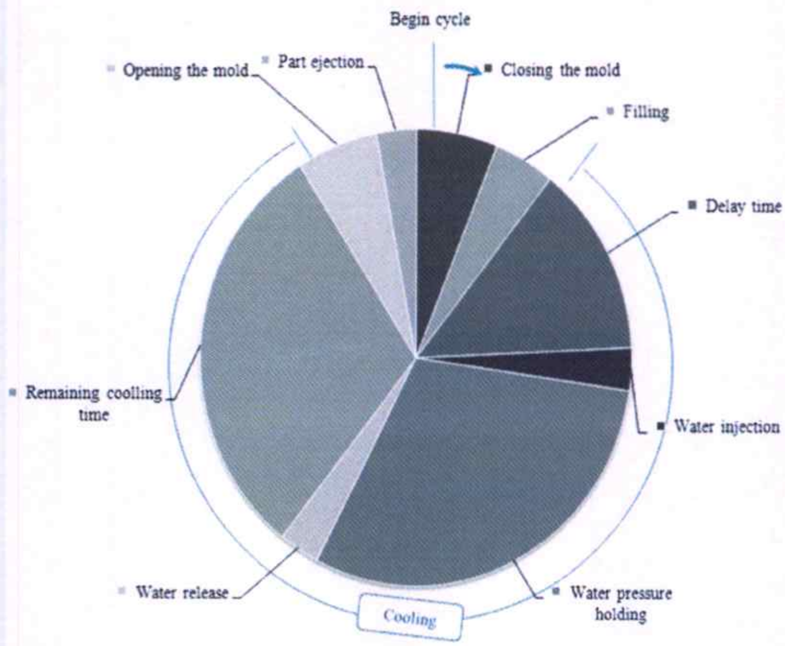

(1) Closing of cavity

(2) Polymer injection

(3) holding press

(4) Water injection

(5) Water holding time

(Fluid holding press.)

(6) Pressure release +

water retrieval.

(7) Cooling time

(8) Opening of cavity

(9) Ejecting molding

Figure 2.9 WAIM injection molding cycle possesses should be carried out with regard to the particular application. Beside the pure technical specific advantages and drawbacks. Therefore, the selection feasibilities and challenges, special consideration.

2.3 Techniques for Water-Assisted Injection Molding Process

In principle, the process variants of WAIM are identical to those of GAIM and sandwich injection molding. Figure 2.2 illustrates the four most common process variants for fluid injection. The individual processes can be distinguished by their respective process controls. Therefore, specific advantages and disadvantages, relating to saving material, material strain/damage, changeover marks, superior filling of compact areas in highly integrated molded parts, mold complexity, patent/royalty situation etc., are associated with each process variant.

2.3.1 Short-Shot Process

In general, the short-shot process is the simplest process variant for fluid injection. In this process, the cavity is partially filled to 50-95% of its volume. After a preferably short time delay, the cavity is completely filled volumetrically by means of the fluid. The injected fluid is well directed into the still molten core of the pre-molding, displacing the melt successively to the end of the flow path as show in Figure 2.10. To ensure that the fluid does not break through at the flow front, a sufficient amount of plastic needs to be injected at the beginning. In order to compensate for potential variations in the residual wall thickness, a small compact section at the end of the flow path should remain as a buffer. The advantage of the short-shot process is the can occur, due to stagnation of the short shot and solidifying skin, which is stretched by the subsequent fluid injection. Short time delays and specially modified polymers (retardation of crystallization) help to eliminate hesitation marks.

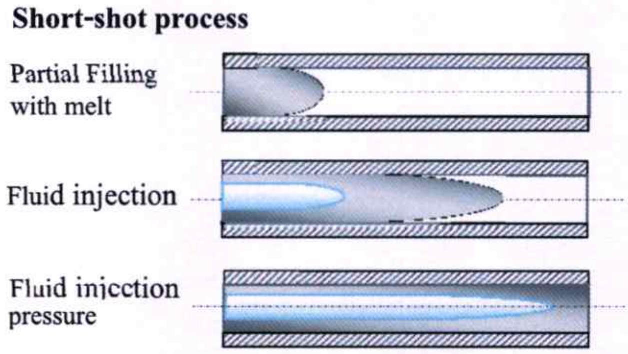

Figure 2.10 Short-Shot Process

2.3.2 Full-Shot Process

In this technique, the melt is completely injected into the mold cavity [16]. The water is injected. Because the cavity has already been filled with plastic, the water can enter only if the volume of plastic shrink. Full-Shot method is shown in Figure 2.11. Thus, the water is playing only as holding pressure and weight reductions of moldings depend on the volumetric shrinkage of polymer. However, the reason to use the full-shot process. The basic advantage is to make moldings that do not have sink marks, do not warp and fulfill demands for high quality.

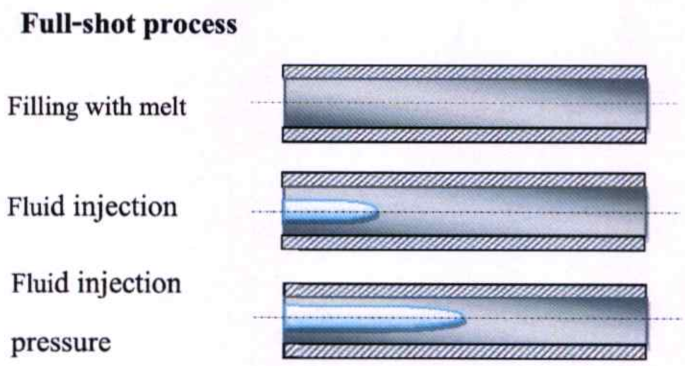

Figure 2.11 Full-Shot Process

2.3.3 Over-Flow Process

One of the limitation of short-shot water-assisted injection-molded parts is the switchover mark on the surface of molded products[14]. The full-shot and overflow process has an advantage of eliminating the switchover mark on the surface of the molded parts. This leads to a reproducible molding of the cavity surface without hesitation marks, different gloss levels, or sink marks. Similar to conventional injection molding, melt back pressure is then applied over the gating system before injecting the fluid in order to mold compact, thin-walled sections such as mountings or other functional elements. Regarding injector positioning and the adjacent melt displacement, there are two different overflow processes, which can be subdivided into an overflow process with shut-off and without shut off.

2.3.3.1 Overflow Process with shut-off

Another interesting technique is to fill the cavity completely and then to expel some plastic into the overflow cavity. The so-called the spillover cavities, as show in Figure 2.12. For better control of the process, a valve can be provided between the cavity and the overflow cavity. The start time of the water injection has direct influence on the residual wall thickness. By increasing the water delay time between mold filling and the start of water injection, the residual wall thickness can be increase because a plastic layer in the cavity has already solidified. The water delay has no influence on the surface quality, because the cavity has been filling completely.

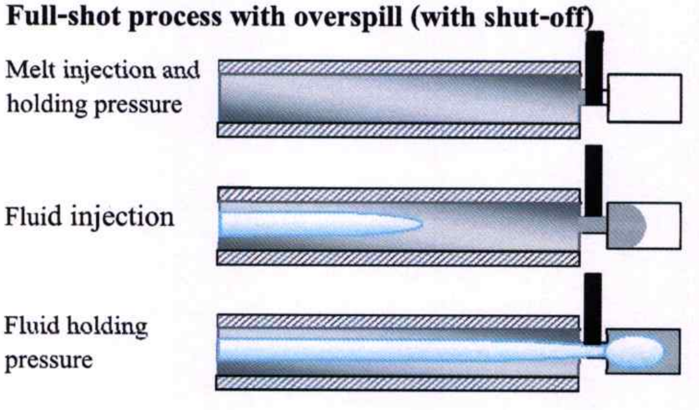

Figure 2.12 Full-Shot Process with shut off

2.3.3.2 Overflow Process without shut-off

In the Overflow process without shut-off is moving the position of the melt front at the end of filling outside of the product by without valve gate, The process sequence is the same as for short shot. The molten is short-shot injected at the end of product "envelope".[7] Immediately or after a delay time, the water is injected and then to expel some plastic into one or more separate cavities, so-called overspill or overflow cavity. The principle is show in Figure 2.13

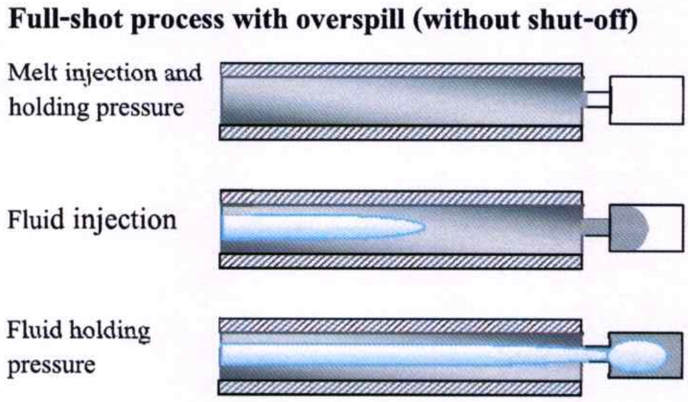

Figure 2.13 Full-Shot Process without shut off

2.3.4 Melt Push Back Process

The melt pushback process or the back to screw process, the method is closely related to the overspill cavity method [12,17]. The mechanism melt pushback process is that the melt is injected at the end of the flow path and the water is injected at the other end of the molding, and then melt is pushed back to the barrel as show in Figure 2.14. The stroke of the screw being pushed back by the plastic must be set accordingly to accept the volume of the displace plastic.

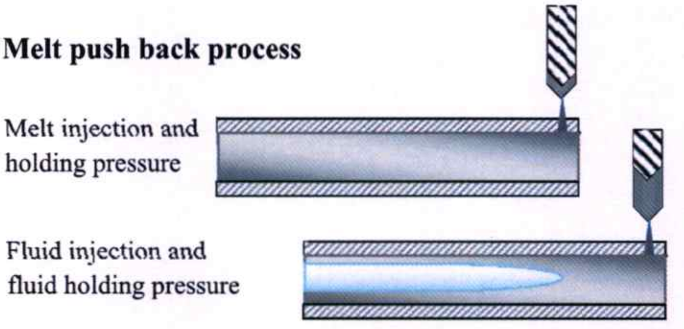

Figure 2.14 Melt Push Back Process.

2.3.5. Core pulling process

A fifth process is the core-pulling process. The process method is show in Figure 2.15. The melt is injected into a cavity of variable volume. After closing the mold, the cores are moved into forward position to reduce the initial cavity volume. Then, the cavity is completely filled with polymer and after a set delay time with optional melt back pressure, the cores are pulled back to increase the cavity volume. In order to keep the polymer in contact with the cavity walls, the water needs to be injected simultaneously. However, the area where the core movement occurs is more or less visible on the molding.

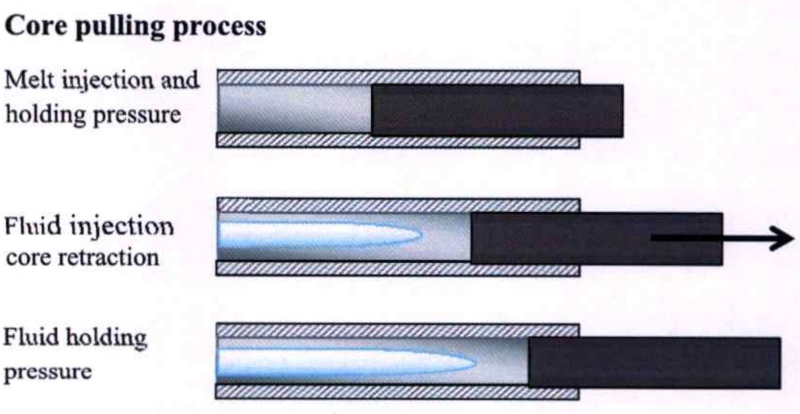

Figure 2.15 Core pulling process

2.4 WAIM and GAIM comparison.

Water assisted injection and gas assisted injection molding techniques are closely related process But WAIM has advantage over its better known competitor, gas assisted injection molding. [2, 4, 17-21 and 27] Both techniques are not concerning plant and injection technology or cycle time, but also concerning part properties and design options. The fields of application overlap only partially, so that WAIM technique is an additional to rather than a substitute for GAIM. Regarding the geometry for fluid injection, three different classes of molded parts can be observed:

- Thick-walled and rod-shaped parts (GAIM and WAIM)
- Compact part with integrated thick-walled sections (GAIM and WAIM)
- Flat thin-walled parts with suitably shaped stiffening ribs (only GAIM)

The difference applications are show in Figure 2.16

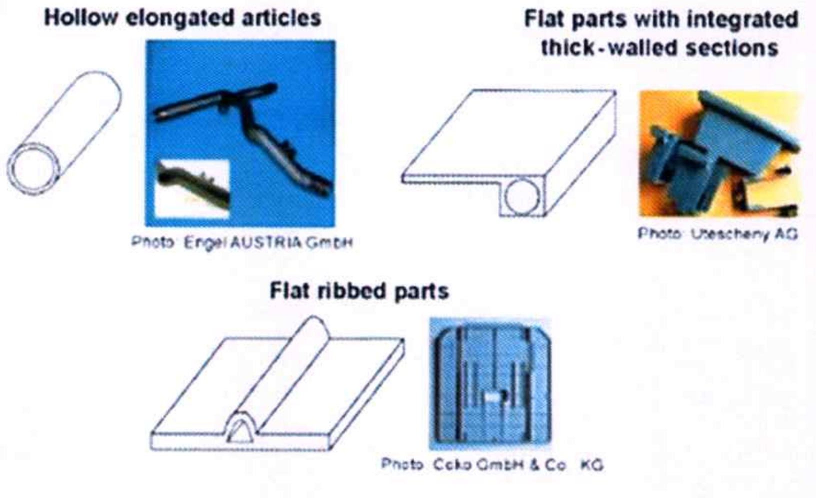

Figure 2.16 Difference part geometry for WAIM

There are set physical limitations for GAIM, for manufacturing parts, the cross sectional size should not exceed 30 millimeter in any diameter (Figure 2.17) and the cross sectional shapes should approach a circle (Figure 2.18) [22]. This can be attributed to extensive wall thicknesses and a pouring down of non-solidified melt inside the hollow mold during the gas holding time. Due to the strong cooling effect of water, this problem can be prevented completely with WIT, even for large diameters.

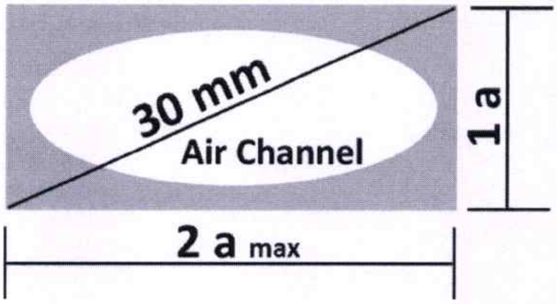

Figure 2.17 Diagram of rectangular cross-sectional maximum proportions

(illustration courtesy Integrated Design Systems, Inc.)

Figure 2.18 Ideal cross-section for a contained channel part

(illustration courtesy Integrated Design Systems, Inc.)

2.4.1 Cycle Times

The most demonstrative advantage of WIT, compared to GAIM, is the considerably more efficient cooling effect of water versus gas, as mentioned above. Nitrogen has approx. 40 times lower heat capacity, and four times lower heat capacity, compared to water; therefore, nitrogen has less than 25% of the cooling impact of water on the part interior as show in table 2.1. These results in significantly reduced cooling time when using the water injection technique compared to that with GAIM, depending on the part size and geometry and on the specified product properties. Figure 2.19 depicts this phenomenon, as indicated by infra-red thermal images after de-molding.

Table 2.1 A comparison of heat capacity between nitrogen and water

	Nitrogen 1 bar, 20 °C	Water 1 bar, 20 °C	
Thermal conductivity λ [W/m K]	0,0143	0,604	> Factor 40
Specific heat capacity c_p [J/kg K]	1038	4182	> Factor 4

Reference: IKV Aachen

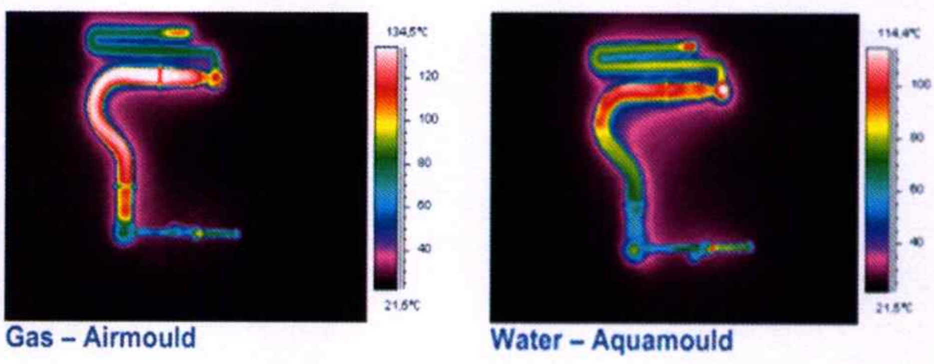

Figure 2.19 Infra-red heat images after demolding (courtesy of Battenfeld)

Moreover, Liu et al. [5] demonstrated the temperature profile of cooling time, the measured result reported that the cooling time for water assisted injection molding is much shorter than of conventional injection molding and gas assisted injection molding as show in Figure 2.20.

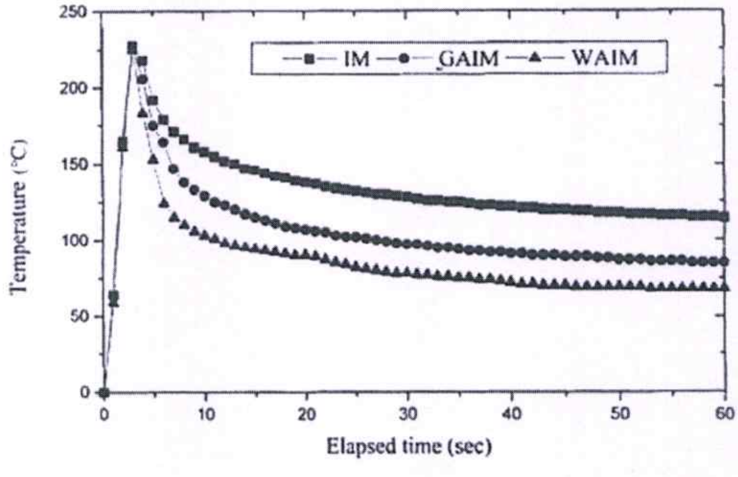

Figure 2.20 Temperature variation of injection molding (IM), Gas-assisted injection molding (GAIM), and Water assisted injection molding.

2.4.2 Part Properties

Generally, both GAIM and WIT facilitate a very efficient and cost-saving production of high- quality hollow plastic articles, with minimized warpage and sink marks. Nevertheless, the different process media influence different part properties, such as residual wall thicknesses, concentricity of the hollow section, fluid-side surface qualities, or morphology across the residual wall.

2.4.2.1 Residual Wall Thicknesses (RWT)

It is a known fact that material viscosities have an impact on residual wall thicknesses. Additionally, due to the different viscosities of gas and water, residual wall-thicknesses are less when using water in comparison to gas. One theory attributes this smaller residual wall thickness to higher heat transfer through the water inside the part. The water increases the viscosity of the melt at the flow front and forces the melt to move forward instead of being pushed to the side, resulting in a smaller residual wall thickness [26] as shown in Figure 2.21.

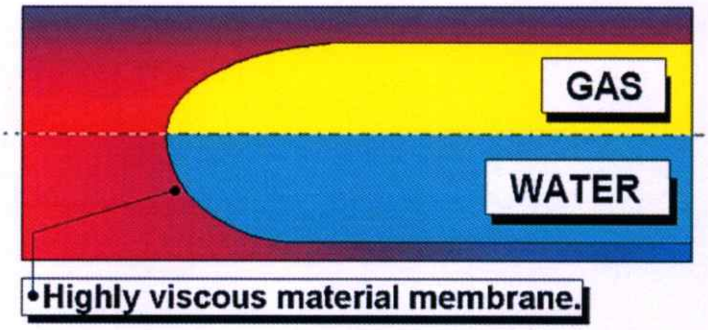

Figure 2.21 Highly viscous membrane forces the material forward instead of being moved to the side

The distribution of the residual wall thickness across and along the flow path is one of the essential quality criteria of hollow parts. On the one hand, the mechanical part properties are directly affected by the RWT distribution. On the other hand, the flow section of media conveying lines is determined by the RWT. Moreover, shrinkage and warpage are strongly influenced by the RWT distribution. The resulting wall thickness for GAIM, as well as for WIT, is predominantly determined by the rheological and thermal melt properties. Process parameters, such as time delay, fluid pressure, volume flow rate, and processing temperatures have only a limited effect on the RWT [5]. With the water injection technique, it is generally possible to achieve larger part dimensions and lower residual wall thicknesses than with the gas injection technique, when suitable materials are employed. Figure 2.22 shows a comparison of the resulting residual wall thicknesses for different polypropylenes.

The differences in RWT using GAIM or WIT are small. Only for one special material (WB130 HMS; HMS = high melt strength) were smaller RWTs achieved by GAIM.

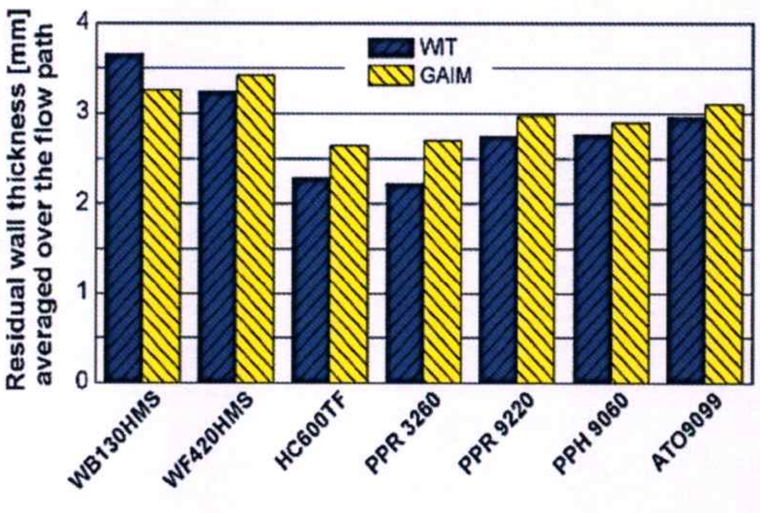

Figure 2.22 Comparison of the RWT for GAIM and WIT

Finally, compared to GAIM, significantly better concentricity of the hollow section can be realized by using WIT, particularly in curves and redirections. The results of investigations performed at IKV regarding the differences in residual wall thickness of a flow path are shown in Figure. 2.23. In additional, BASF demonstrated that WAIM created thinner wall approximately 25% thinner than GAIM as show in Figure 2.24 [24]

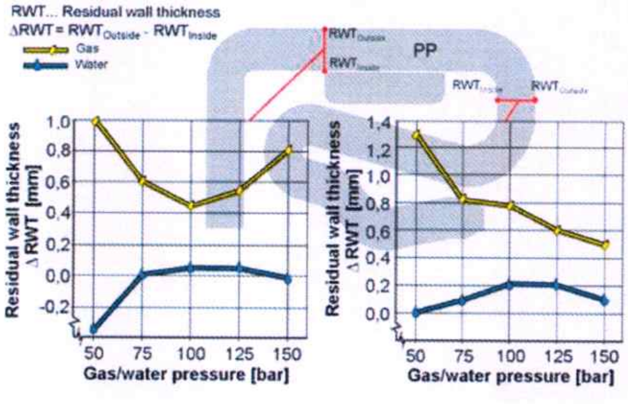

Figure 2.23 Comparison of the RWT for GAIM and WIT

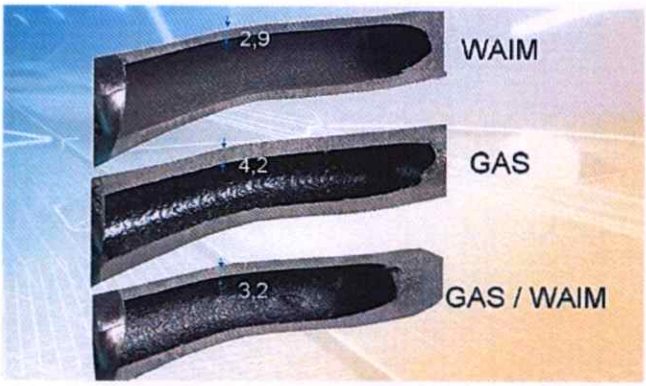

Figure 2.24 Internal surface finish and wall thickness of

Ultramid® B3GM35 Black Q642 (courtesy of BASF)

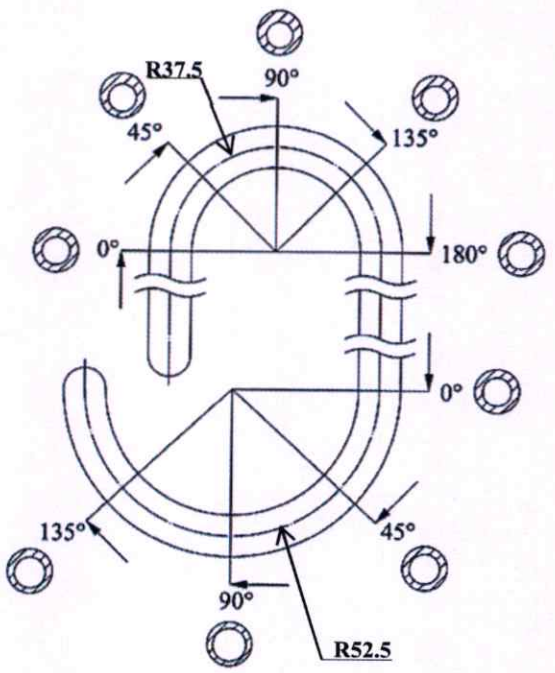

Figure 2.25 Wall thickness difference at different positions along the upper and lower curved sections

During the forming of the hollow section, the fluid takes the path of least resistance, which is located closer to the inner side of any curve that may be in the part. Compared to gas, water has more inertia, partially compensating the variance in pressure drops in the curve section of the part. However, extreme redirections (sharp corners) should be avoided if possible. Furthermore, Lin and coworker [13] reported the wall thickness was not uniform at curved sections in spiral tube cavity with diameter of 16 mm. that consists two curved section: a curvature radius of 37.5 mm. at upper curved section and a curvature radius of 52.5 mm. at lower curved section, there are eight curved water channels as show in Figure 2.25. They found out that the residual wall thickness around mold curved section was not axial-symmetric. The outer wall thickness was greater than the inner wall thickness. Furthermore, the residual wall thickness difference of gas assisted injection molded tubes was smaller than that of water assisted injection molded part at the upper curved section, but was greater than that water molded parts at the lower curved section as show in Figure 2.26 and 2.27

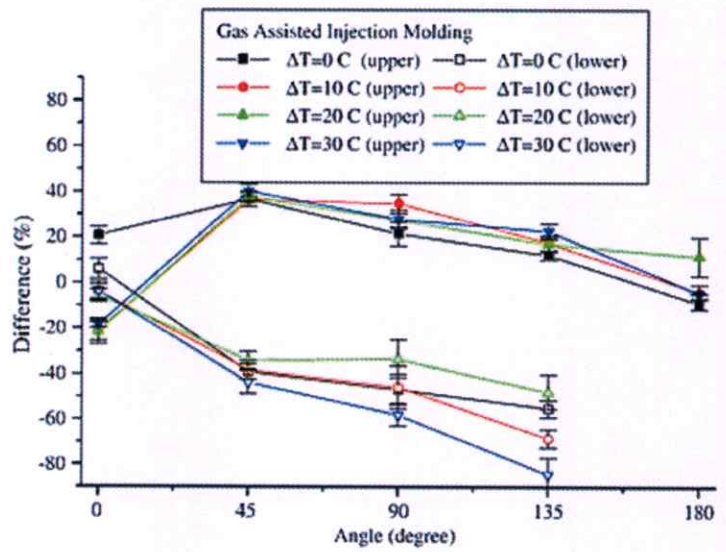

Figure 2.26 Measured wall thickness difference at various positions along curved sections of gas assisted injection molded parts

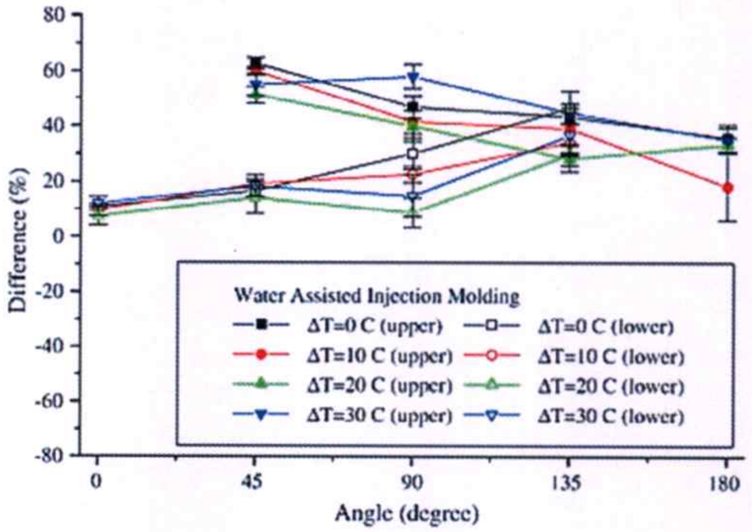

Figure 2.27 Measured wall thickness difference at various positions along curved sections of water assisted injection molded parts

2.4.2.2 Shrinkage/Warpage

Shrinkage and warpage are crucial quality criteria for plastic moldings, particularly if they are integrated in complete assembly groups. One reason for the broad acceptance of GMM is that the volume shrinkage is reduced significantly compared to that of conventional injection molding. The extent of shrinkage is mainly affected by the holding pressure. Figure2.28 shows the shrinkage for GAIM and WIT, for the flow path test molding using a virgin poly-propylene. Basically, shrinkage decreases with increasing water or gas pressure. In most cases with GMM, slightly less shrinkage values are obtained as compared to WIT, since the effect of the holding pressure of gas is better than that of water. Due to the strong cooling effect of water, the fluid side polymer layers solidify rapidly. Therefore, the remaining melt cannot be pushed as forcefully to the cavity wall as with GAIM. Warpage is mainly determined by the cooling conditions, which are again a result of wall thickness distributions and thermal conditions in the cavity. Due to the complexity of the interacting effects, no general statement can be made about which process leads to less warpage. Obviously, the warpage values strongly depend on the measuring position and the processed material. Thus, no general trend for WIT or GAIM can be observed.

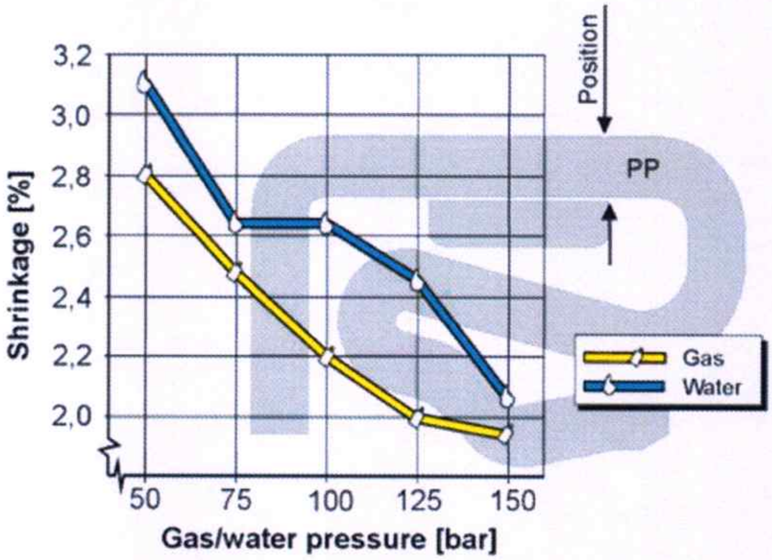

Figure 2.28 Shrinkage for GAIM and WIT vs. fluid holding pressure

2.4.2.3 Fluid-Sided Surface Qualities

The resulting qualities of the fluid-sided surfaces are of great importance for media-conveying lines. Obviously, the flow resistance of the application is influenced by the surface quality. However, of much greater importance is how the surface can resist the applied media during use, for instance, water/glycol mixtures in case of automotive water-cooling pipe applications. In this context, a smooth, uniform surface structure is required in order to achieve the least effective contact surface possible. For most of the pipe applications, glass fiber reinforced materials are used. In this case, it is important that the fibers are well embedded to prevent erosion or wear on the system.

The main effect on the fluid side surface quality has the processed material itself. Which process, GAIM or WIT, leads to better surface quality again depends on the processed material. For instance, most of the investigations during the early years after development of WIT were made with polypropylenes (PP), which are quite comfortable to process. For most of the polypropylenes, the application of WIT leads to significantly improved surface quality. That is the reason why, in several publications, the fluid-sided surface quality is listed as a strong were made with polypropylenes (PP), which are quite comfortable to process. For most of the polypropylenes, the application of WIT leads to

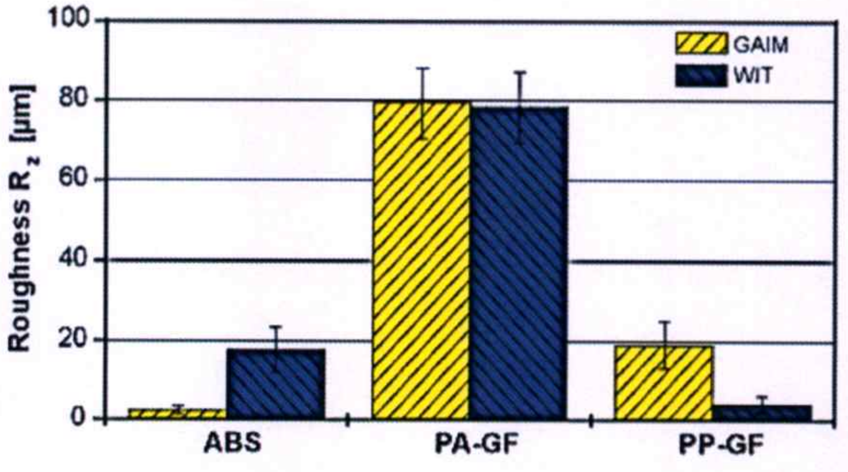

Figure 2.29 Average fluid-sided roughness

significantly improved surface quality. That is the reason why, in several publications, the fluid-sided surface quality is listed as a strong advantage of WIT [23]. In fact, this is only valid for PA With other resins, surface quality of GAIM is comparable or even smoother than WIT formed surfaces. Figure 2.29 depicts this phenomenon, showing the fluid-side surface roughness of three different materials.

2.4.2.4 Typical Part Defects

Apart from defects already associated with conventional injection molding, there are some typical defects that can be directly attributed to fluid injection. For gas-assisted injection molding, typical defects include gas dissolution into the polymer and thus foaming of the fluid-side surface, as well as fingering. Both defects are described comprehensively in GAIM for foaming of the inner surface can be prevented completely for WIT, because the water normally hollows out the cavity without evaporating. Fingering is also normally not observed for WIT, since this problem typically occurs for flat, ribbed parts, for which WIT is typically not used. In that case, the fluid is only used for compensation of shrinkage and the cooling effect by water could not reduce the cycle time significantly. Defects typical of WIT are various types of non-continuous hollow sections shown in Figure 2.30, as well as extensive voids.

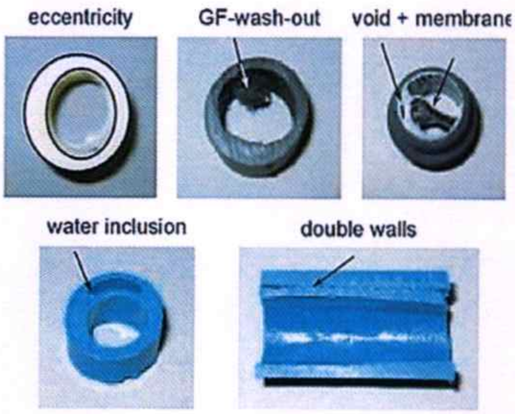

Figure 2.30 Typical Part Defects for WAIM

For WIT-suitable materials, both types of defects can be prevented, using proper injector technology and suitable process parameters. A comprehensive description of the development of such defects has not been made so far. The analyses and understanding of the exact mechanisms is the subject of current research activities. For most of the results, there is evidence suggesting that the defects occur during water injection at the contact surface between the water and the polymer. Identification of the polymer melt of the physical properties that are ultimately decisive for WIT process ability has not yet been clarified unambiguously. There is a number of properties, such as viscosity, structural viscosity, stretching viscosity, elasticity, and interfacial tension, which effect the forming of the hollow section significantly, in most cases, the WIT process ability of each polymer has to be proved in practical trials.

2.5 Equipment for WAIM.

The basic equipment for WAIM process is composed of five components:

- Injection molding machine
- Water pressure generate unit.
- Pressure control unit
- Water pressure control and water injection modules.
- Water injection pin

2.5.1 Injection molding machine.

The injection molding machine used in conventional molding is the primary item required to produce water assist molded parts and also implemented in WAIM by only modifying the interface between water injection unit and molding machine.

2.5.2 Water pressure generate unit.

Pressure generating units for water are compact mobile units. All elements which come into contact with the water are made from copper (low-pressure areas) or stainless steel (high-pressure areas). The mobile pressure generating unit is linked to the injection molding machine with stainless steel pipes [25], high-pressure hoses and screw couplings. Effective working pressure of 200 bars is sufficient. In additional, the unit can provide water heating to 70 °C are available. An as sample for pressure generate unit for water, the Aquamould® series"WE" by Battenfeld as shown in Figure 2.31 and the appropriate size depends on the number of machines to be connect to the pressure generation unit.

Figure 2.31 Aquamould® water generating unit

2.5.3 Water pressure control unit

The control is links to the conventional injection molding machine by means of an interface. An as sample for pressure control unit, the Aquamould® Unilog B 4 by Battenfeld as shown in Figure 2.32.

The modern system offers advantage such as:

- Easy control (i.e., by touch screen)
- Real value graphic for pressure curves (Figure 2.33)
- Standard for up to four pressure control modules
- Suitable for water-assisted injection molding techniques
- External data storage

Figure 2.32 The mobile pressure control unit Aquamould®UNILOG B4

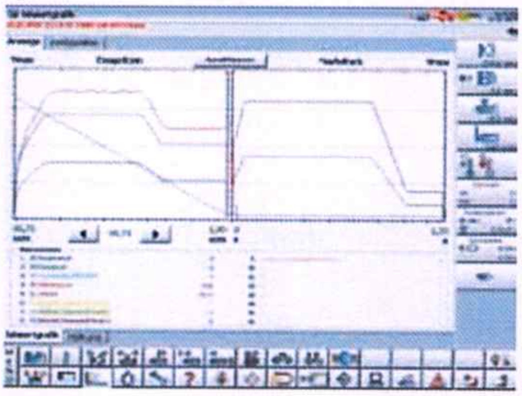

Figure 2.33 Actual value graphic displays for pressure curves

2.5.4 Water pressure control and water injection modules

The water pressure is controlled with pressure control modules (Figure 2.34) are designed as compact unit and to be positioned close to the mold. Leakage-free values are used for precise control of the water pressure. They are suitable for low and high water volumes. The values are actuated electrically which dispenses with the need for a supply of hydraulic oil or compressed air. Prior to de-molding, the removal of water after molding is also a challenge [21] and can be achieved in different ways such as:

- By gravity through the water injection points
- Alternating injection of compressed air through water injector
- The use of gas pressure applied to a second inlet (additional air injection) of the injection mold component

Figure 2.34 Water pressure and water control module

2.5.5 Water injector

The gas pin, which is commercially available from a gas injection unit suppliers, consists of an annular opening 0.05 mm. between a cap for nitrogen discharge and the pin body. For water assisted injection molding, three types of injector pin, the ring type, the orifice type and the porous type. The water injector is made of stainless steel for corrosion resistance and normally varies in a range from 2-15 mm. In addition, Liu and Lin [9] investigated for the volumetric flow rate and outlet pressure of the orifice type and the porous pins types, the porous type water injection pin has pore diameter of the surface ranges from 50 to 70 μm and porous surface is made from the sintering of stainless steel powers (Figure 2.35). The orifice pin has a small orifice of 0.5 mm. in diameter at the side of the pin body (Figure 2.36). They reported that both the volumetric flow rate and outlet pressure of the porous pin are much higher than orifice pin as show in Figure 2.37. Moreover, Liu et al. [16]

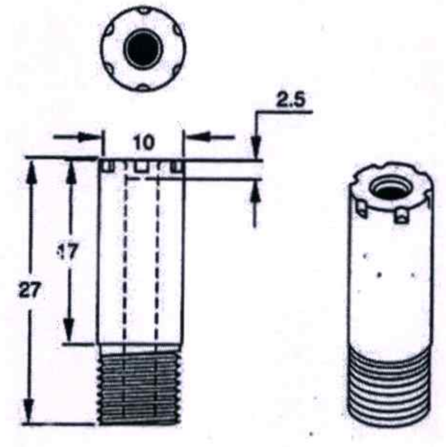

Figure 2.35 Structure and dimension of porous pin (unit: mm)

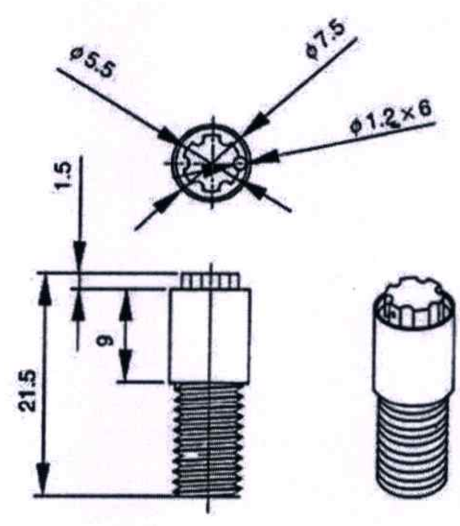

Figure 2.36 Structure and dimension of orifice pin (unit: mm)

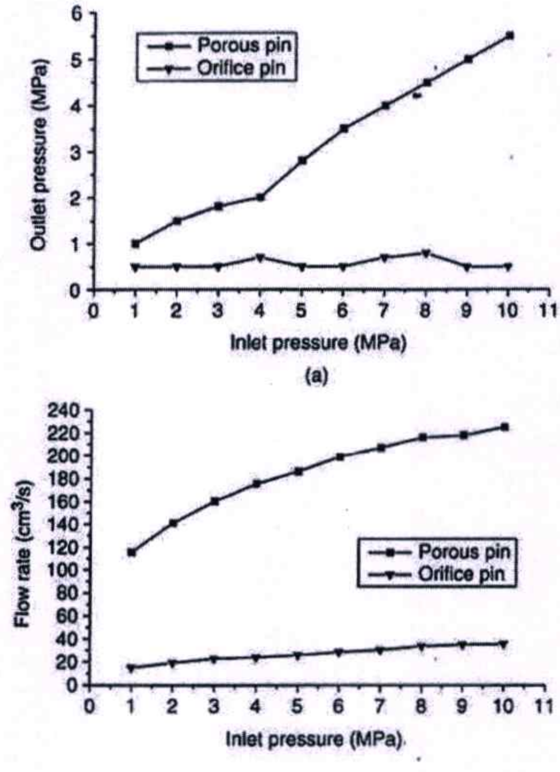

Figure 2.37 (a) Outlet pressure, and (b) volumetric flow rates of the pins subjected to different inlet water pressure

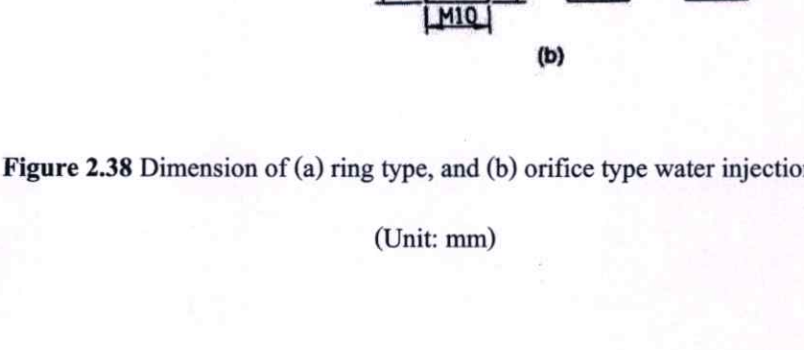

Figure 2.38 Dimension of (a) ring type, and (b) orifice type water injection pins

(Unit: mm)

proposed the moldability compared between the ring type and orifice type by tested on polypropylene material. The ring type pin has four shallow openings (0.1x2.0 mm in cross section) between the body and the cap around the water injection (Figure 2.38a). The orifice type water injection pin has a small orifice at the side of the pin body. There are three different of orifice hold sizes 0.5, 1.0 and 1.5 of diameter (Figure 2.38b). The result reported that the orifice type water pin had a higher chance to get stuck by the polymer melt as shown in Table 2.2.

Table 2.2 Moldability of water injection pin designs against polypropylene material.

Parameter		Type of water pin			
Melt filling pressure MPa	Water pressure MPa	Ring (0.1 mm x 2.0 mm.)	Orifice Ø0.5 mm.	Orifice Ø1.0 mm.	Orifice Ø1.5 mm.
100	5	O	O	O	O
100	7	O	O	O	O
100	9	O	O	O	O
140	5	O	O	O	X
140	7	O	O	O	X
140	9	O	O	O	X
180	5	O	O	X	X
180	7	O	O	X	X
180	9	O	O	X	X

* O = Pin unstuck; X = Pin struck

As openings in this dimension, the water injector is designed so that the plastic forms a water-tight seal. Therefore, an active closing mechanism is required to prevent the melt from unintentional flowing into the injector during the melt injection phase. It is obvious that the constructing engineer has to deal with two conflicting demands. On the one hand, the injector should be preferably small sized in order to prevent a strong impact on the design of the part and to allow an easy integration of the injector system into the mold. The design of the part and to allow an easy integration of the injector system into the mold. On the other hand, preferably high water flow should be discharged into the melt without strong jetting of the water at the injector orifice, to enable a reproducible forming of the hollow section. Therefore, a diameter of the outlet orifice must be carefully chosen. As a general rule, the injector orifice diameter has to be increased with increasing part diameter. Which value exactly should be chosen for each diameter additionally depends on the injector embedding, the general injector concept, and the processed material. Definitive guidelines have not been worked out at this time. As a recommended value, the injector orifice should be in the range of 1/10th to 1/3rd of the part diameter.

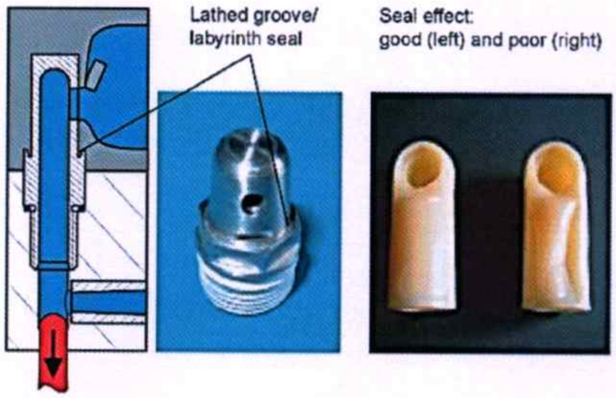

Figure 2.39 Seal principle and seal effect of WIT-injectors

Another important demand on the WIT injector system is proper sealing against leakages between injector and the melt. Several different sealing design details should be taken into consideration. The sealing effect around the inlet area is particularly important.

The most common principle is shown in Figure 2.39 and Figure 2.40 shown the WIT injector sealing design by Battenfeld.

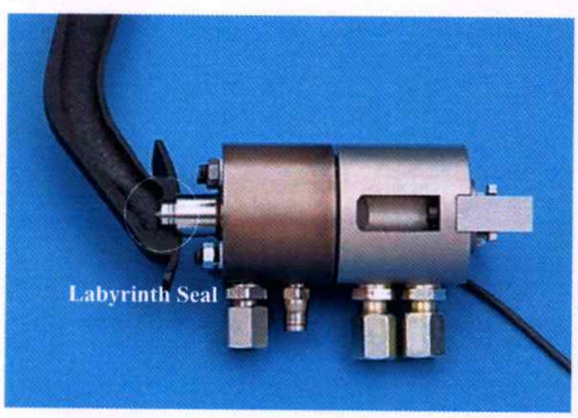

Figure 2.40 Water nozzle injecting direct into the mold cavity

2.6 Applicable materials for WAIM.

Most thermoplastic, thermoset polymer thermoplastic composite materials are capable of being used in water assisted injection molding.

Liu et al. [5] performed an experimental study on WAIM of thermoplastic material, polystyrene (PS), high impact polystyrene (HIPS), Polypropylene (PP), polyethylene (PE), and acrylonitrile-butadiene-styrene (ABS). A spiral cavity with a square cross section of 15 mm. x 15 mm. was used in the experiment. They found out that all materials can be capable molded by WAIM. Figure 2.41 shows the cross sections and the void shapes.

Huang et al. [29] studied WAIM process, effect of processing parameters on the penetration behavior of water in the WAIM process of acrylonitrile-butadiene-styrene (ABS) material.

Liu and Chen. [16] Studied the effects of different processing parameters on the WAIM of the short glass-fiber filled polypropylene composites. Composites molded by WAIM have a shorter cycle time than those molded by conventional injection molding and GAIM.

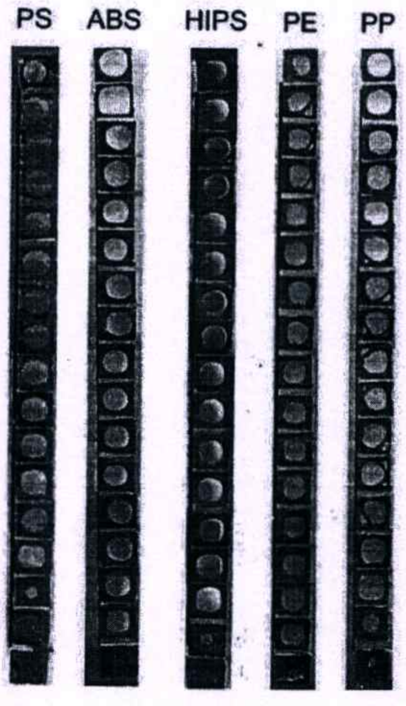

Figure 2.41 Void shapes of water assisted injection molded thermoplastic material

Liu et al. [30] performed an experimental study on WAIM of glass fiber filled poly-butylene terephthalate (PBT) composites. A plate cavity with a rib crossing the center was used in the experiments. The influence of various processing variables on the length of water penetration in molded parts was examined. They found out that the melt filling pressure, melt temperature, and short shot size were the dominant parameters affecting the water penetration behavior. A higher degree of crystallinity was exhibited at the mold-side than that at the water-side. They reported that glass fiber filled composites exhibit more severe water fingerings than those of un-filled materials.

Liu and Shih [31] studied experimentally the water-assisted injection molding process of glass fiber-reinforced polyamide-6 (Nylon-6) composites on spiral mold cavity.

2.7 Part design consideration

Design guidelines for water assisted injection molding should focus on three objectives:

2.7.1. Cross Sections

For the design of the cross section, it should be taken into account that the fluid flow channel develops distribution over the cross section, which leads unavoidably to sink marks or warpage, the exterior contour should be designed as circular as possible.

Up to a certain extent, the fluid channel can approximate the cavity contour. For a rectangular cross section, for instance, an elliptical fluid flow section develops. If a circular exterior shape cannot be realized, owing to design or functional restrictions, the following indications should be taken into consideration (see Figure 36):

- Realization of best possible approximation to circular contour
- Prevention of edges
- Prevention of material accumulations
- Uniform distribution of the residual wall thickness over the complete part

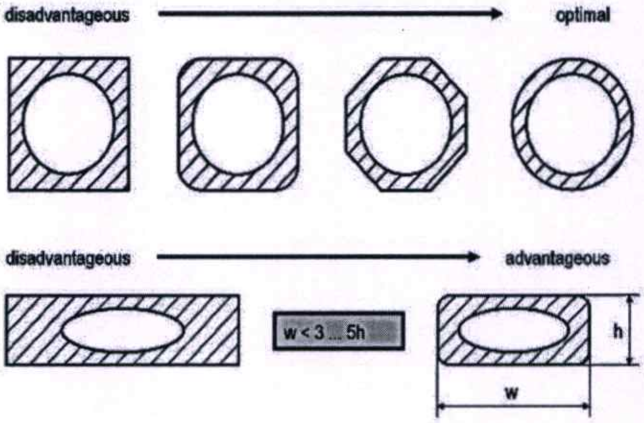

Figure 2.42 Cross sections for rod-shaped articles

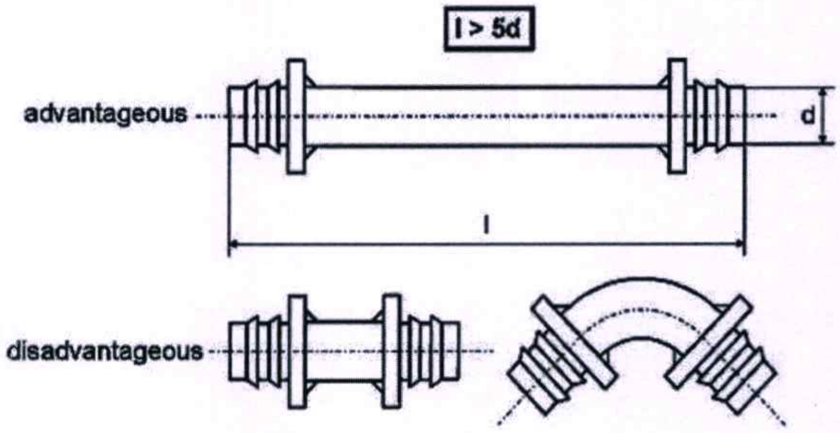

Figure 2.43 Aspect ratios for WAIM molded parts

For thin rectangular cross sections, the narrow-sided melt often cannot be displaced. Accordingly, as a rule of thumb, the maximal part width should be smaller than three or five times of the part height.

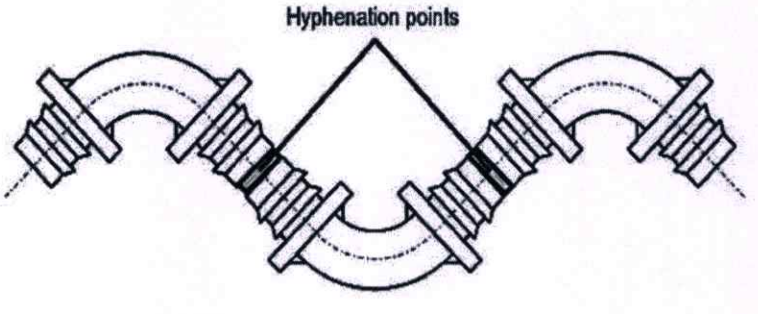

Figure 2.44 Multi cavity mold with connected cavities

2.7.2 Aspect Ratio

Generally, after injection, the fluid requires a certain How length to hollow out the cross section completely. For this reason, a certain aspect ratio, as shown in Figure 2.43, should (preferably) be taken into consideration.

In practice, the aspect is often determined by functional or design requirements, and it is smaller than the feasible minimum for WIT . One possible solution is the "multi-cavity" mold with sequentially connected cavities, as shown in Figure 2.44.

This concept offers the process reliability of a one-cavity mold with reduced investment cost (half the - number of injectors) at the productivity of a multi-cavity mold.

2.7.3 Curves and Redirections

When redirections have to be realized by WAIM, there is a general risk of material accumulations at the outer radius. The fluid channel, following the least flow resistance, is located closer to the inner radius. With WIT, narrower redirections can be realized, due to partial compensation of the above-described effect by the inertia of the injected water. Nevertheless, it is essential for WIT parts:

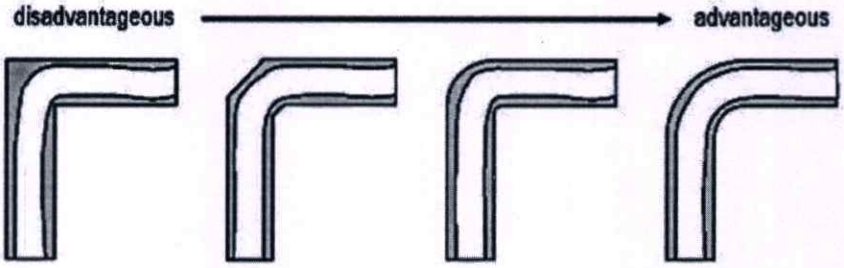

Figure 2.45 Design of re-directions and turnings

- To prevent sharp-edged redirections
- To choose the biggest possible radius of the redirection as shown in Figure 2.45

2.7.4 Change of Diameter

Abrupt changes in the diameter of the parts are critical. On the one hand, there is a risk of jetting during melt filling and, on the other hand, abrupt changes in the part diameter lead to dead water areas, which remain compact during fluid injection and generate material accumulations with the familiar problems. Furthermore, thin-walled wash-outs develop directly at sharp edges, representing mechanical weak points. If possible, the following points should be taken into consideration, as shown in Figure. 2.46

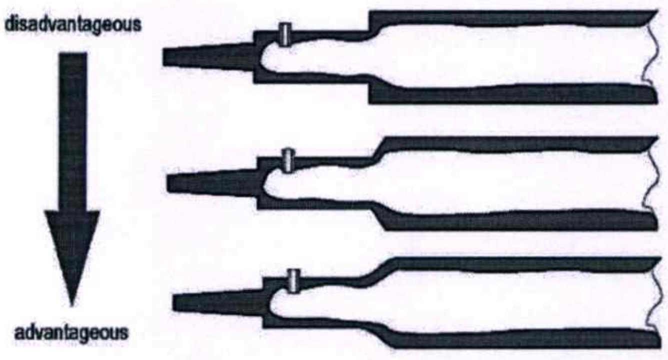

Figure 2.46 Change of diameter in the cross section

2.8 Fields of Application and Examples

Water assist injection molding is well-suited for the following types of potential applications automotive components such as handles; fluid handling tubes; office furniture components; appliance handles; and other structural components: example of automotive products show in the Figure 2.47-2.51.

Figure 2.47 BMW oil guide dipstick tube is molded with Engel's Watermelt process and a new WIT nylon grade from DuPont

Figure 2.48 Automotive air support system is molded with Engel, material is PP

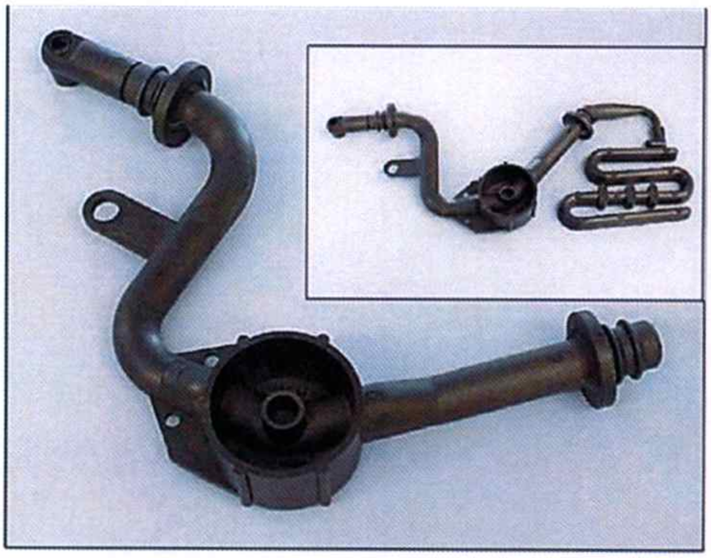

Figure 2.49 Automotive cooling water pipe, glass filled nylon 6.6

Figure 2.50 Volkswagen clutch pedal IS molded with Battenfeld's Aquamould, material is a 30% glass filled nylon 6

Figure 2.51 Handle for car seat adjustment: PA 6 GF 30, produced by Aquamould: Battenfeld

CHAPTER 3

EXPERIMENTAL PROCEDURES

3.1 Materials

In this research, semi-crystalline polypropylene (PP) were used to study the effect of processing parameters on water-assisted molded part properties by means of residual wall thickness (RWT) and hollow core ratio as shown in Table 3.1. The grade of PP is commercially available in the plastic market.

Table 3.1 Varios Thermoplastic Materials Used in the Experiment.

Material type (Grade)	HP400K	HP400M	HP550R	ASTM METHOD
Melt flow index (g/10 min)	**4**	**7.5**	**22**	**D 1238**
Density (g/cm^3)	0.9	0.9	0.9	D 792B
Tensile strength at yield (Mpa)	33	34	34	D 638
Elonation at yield (%)	11	10	9	D 638
Flexural modulus (Mpa)	1400	1450	1480	D 790A
Notch izod impact strength (J/m)	32	27	22	D 256A
Deflection temperature ($^{\circ}$C)	93	96	97	D 648

3.2 Experimental

The instruments used in this experiment are listed in Table 3.2.

Table 3.2 List of instruments

Instrument	Model
Water assisted injection unit	MTEC
Water Injection Pin	MTEC
Mold	Automotive fluid handling tube
Injection molding machine	JETMASTER Ai-Series
Mold temperature control	Water heaters STM-W Series

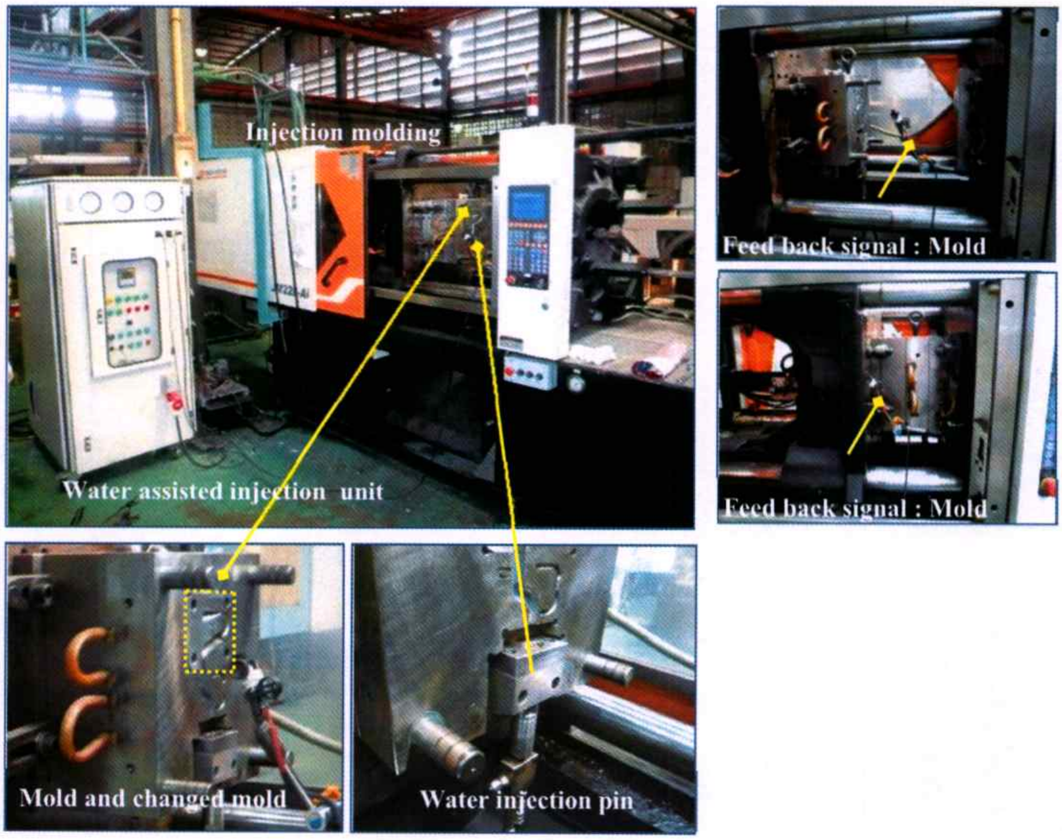

Figure 3.1 Experiment set up and instruments

3.2.1 Water assisted injection unit

A lab scale water injection unit developed earlier in National Metal and Materials Technology Center of Thailand : MTEC laboratory was used for all experiments. During experiment, the control circuit of the water injection unit received a signal from the molding machine and controlled the time and pressure of injected water.(Figure 3.2)

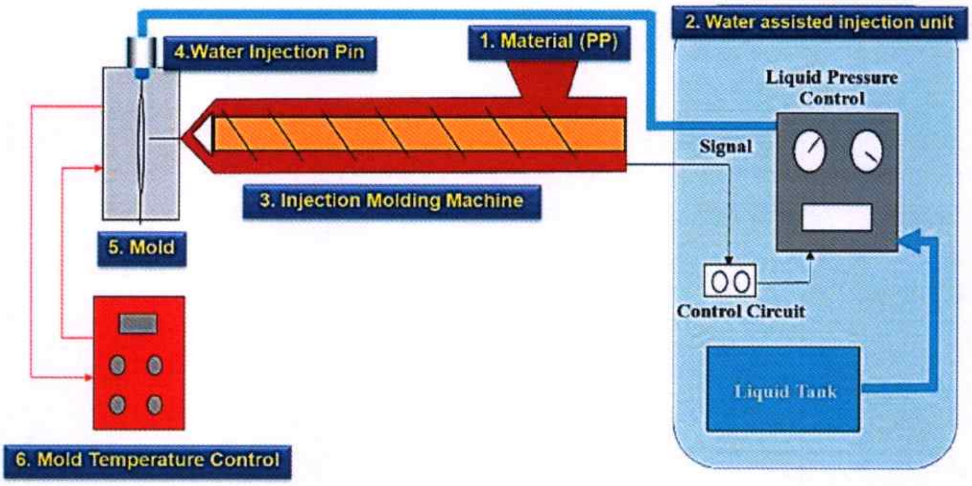

Figure 3.2 Schematically, the setup for water-assisted injection-molding

3.2.2 Water Injection Pin

Type of water pin design was developed in MTEC lab: Figure 3.3 shows the dimensions of the water injection pin used in this study. The water injection pin has a small orifice at the side of the end of pin body.

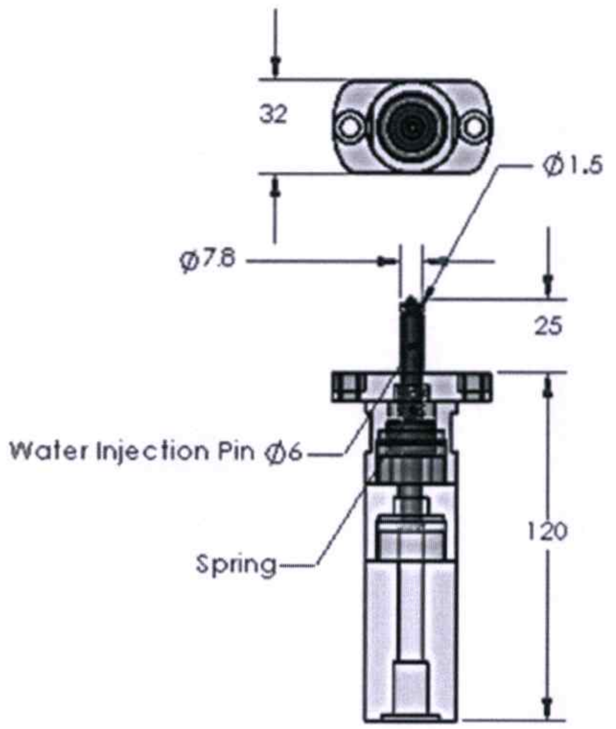

Figure 3.3 Structure and dimensions of injection water pin (unit: mm)

3.2.3 Injection Molding Machine and Mold

Water assisted injection molding experiments were conducted on a 228-ton conventional injection-molding machine. The specification of injection molding machine is show in appendix A. The mold cavity that is tubular with diameter of 17 mm. and a flow length of 150 mm. The overflow geometry is a haft of cone. Seven sets of molds for cavity with different corner angle (0°, 15°, 30°, 45°, 60°, 75° and 90°) by changing the moving inserts and additional geometric features by include thin walled mounting brackets The typical geometry of the cavity in the mold construction for the experiment is shown in Figure 3.4 and Figure 3.5 shows the dimensions and the detailed structure of mold cavity includes the exchangeable mold inserts. The mold was installed with water pin at underneath the parts. The temperature of mold was regulated by a water-circulating mold temperature control unit.

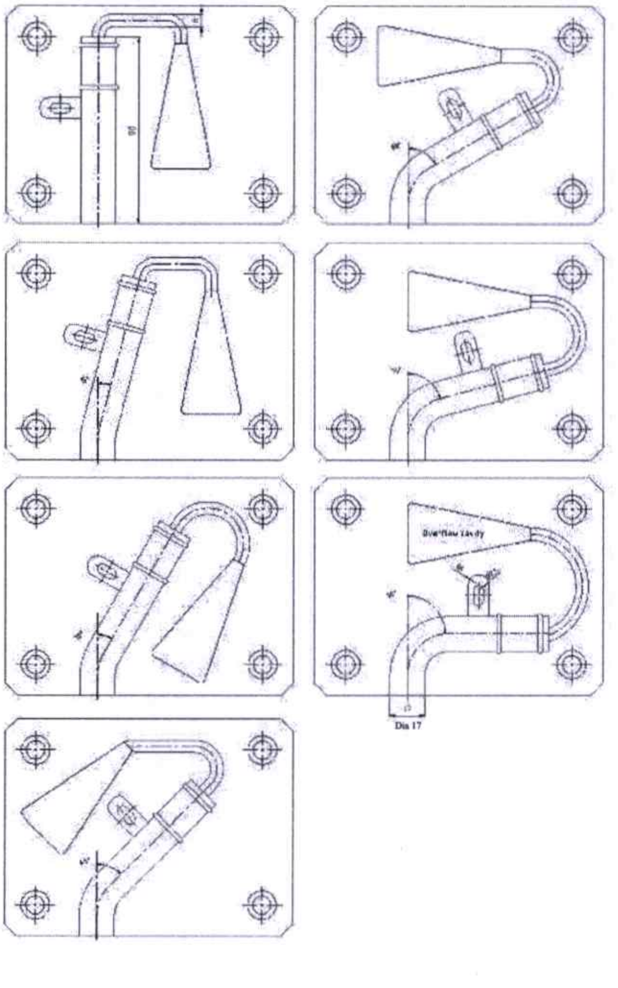

Figure 3.4 Seven sets exchangeable mold inserts for cavity with different corner angle by 15 degree

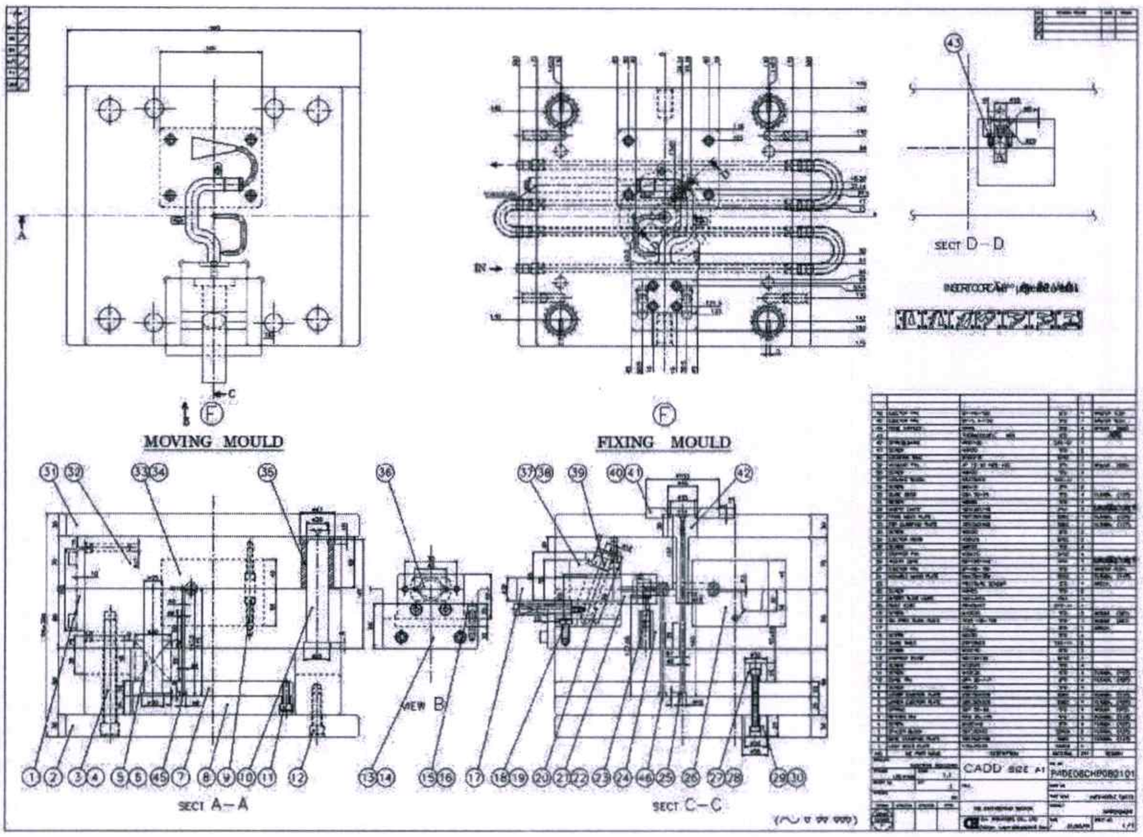

Figure 3.5 Layout and dimensions of mold cavity

3.2.4 Water assisted injection unit

A lab scale water injection unit developed earlier in National Metal and Materials Technology Center of Thailand (MTEC) laboratory was used for all experiments. During experiment, the control circuit of the water injection unit received a signal from the molding machine and controlled the time and pressure of injected water.

3.3 Process Parameter

The water assisted injection molding cycle can be divided into several, which partly overlap one another as following sequence of phases in Figure. 3.6 The process parameters chosen were listed in Table 3.3. They were chosen based on material and equipment supplier's recommended processing ranges. When one parameter was varied the other parameters were kept constant. Various processing variables were studied in terms of their influence on the residual wall thickness of molded parts: melt temperature, mold temperature, water pressure, water injection delay time, hold time and overflow process without shut off were molded for this study. After the molding process had stabilized, three parts were examined for each.

Table 3.3 The processing variable as well as the values used for molding in the experiments

Melt temp (°C)	Mold temp (°C)	Water pressure (bar)	Water injection delay time (sec)	Water hold time (sec)
190	40	120	1	**10**
200	**50**	**150**	**3**	15
210	60	180	5	20
220	70	210	7	25

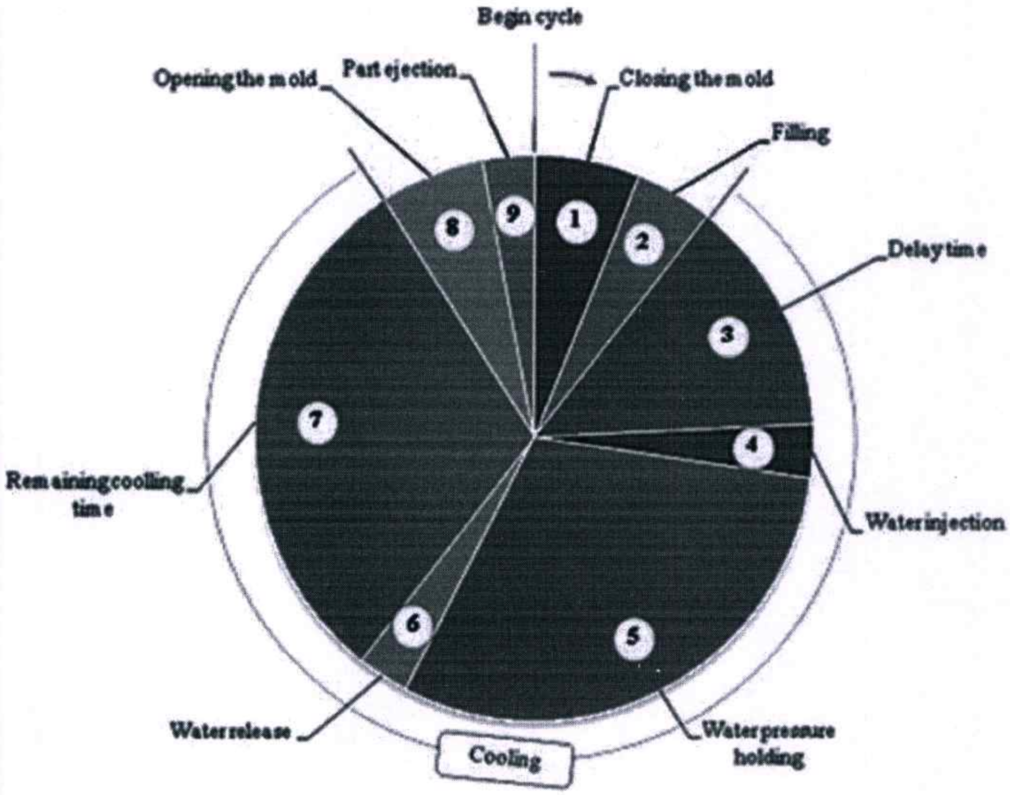

Figure 3.6 Water assisted injection molding cycle

3.4 Injection molding process

This study used WAIM technique of overflow without shut off. The advancetage of overflow process can eliminate the switch over mark from the final product by moving the position of plastic melt front at the end of the product. Then, injected water will push the melt into the overflow cavity. Delay time was not effect and was not obvious on the external surface of product. The process sequence is a follow (Figure 3.7):

- Injected melt to fill the mold
- Stop melt injection and inject water to push melt into over-flow cavity
- Maintain a water pressure during cooling – Release the water – demold

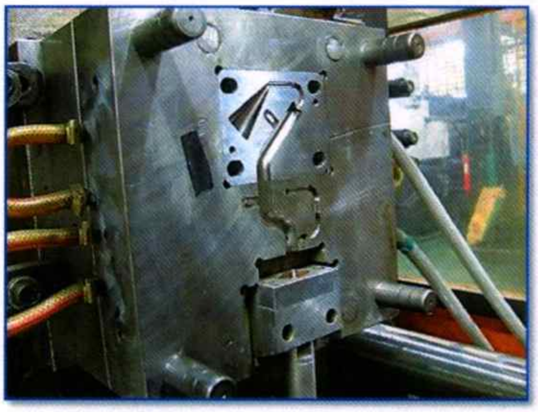

(a)

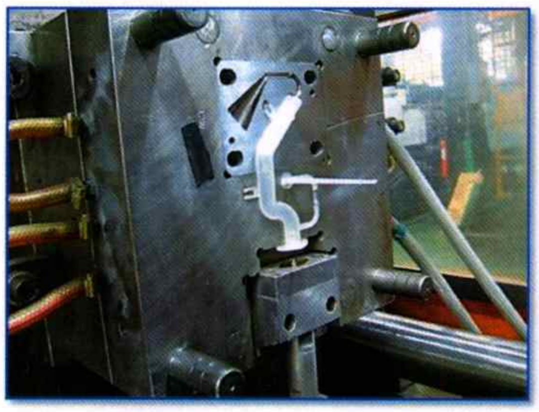

(b)

(c)

Figure 3.7 Overflow process without shut-off valve (a) Mold opening (b) Melt filling

(c) Product after injected and holding by water

3.5 Residual wall thickness distribution

3.5.1 Measurement of residual wall thickness.

After the tubes were water-assisted injection molded, the section at the center of corner tubes were sectioned and deburr the chips surrounding the sectioned parts as show in Figure 3.8. The images were then scanned into a computer an image analysis system was used to characterize the projected area of residual wall thickness. Each of samples would be measure in four sides comprising left, right, inner and outer sides as demonstrated in Figure 3.9.

Figure 3.8 The location of sectioned part for determining the residual wall thickness

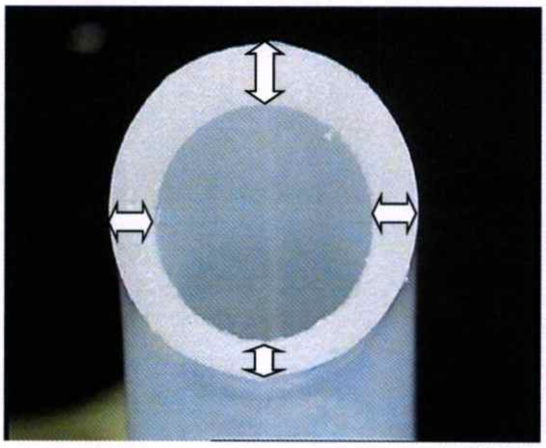

Figure 3.9 Four sides of measuring the RWT

3.5.2 Measurement of hollow core ratio and the percentage difference of the residual wall thickness.

Proporation relation between part channel and core out channel after molded. The variation of the hollowed core ratio of water- assisted injection molded parts was measured and calculated according to the following:

$$\text{Hollowed core ratio} = (A_{bubble} \ / \ A_{channel})*100$$

Where $A_{channel}$ is the cross-section area channel, and A_{bubble} is the area of the water bubble in molded parts. In addition, to understand the thickness uniformity of molded tubes, the percentage difference of the residual wall thickness is defined as:

$$\text{Difference (\%)} = (\text{outer wall thickness} - \text{inner wall thickness}) / \text{average thickness}*100$$

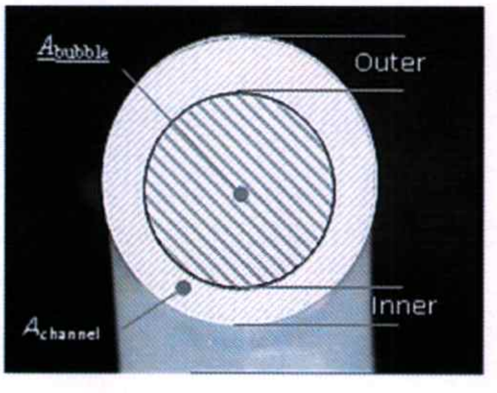

Figure 3.10 Cross section of area channel

3. 6 Physical properties

3.6.1 Inner surface roughness

Pressure drop during internal flow is one of the most important considerations in designing a fluid flow system. Surface roughness was identfied as an important parameter in fluid flow as early as in the nineteenth century by Darcy [31]

The surface roughness analysis was performed with Surftest SV-3000 as showed in Figure 3.11. The most common parameter for surface texture is arithmetical mean roughness (Ra). Ra is calculated by an algorithm that measures the average length between the peaks and valleys and the deviation from the mean line on the entire surface within the sampling length (Figure 3.12) according to Equation (3.1). Rz is common parameter for roughness is Mean Roughness depth (Rz). Rz is calculated by measuring the vertical distance from the highest peak to the lowest valley within five sampling lengths (Figure 3.13), then averaging these distances. Rz averages only the five highest peaks and the five deepest valleys, therefore, extremes have a much greater influence on the final value according to Equation (3.2)

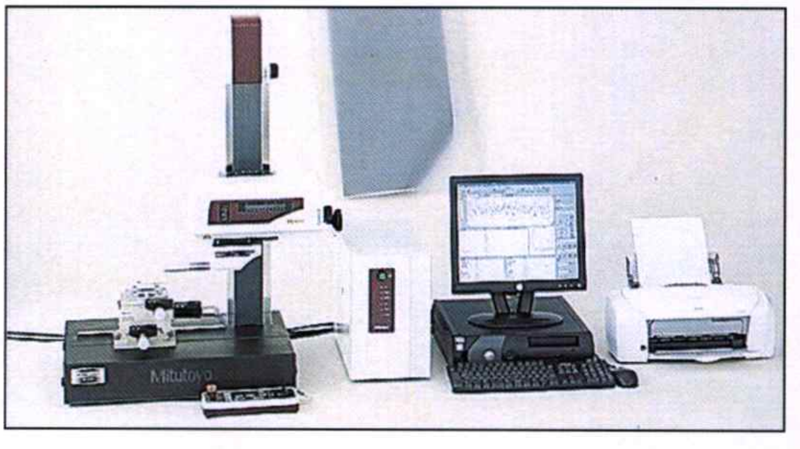

Figure 3.11 Surface roughness measuring machine (Surftest SV-3000)

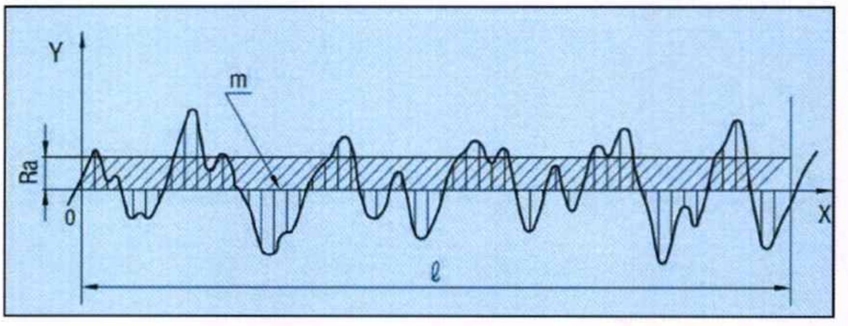

Figure 3.12 Ra Roughnesses Analytical Function

$$Ra = \frac{1}{\ell}\int_0^{\ell} |f(x)|\, dx \tag{3.1}$$

R_a is the arithmetic average deviation from the mean line within the assessment length (L)

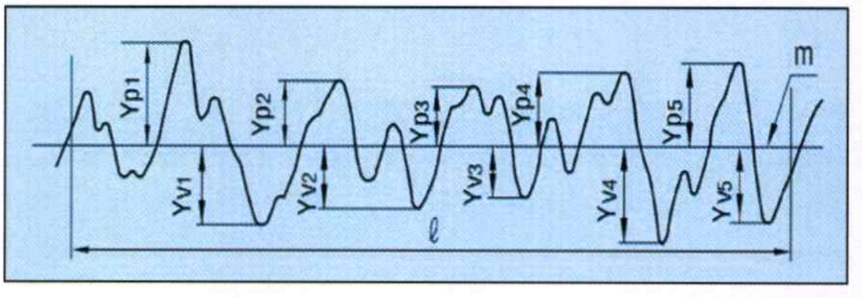

Figure 3.13 Rz Roughnesses Analytical Function

$$Rz = \frac{|Yp1+Yp2+Yp3+Yp4+Yp5| + |Yv1+Yv2+Yv3+Yv4+Yv5|}{5} \tag{3.2}$$

Yp1, Yp2, Yp3, Yp4, and Yp5: Tallest 5 peaks within sample.

Yv1, Yv2, Yv3, Yv4 and Yv5 : Lowest 5 peaks within sample.

3.6.2 Switch over mark observed

The switchover point from resin injection to water injection may cause hesitation marks on the surface of the part so call "switch over mark". Due to hesitation marks on the surface of the molding due to the stop of the melt flow during the polymer-to-water switch-over as showed in Figure 3.14 The stagnation of the already injected plastic before new acceleration through the water can lead to visible surface defects as showed in the Figure 3.15. The profile of surface on marked area was tracing the line into a computer and measurement analysis system was used to measuring the length and depth for the characterization of surface quality.

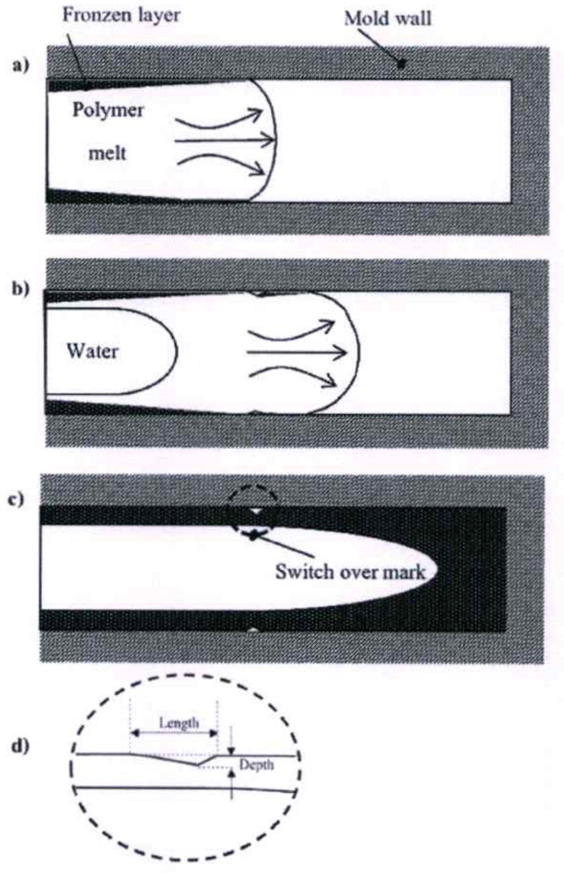

Figure 3.14 Consecutive steps of water-assisted injection moulding process,

(a) after injection phase, (b) during water injection phase, (c) during water holding pressure phase (d) characterize the length and the depth on switch over mark surface

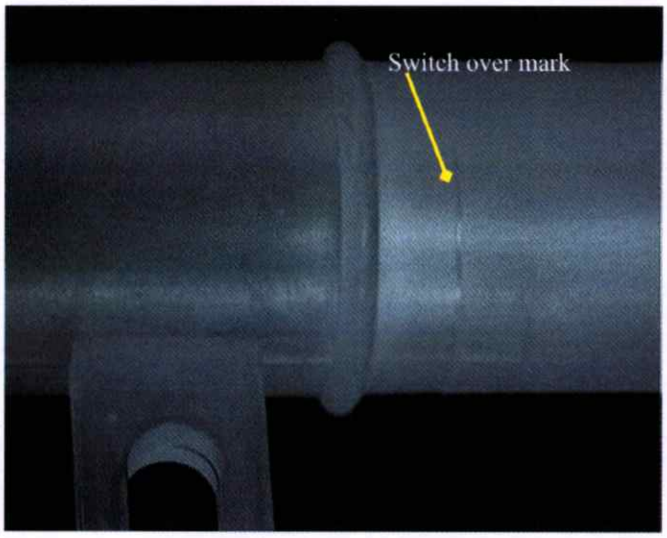

Figure 3.15 Visible surface defect of switch over mark as molded by Short-shot process of WAIM

The switch over mark observation was performed with Formtracer SV-C3000 as showed in Figure 3.16 and the workpiece set up showed in Figure 3.17.

Figure 3.16 Contour measuring machines (Fromtracer SV-C3100)

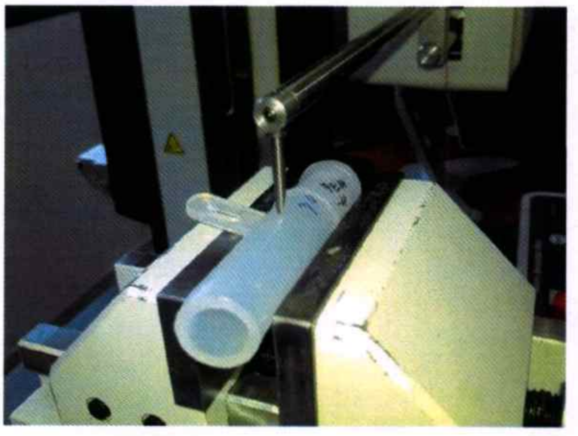

Figure 3.17 workpiece set up condition

3.6.3 Stiffness

The stiffness parameter is essential in the design or the analysis of any plastic pipe installation and is closely related to material properties and is an important design parameter. [33] Parallel-plate loading mechanism (ASTM D2412 standard test method) was used for investigating the pipe stiffness values. In this experiment, Stiffness test were performed on speciments obtained from the water assisted injection mold parts (See Figure 3.18). The dimensions of specimens for the experiments were 25.4 mm. of length. Stiffness test were performed in a Universal Testing Machine in Figure 3.19 (Instron Model 3382) and compress the specimen at the constant rate of 12.5 mm./min.

Calculate the stiffness, PS, for any given defection as follows:

$$PS = F/\Delta y \tag{3.3}$$

Where F = the load applied to the pipe (N/mm)

Δy = measured change of the inside diameter (mm)

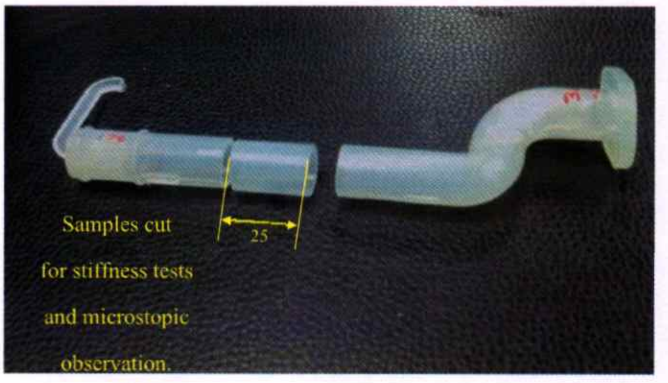

Figure 3.18 Schematicallly, the positioning of the samples cut from the molded parts for stiffness tests

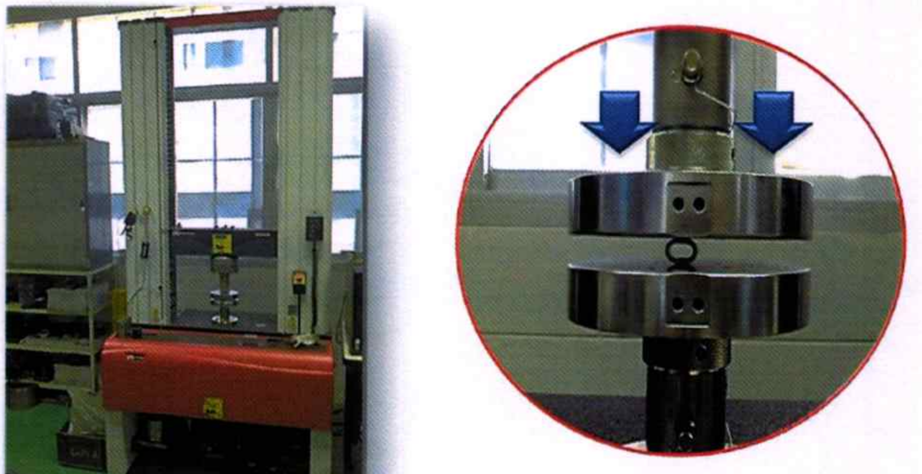

Figure 3.19 The universal testing machine Instron Model 3382

3.6.4. Microstopic observation

Struction observations were done with the use of Polarizing microscope NIKON Eclipse LV100 POL (Figure 3.20 (a)) on surface of the samples cut from the parts, from the region with the water channel. Then microtomed slices were taken out of the parts in order to investigate the structure of the parts. The microtome (Figure 3.20 (b)) used for preparation the slices with thickness of 0.014 mm. The slices were put between two glasses and observed at Nikon Eclipse LV100 microscope in polarized light.

(a) (b)

Figure 3.20 (a) NIKON Eclipse LV100 POL Polarizing Microscope

(b) Semi-automated Rotary Microtome Leica RM2245

CHAPTER 4

RESULTS AND DISCUSSION

The effect of part geometries, process variables and material properties can be devided into five aspects: (1) residual wall thickness distribution (2) Inner surface roughness observation (3) switch over mark on ourter surface observation (4) stiffness and (5) microstopic observation.

4.1 Residual wall thickness distribution.

4.1.1 The effect of curve corner angle.

According to Figure 4.1, the relationship between the inner residual wall thickness and the shear rate at the inner sharp corner is shown. Moreover 7 different of sharp coner angle geometries in step of 15 degree are compared. The shears were obtained from the apparent values reported by the software. The simulation results were showed the maximum shear rate is located in the inner wall of sharp corner as shows in Appendix F. The inner RWT showed the highest value of 2.47, 2.42, 2.32, 2.15, 2.07, and 1.94 mm. for at the shear rate on the inner wall of 34.12, 37.9, 39.74 40.91, 42.14 and 44.46 sec^{-1}, respectively. From their results showed that increasing the sharp corner angle, increased the magnitude of the shear rate and relative with shear thinning power-law fluids, the viscosity decreases with increased shear rate. Because of the model of shear thinning is the power-law model. This states that the viscosity is proportional to the shear rate ($\eta \propto \dot{\gamma}$). And from the simulation result reported that increases the sharp corner angle increases the shear rater at inner wall ($\theta \propto {}_{inner}\dot{\gamma}$). In additional, the experiment result suggested that increases the sharp corner angle decreases the inner RWT. These representatives can be obtained as

$$\text{Inner RWT} \propto \eta \propto \frac{1}{\theta} \propto \frac{1}{inner\,\dot{\gamma}}$$

The relationship between sharp corner angle and inner wall shear rate, higher shear rate caused the melt viscosity and the flow resistance to decrease. With low flow resistance which was higher near the inner wall, result in the inner residual wall thickness was thinner than the outer wall.

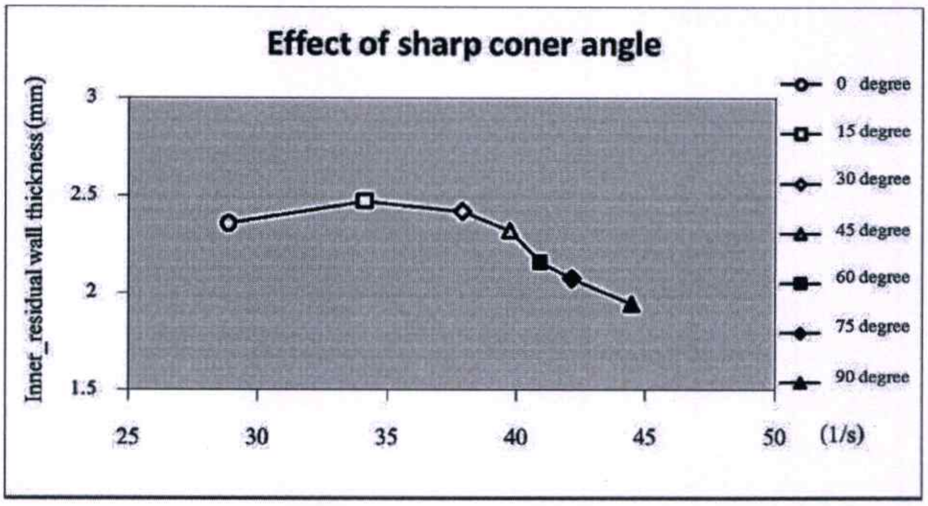

Figure 4.1 inner residual wall thicknesses versus inner wall shear rate

4.1.2 The effect of melt flow index

Melt flow index (MFI) is a measure of the ability of the material's melt to flow under pressure. Melt flow rate is inversely proportional to viscosity of the melt at the conditions of the test. Flow of the plastic in the mold is quite important to ensure adequate fill in cavities. Typically, viscosity decreases with increasing shear so that design of the mold geometry can be used to optimize the flow. In this study, the virgin polypropylene (PP) was employed in order to investigate the effect of melt flow property. In the case of a tube cavity with a diameter of 17 mm. and sharp corner angle at 45 degree was used. Three grade of melt flow rate, ranging from 4, 7.5 and 22 gram per 10 miniute were injected with melt temperature 200 °C and filling time is 2.5 sec. with the estimate volume flow of 10000 mm^3/sec., the mold temperature was set at 50 °C, the mold cavity is filled with the polymer melt and then the water injection pressure of 15 Mpa with delay time used was 3 seconds and the water holding time set at 10 seconds. The Figure 4.2 and 4.3 showns the effect of melt flow properties on the inner and outer residual wall thickness, the result showed that the 22-MFI parts had the inner RWT thinner than the 4-MFI and 7.5-MFI. Because of the melt resistance is lower viscosity. Water has higher viscosity and incompressibility. It seeks the path of least resistance and makes a "short-cut" at corner of molded part. On the other hand, the difference percentage between inner and outer wall thickness were increased with increased the melt flow index as showed in Figure 4.4. On the contrary, the hollow core ratio of molded part decreases accordingly (Figure 4.5) with increased the melt flow index.

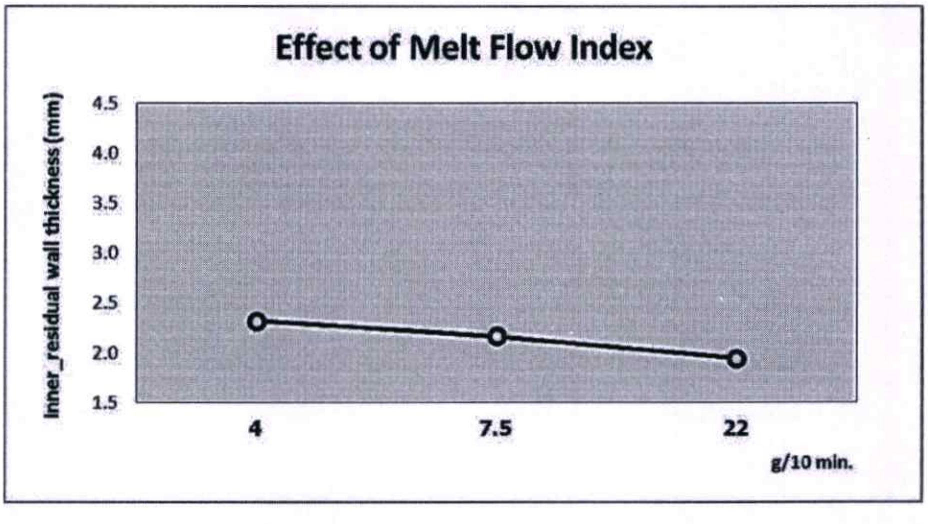

Figure 4.2 Effect of melt flow index on inner residual wall thickness, 45° curve corner angle

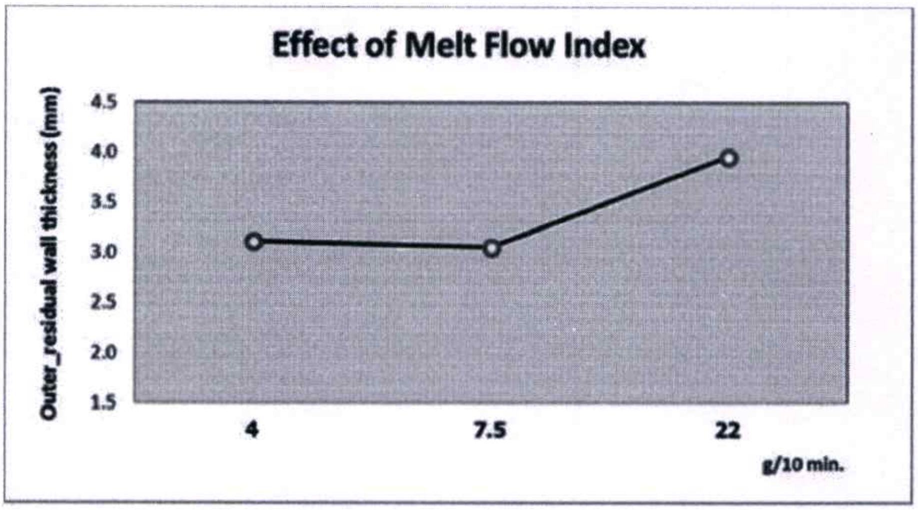

Figure 4.3 Effect of melt flow index on outer residual wall thickness, 45° curve corner angle

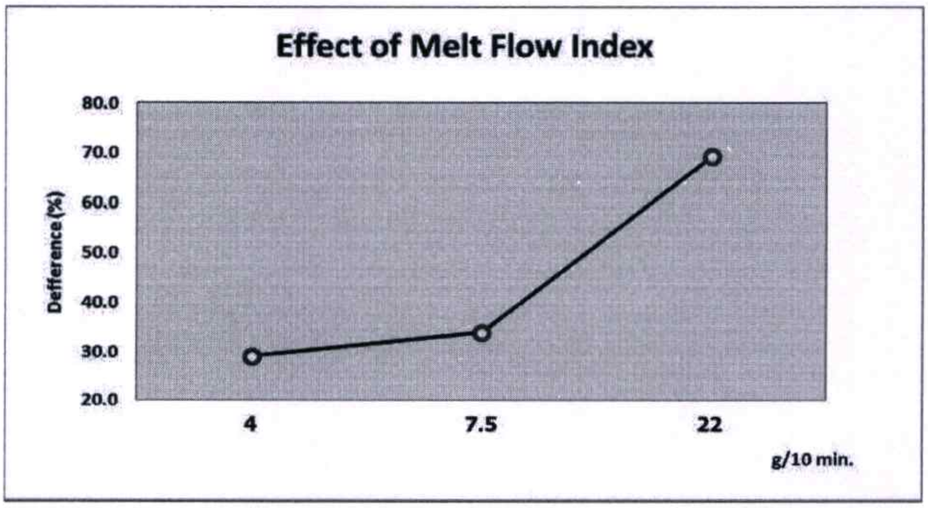

Figure 4.4 Effect of melt flow index on the difference percentage

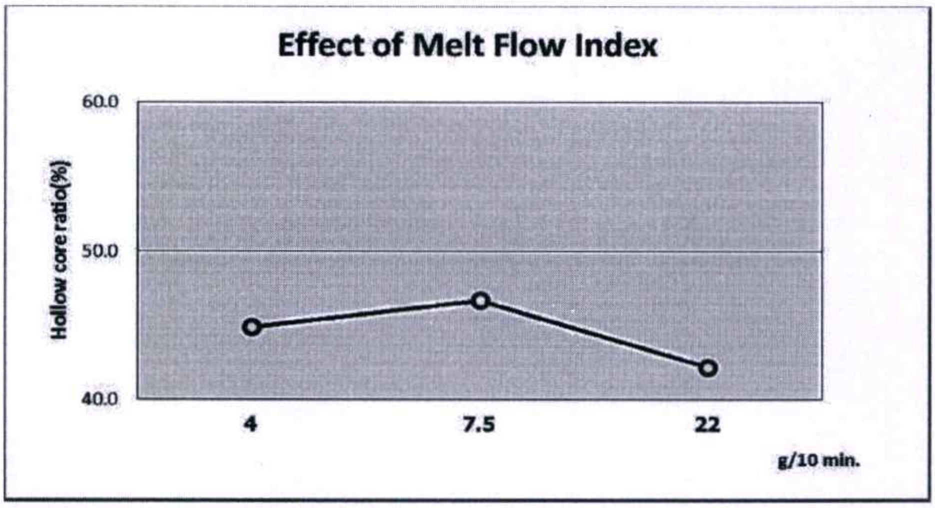

Figure 4.5 Effect of melt flow index on hollow core ratio

4.1.2 The effect of melt temperature

Melt Temperature is the temperature of the cylinder of the machine which determines the temperature of the material that will be injected into the mold. In this research found that the inner RWT was dropped continuously with increasing melt temperature.

According to Figure 4.6 and 4.7, in the straight molded tube part, the result shows that the RWT was dropped continuously with increasing the melt temperature. All the inner RWT of straight molded tube parts showed the lowest valve worth 2.56, 2.48, 2.35 and 2.31 mm. for at with melt temperature 190, 200, 210 and 220 °C, respectively. In opposite side, all the outer RWT showed the highest valve of thickness 2.78, 2.71, 2.6 and 2.53 mm. respectively. From their result of rheological properties, increasing melt temperature led to decrease in elogational and slight decrease in shear viscosity. The impact of melt temperature on the inner RWT of the shape corner angle at 15 degree and 30 degree, the inner RWT were slightly decreased, while the inner RWT were obviously decreased for the shape corner angle at 45 degree, 60 degree, 75 degree and 90 degree respectively. On the contrary, the outer RWT were slightly increased on the molded parts of sharp corner angle at at 15 degree and 30 degree., Meanwhile, for the shape corner angle at 45 degree, 60 degree, 75 degree and 90 degree, the outer RWT of molded parts were obviously increased regarding with simulation result.

On the other hand, the residual wall distribution were not uniform as showed in Figure 4.8 and the measurement result as showed in Figure 4.9, the RWT difference percentage can be estimated about 8.4% – 9.6% with melt temperature,190–220 °C by increasing in step of 10 °C.

The hollow core ratio of molded part decreases accordingly (Figure 4.10) with increased the melt temperature as well as the viscosity of the materials. It is thus not difficult for water to push the melt forward to overflow cavity for the molding of sharp corner angle 0 degree (straight shape), 15 degree and 30 degree molded parts. Meanwhile, for the shape corner angle from 45 degree to 90 degree, the hollowed core ratios were slightly decreased. The impact of corner angle, the corner angle lower than 45 degree, increased the corner angle decreased the hollowed core ratio. But for the corner angle more than 45 degree, increased the corner angle increased the hollowed core ratio.

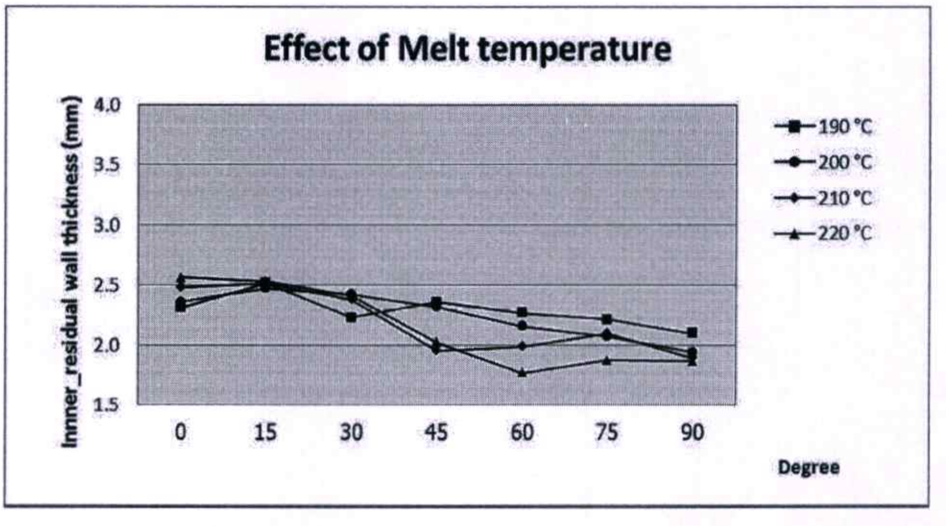

Figure 4.6 Effect of melt temperature on inner residual wall thickness

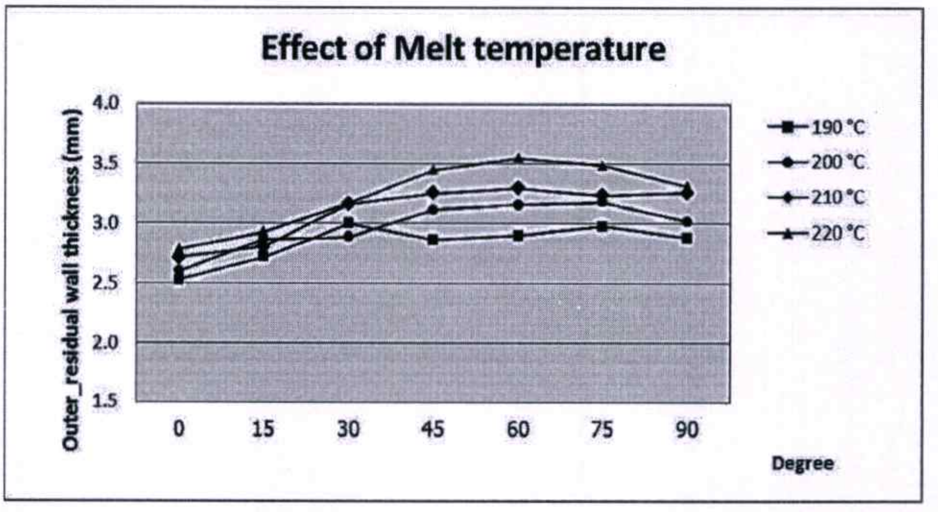

Figure 4.7 Effect of melt temperature on outer residual wall thickness

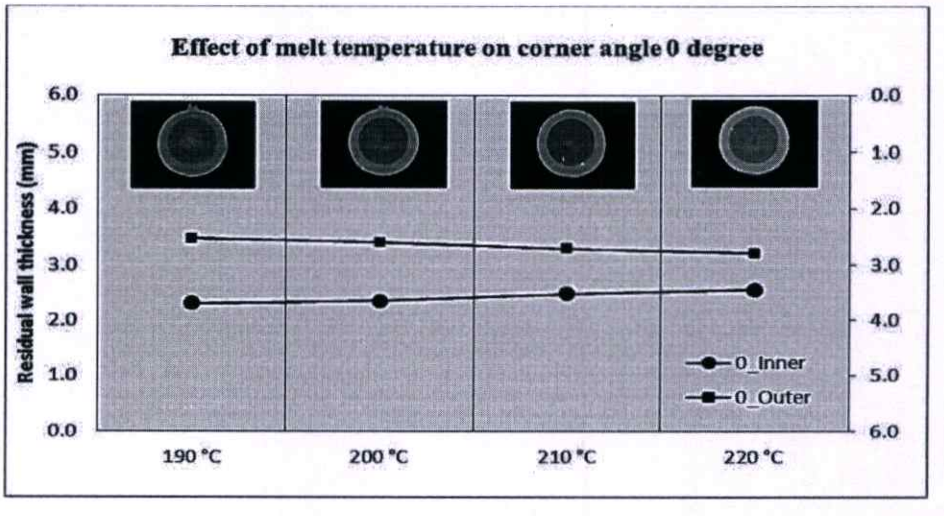

Figure 4.8 Effect of melt temperature on the inner RWT and the outer RWT of mold parts with sharp corner angle 0 degree

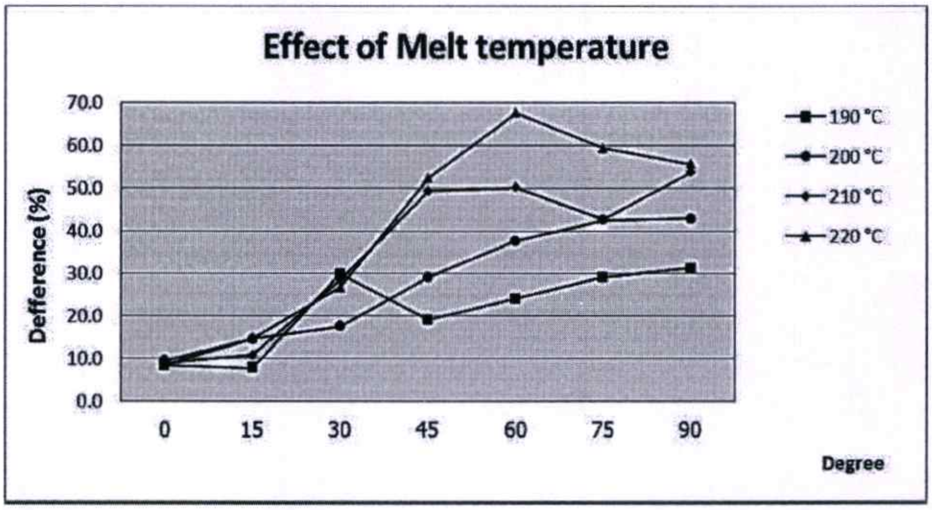

Figure 4.9 Effect of melt temperature on the difference percentage

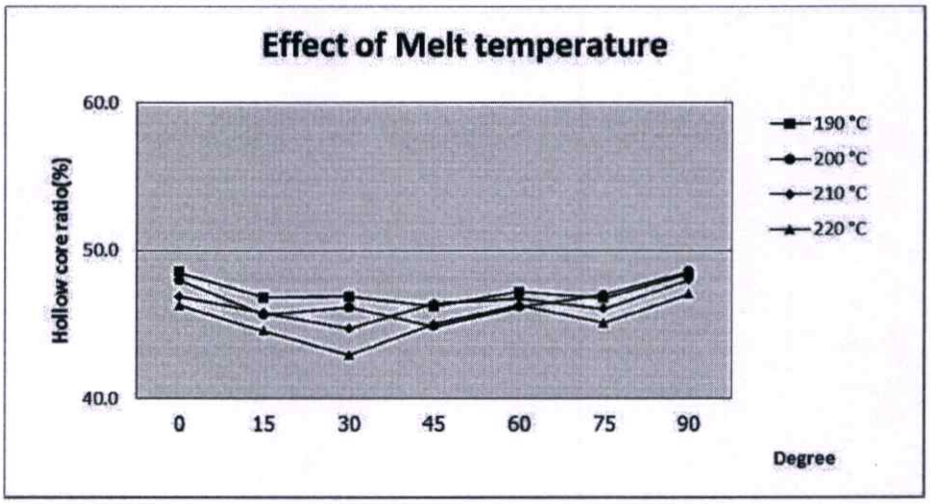

Figure 4.10 Effect of melt temperature on hollow core ratio

4.1.3 The effect of mold temperature.

The benefit of using higher mold temperature in the process is to improve the hesitation mark [32] in gas assisted injection molding and water-assisted injection molding. In the study the polymer grade with 4-MFI was used for the material, which were injected with the same melt temperature of 200°C. The mold temperatures were ranging from 40 °C to 70 °C by increasing in step of 10 °C. The effect of the mold temperature variation on the inner and outer residual wall thickness distribution are shown in Figure 4.11, 4.12 and 4.13. It was found that the effect of the mold temperature does not lead to major significant changes in residual wall thickness distribution and the result of their trendency are similar to the result of item 4.2 at melt temperatue of 200°C. Because only the local melt temperature near the wall was affected by the mold temperature. The RWT difference percentage increased with corner angle increased as showed in Figure 4.14. Because of shear rate at the inner wall as discussed in item of effected from the sharp corner angle.

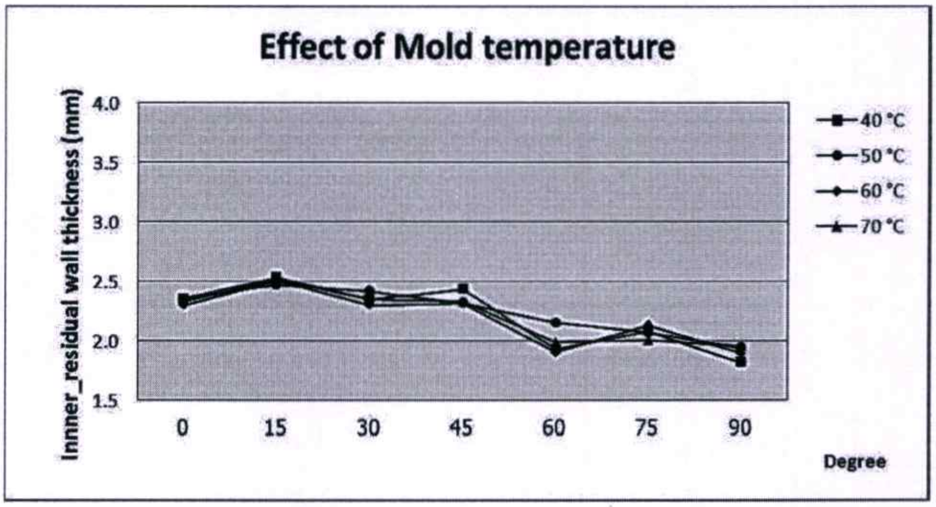

Figure 4.11 Effect of mold temperature on inner residual wall thickness

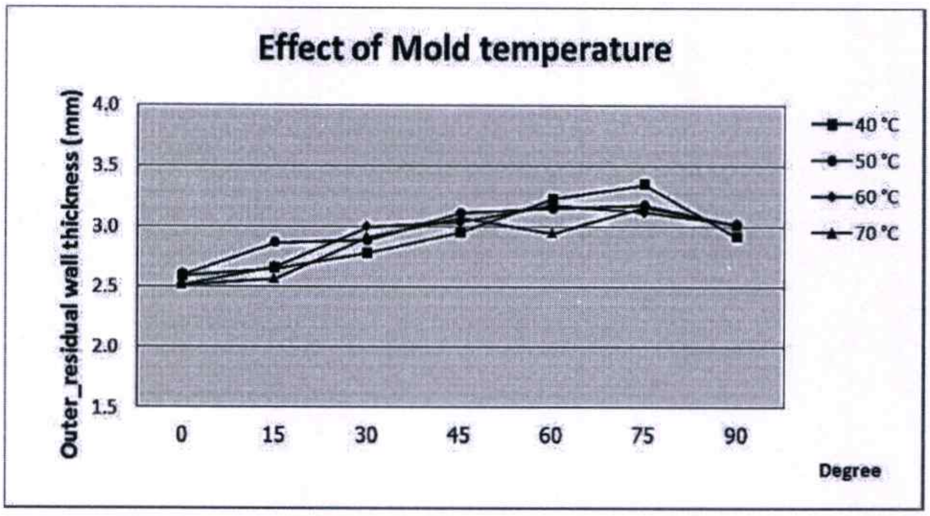

Figure 4.12 Effect of mold temperature on outer residual wall thickness

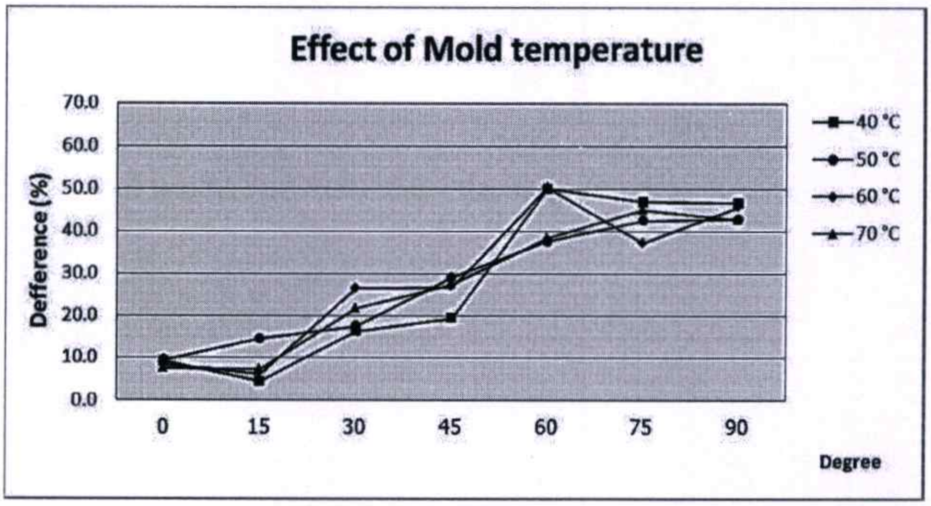

Figure 4.13 Effect of mold temperature on the difference percentage

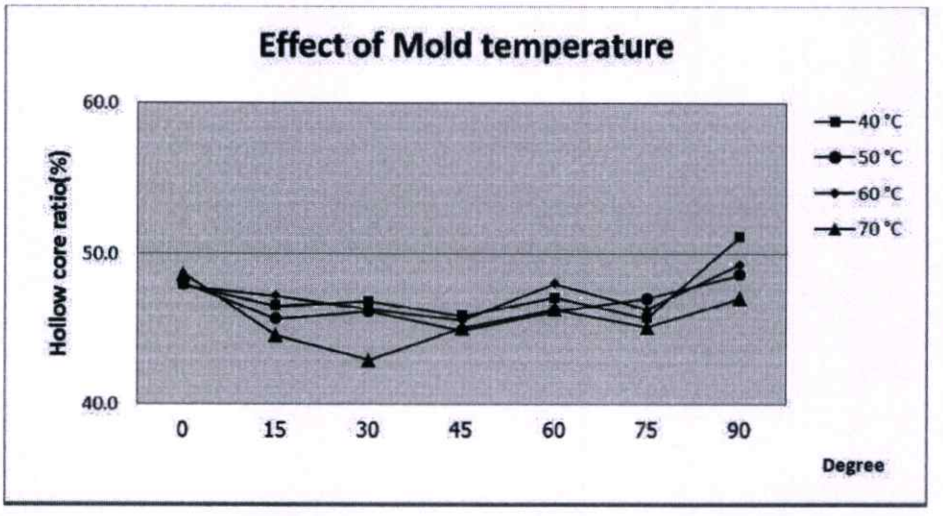

Figure 4.14 Effect of mold temperature on hollow core ratio

4.1.4 The effect of water delay time.

Water delay time is the most important parameter having effecting on residual wall thickness distribution and having been examined by many researchers. Liu and Chen [5] and investigated the influence of processing parameter in the WAIM process. Liu et al. [21] and Liu and Shih [31] looked into the effect of thermoplastic composites material and process parameter on this technique. Liu et al. [8] and Liu et al. [9] reported some useful qualitative statements concerning the influence of process parameters on plastic tube with dimensional transitions by WAIM.

An increase of water delay time caused the cooling time of the polymer melt to increase. Therefore, the increase of the water delay time parameter was correlated with a decrease of melt temperature. A short water delay time resulted in a high melt temperature, which caused the melt viscosity and flow resistance to decrease as well. In the other hand, increased the water delay time increased the cooling time as well as the solidifying layer of polymer melt in the water channel. Figure 4.15 and Figure 4.16 showed that the inner RWT and the outer RWT increased as the delay time increased. Figure 4.17 showed the difference between inner RWT and outer RWT, increased the corner angle, increased the percentage difference of inner RWT and Outer RWT. The measurement results in the Figure 4.18 can be divided into 2 groups which corner angle lowers than 45 degree and more than 45 degree. The group of corner angle are lower than 45 degree, increased the corner angle decreased the hollow core ratio. The opposite side, the group of corner angle are more than 45 degree, increased the corner angle from 45 degree increased the hollow core ratio as well.

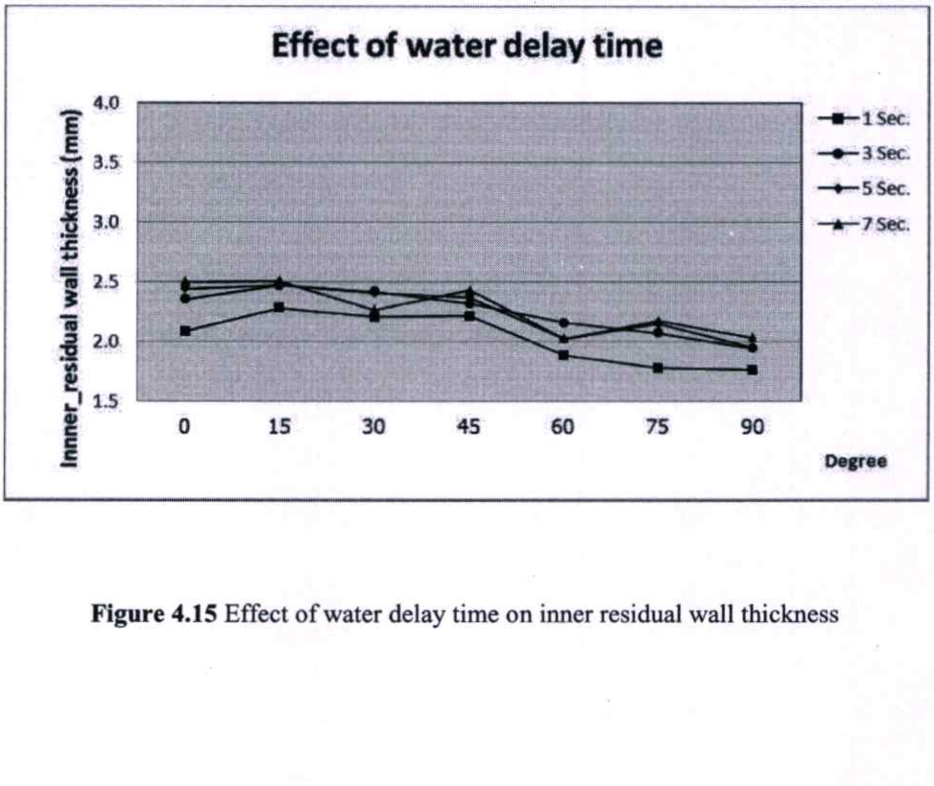

Figure 4.15 Effect of water delay time on inner residual wall thickness

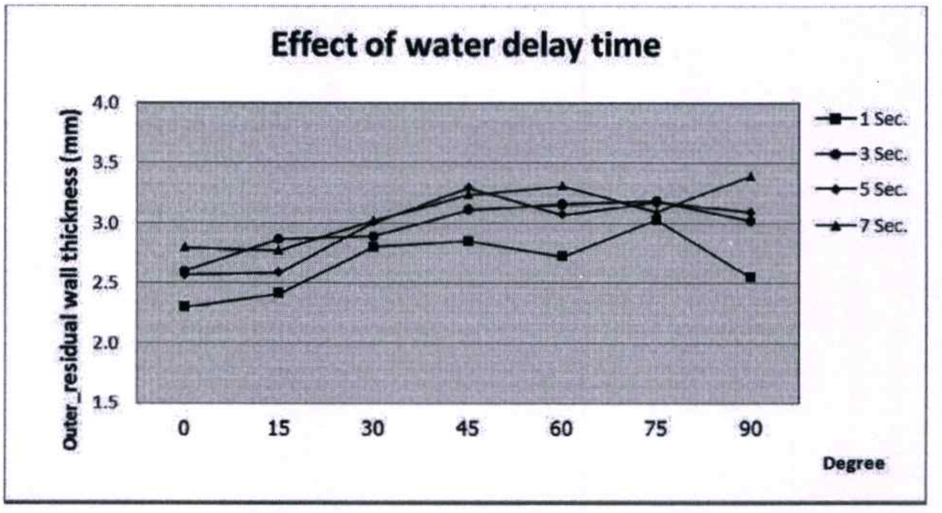

Figure 4.16 Effect of water delay time on outer residual wall thickness

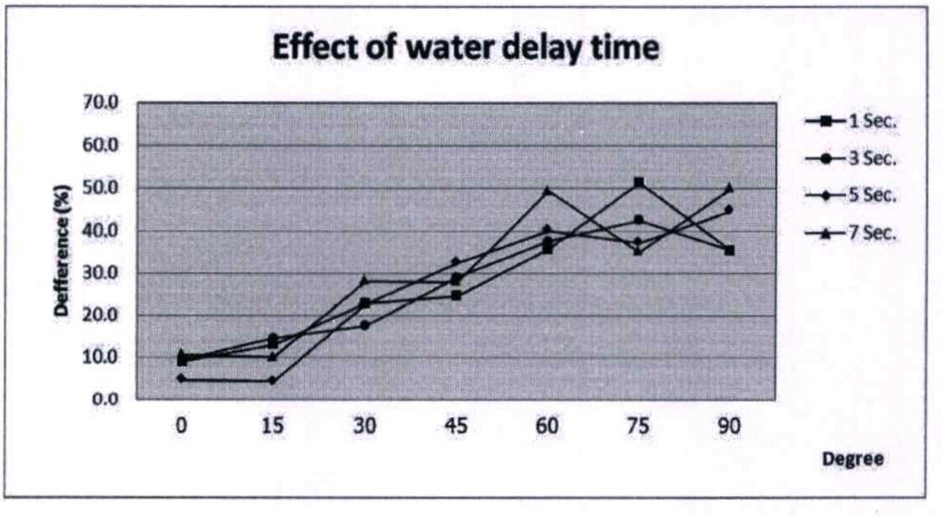

Figure 4.17 Effect of water delay time on the difference percentage

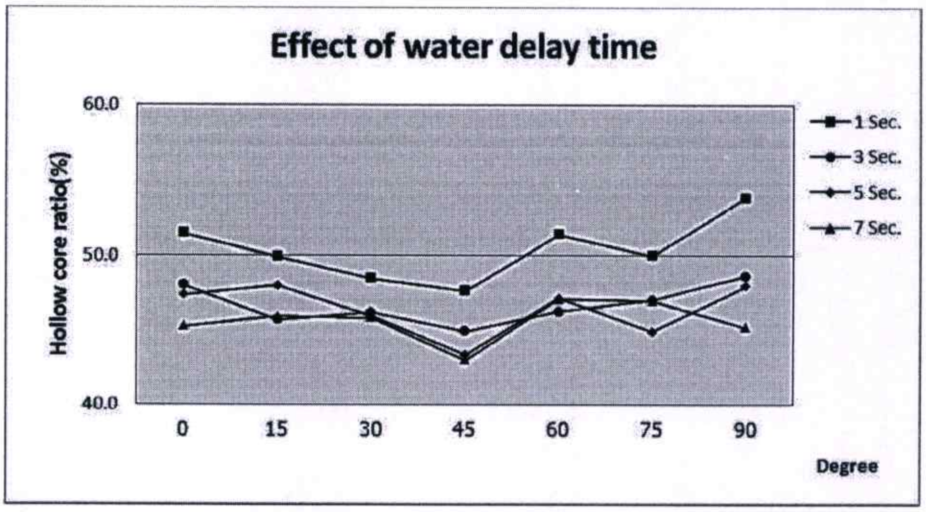

Figure 4.18 Effect of water delay time on hollow core ratio

4.1.5 The effect of water pressure

Water pressure is pressure of water injecting from the water injection unit. In the study the polymer grade with 4-MFI was used for the material, which were injected with the same melt temperature of 200°C. The water pressures start at 120 bars until 210 bars respectively by increasing in step of 30 bars. The effect of the water pressure variation on the inner and outer residual wall thickness distribution are shown in Figure 4.19 and Figure 4.20, from the results it obviously seems that, when the water pressure increases, then the residual wall thickness decreases for all of molded parts. Because the higher water pressure, it helps the water to overcome the viscosity of the polymer melt, the water has push against the mold wall and decreased the residual wall thickness distribution around of the sectioned channel. The difference of inner RWT and outer RWT were increased as well as the corner angle increased as showed in the Figure 4.21. Besides, from the Figure 4.22 the result of hollowed core ratio were showed similar trend with other varying parameters. The hollowed core ratiowere slightly decreased for the molding of parts as the corner angle lower than 45 degree. For the molding of corner angle more than 45 degree, it is seem smaller core ratio.

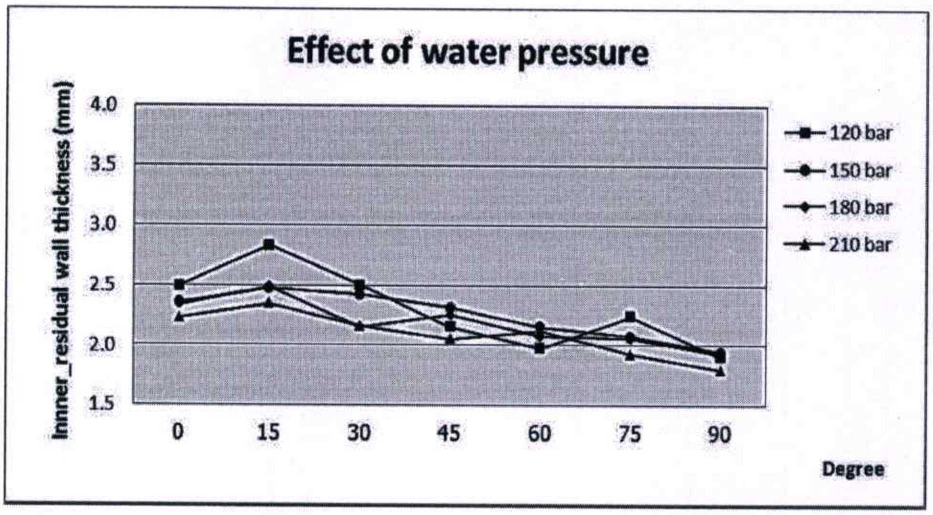

Figure 4.19 Effect of water pressure on inner residual wall thickness

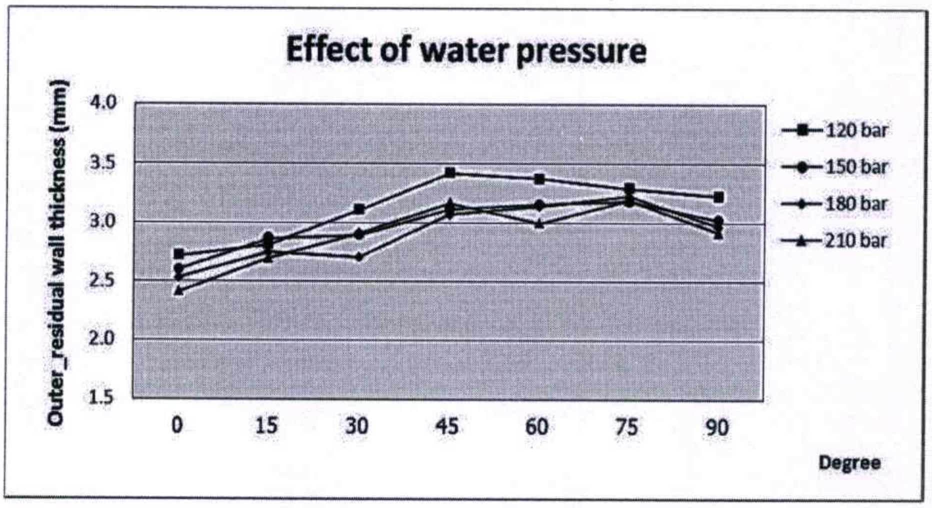

Figure 4.20 Effect of water pressure on outer residual wall thickness

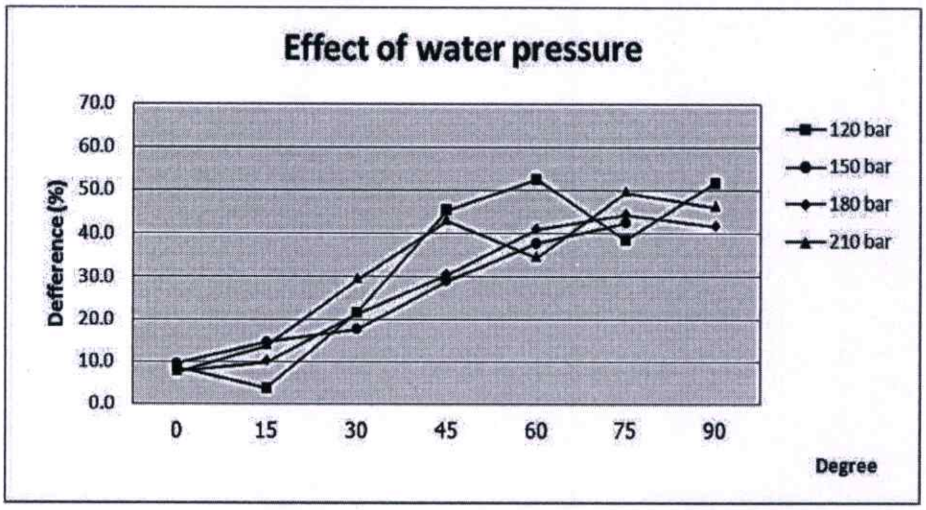

Figure 4.21 Effect of water pressure on the difference percentage

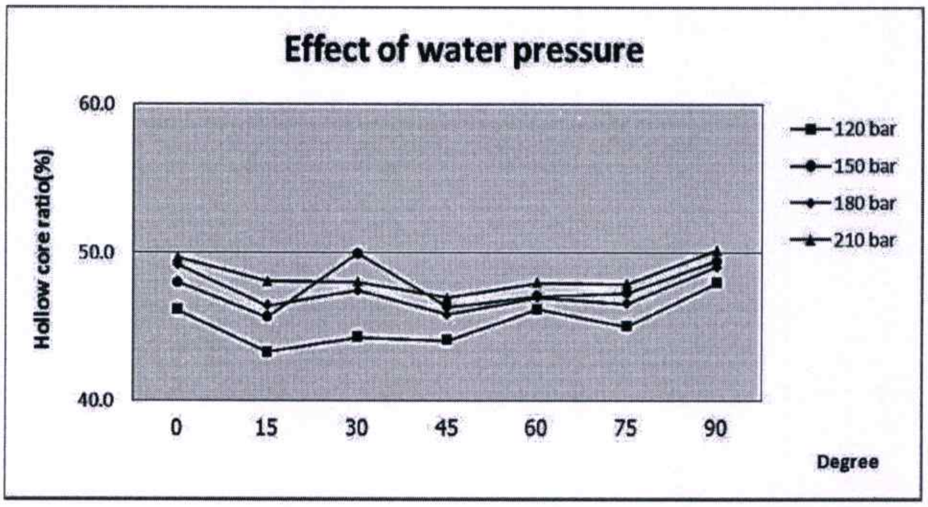

Figure 4.22 Effect of water pressure on hollow core ratio

4.1.6 The effect of water holding time.

The water holding pressure is applied in WAIM process for holding parts to compensate the volumetric shrinkage of molten material. The water holding time in WAIM process is similar with the holding pressure time in conventional injection molding process [5] . The study the water holding time start at 10 seconds until 25 seconds respectively by increasing in step of 5 seconds. Figure 4.23, 4.24 and 4.25, it was found that the effect of the water holding time were minor significant changes in the inner and outer residual wall thickness and then the difference between the inner RWT and out RWT were not obviously different. Increasing the water hold time slightly decreases the residual wall thickness, under the action of the water holding pressure, the volumatic contraction of melt due to cooling process is compensated [33]. According to Figure 4.26, the relationship between the water holding time and the hollowed core ratio is shown. Additional, at the water holding time of 10 seconds, the experiment results showed that the hollowed core ratio had the lowest value. On the other hand, at the water holding time of 25 seconds, the hollowed core ratio of molded increases accordingly.

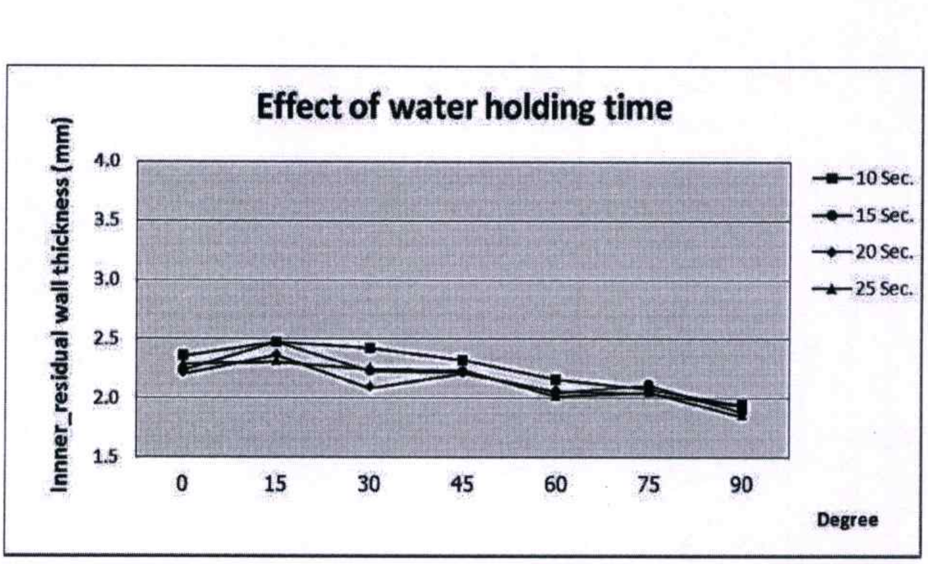

Figure 4.23 Effect of water holding time on inner residual wall thickness

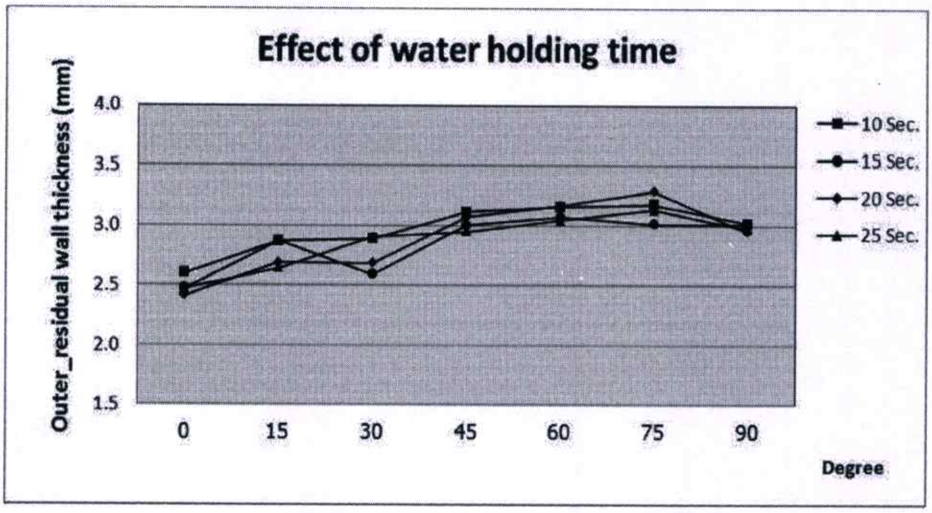

Figure 4.24 Effect of water holding time on outer residual wall thickness

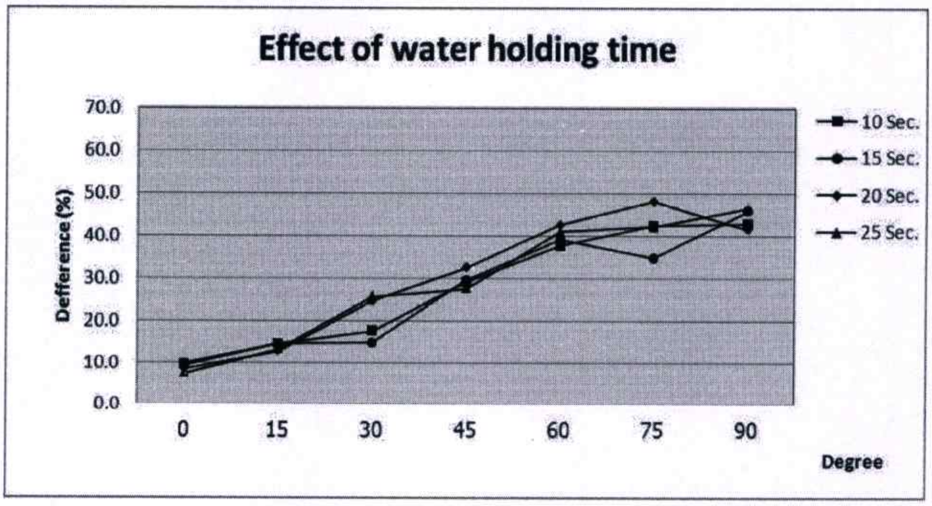

Figure 4.25 Effect of water holding time on the difference percentage

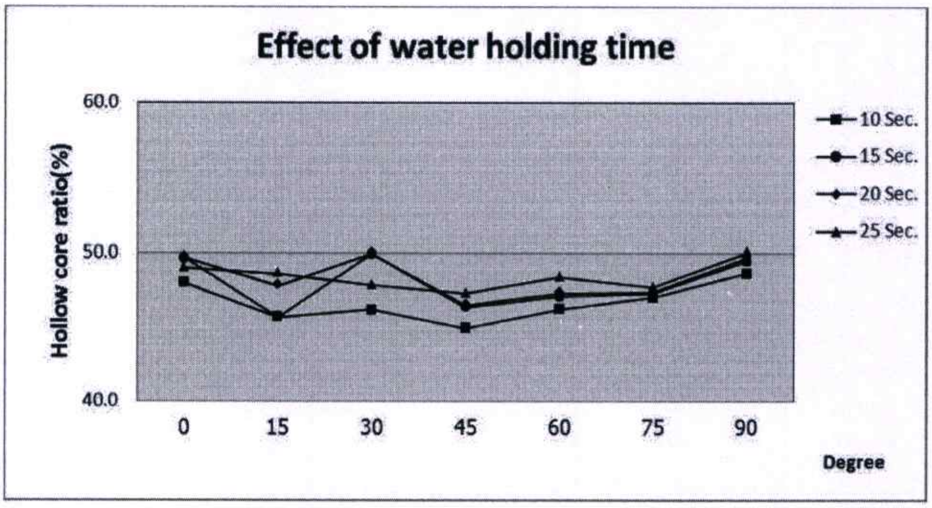

Figure 4.26 Effect of water holding time on hollow core ratio

4.2 Inner surface roughness comparison

The roughness measurements are represented by the roughness parameter Ra and Rz. The measurement length was 3.547 mm. and all of measurements are performed with the stylus tip and velocity. The result in Figure 4.27 presented the roughness parameter as the inner surface of molded tube by WAIM, original metal pipe and metal pipe by bending machine. It is observed that surface roughness of plastic tube by water assisted injection molding (Figure 4.28) is smoother than the original metal pipe (Figure 4.29) about 50%. Moreover, the surface roughness of metal pipe were increased with increasing for bending angle as showed in Figure 4.30 – 4.35.

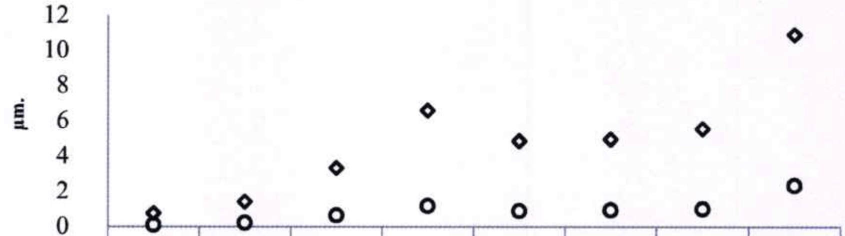

	WAIM molded part	Metal pipe_straight	Metal pipe_15°	Metal pipe_30°	Metal pipe_45°	Metal pipe_60°	Metal pipe_75°	Metal pipe_90°
○ Ra	0.101	0.227	0.643	1.186	0.898	0.953	1.013	2.353
◇ Rz	0.757	1.410	3.333	6.589	4.860	4.965	5.551	10.895

Figure 4.27 Inner surface roughness compairison of WAIM molded part, metal pipe and bending metal pipe

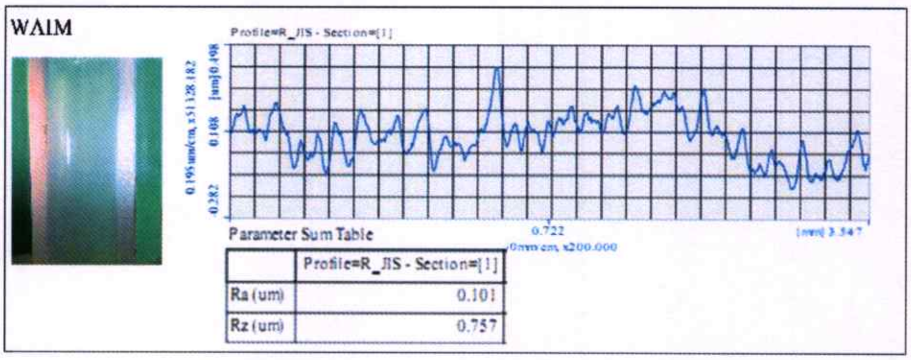

Figure 4.28 Line profile of the surface roughness for WAIM molded part

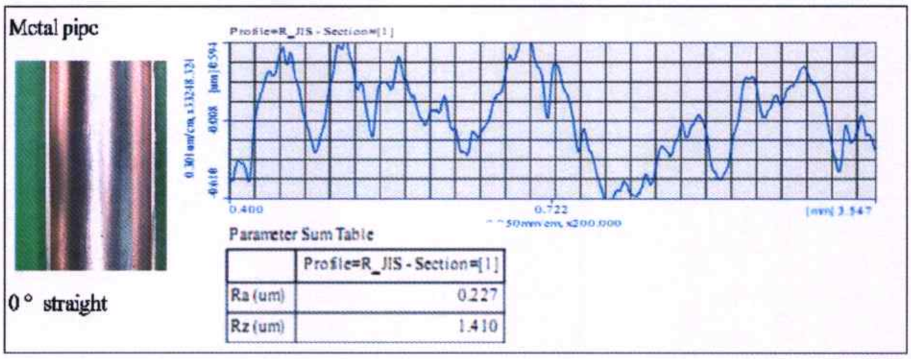

Figure 4.29 Line profile of the surface roughness for stainless steel (straight)

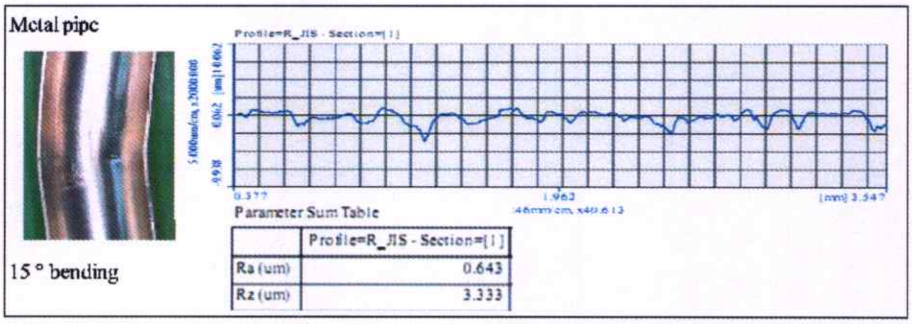

Figure 4.30 Line profile of the surface roughness for stainless steel with 15° bending angle

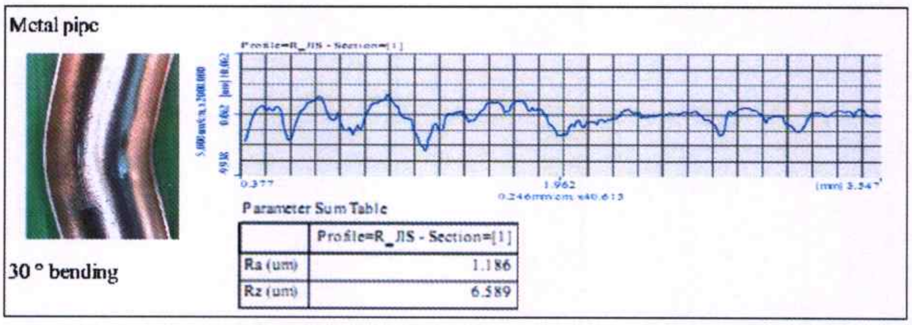

Figure 4.31 Line profile of the surface roughness for stainless steel with 30° bending angle

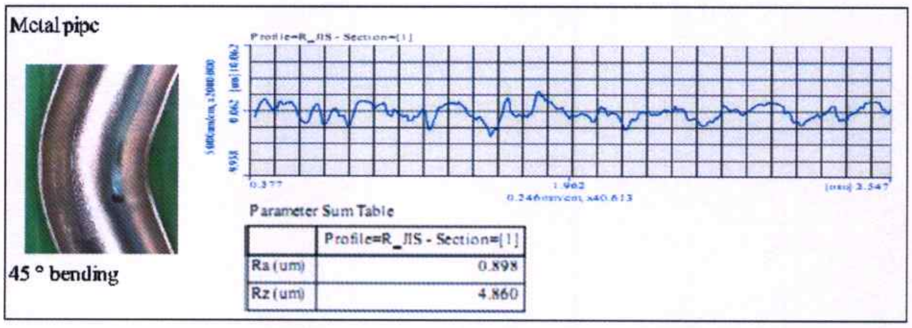

Figure 4.32 Line profile of the surface roughness for stainless steel with 45° bending angle

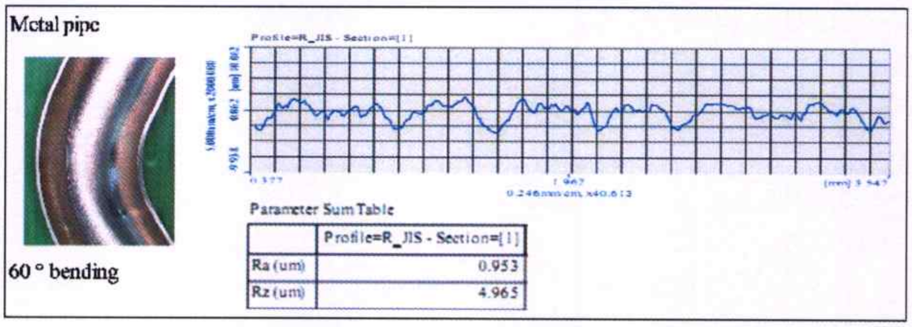

Figure 4.33 Line profile of the surface roughness for stainless steel with 60° bending angle

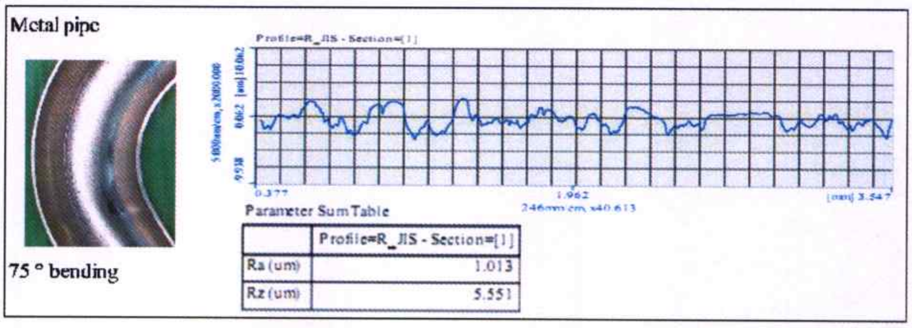

Figure 4.34 Line profile of the surface roughness for stainless steel with 75° bending angle

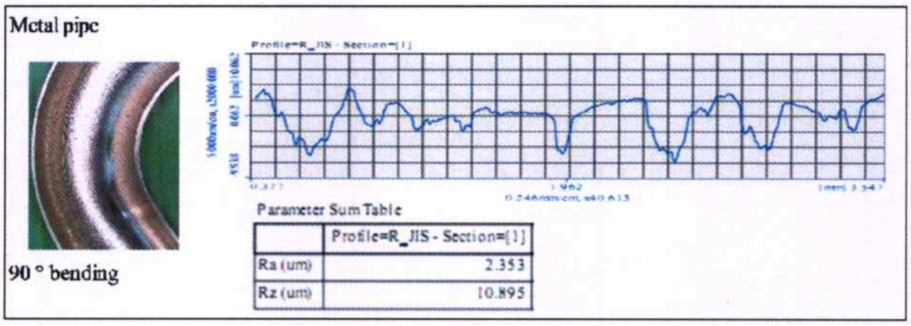

Figure 4.35 Line profile of the surface roughness for stainless steel with 90° bending angle

4.3 Effect of processing parameter on switch over mark

Varios processing variables were studied in term of their influence on the switch over mark characteristic behavior. Table 4.1 lists of result and processing varibles as well as the values used in the experiments. In this study, the virgin polypropylene (PP) was employed in order to investigate the effect of processing parameter. In the case of a tube cavity with a diameter of 17 mm. and sharp corner angle at 45 degree was used for measure.

By changing one of parameters in each test, we were able to understand the effect of every processing parameter on the surface quality of water assisted injection molded parts. The length of switch over mark was found to increase with the mold temperature and water delay time, but increase with melt temperature, the length of switch over mark were decrease accordingly. The observed depth of switch over mark were increase with increase the melt temperature and water delay time as showed in table 4.1

Table 4.1 Effect of processing variables on the surface characteristic of switch over mark

Melt Temp. (C)	Mold Temp. (C)	Delay Time (Sec)	Water Pressure (bar)	Holding Time (Sec)	Length (mm)	Depth (mm)
190	50	3	150	10	0.2686	0.0042
200	50	3	150	10	0.2080	0.0049
210	50	3	150	10	0.2080	0.0051
220	50	3	150	10	0.1510	0.0061
200	40	3	150	10	0.1780	0.0089
200	50	3	150	10	0.2080	0.0049
200	60	3	150	10	0.2154	0.0047
200	70	3	150	10	0.1236	0.0023
200	50	1	150	10	0.0000	0.0000
200	50	2	150	10	0.2080	0.0049
200	50	3	150	10	0.2426	0.0155
200	50	4	150	10	0.2776	0.0107
200	50	3	120	10	0.1950	0.0042
200	50	3	150	10	0.2080	0.0049
200	50	3	180	10	0.1860	0.0047
200	50	3	210	10	0.2170	0.0045
200	50	3	150	10	0.2080	0.0049
200	50	3	150	15	0.1980	0.0191
200	50	3	150	20	0.2570	0.0202
200	50	3	150	25	0.2150	0.0117

4.4 Stiffness

Part strength is the measurement of the load carrying ability of a part. This property depends on part geometry, material properties and loading condition. The Parallel-plate loading mechanism (ASTM D2412 standard test method) was used for investigating the pipe stiffness by conventional and accelerated test procedures. In this research, the stiffness was carried out by using Instron universal testing machine, which is the most widespread-used equipment to characterize the mechanical properities of the plastic parts. The stiffness results for plastic tube as molded by WAIM are shown in Figure 4.36 shows the relationship between the stiffness at 5% and 10% versus with the average inside diameter thickness of molded parts. It was found that the compression load increase with increasing the average thickness. This result can obtain equations 4.1and 4.2.

Stiffness (5%) = 17* Average wall thickness (mm) + 262 (4.1)

Stiffness (10%) = 21* Average wall thickness (mm) + 392 (4.2)

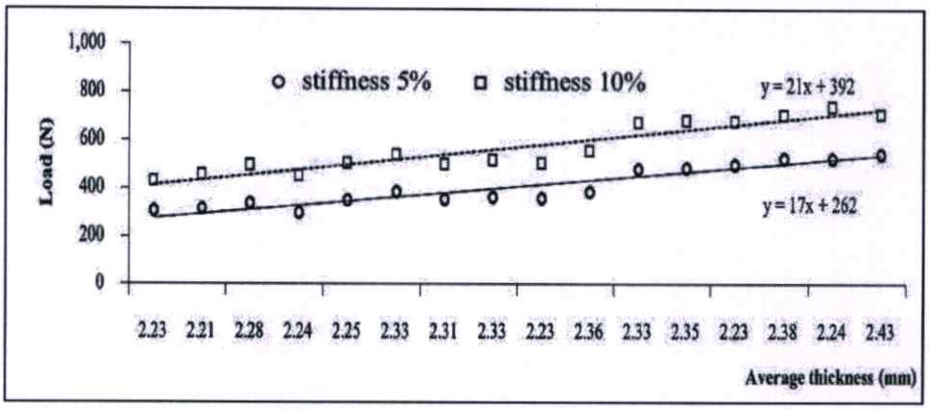

Figure 4.36 The effect of inside average thickness on stiffness at 5% and 10%

4.5 Microscopic observation

The structure observations were observed under a polarizing microscope. All specimens were cut out from the middle of molded parts and mounting with resin. Then microtomed slices were taken out of the parts in order to investigate the structure of the parts.The structure of spherulites formed at water channel wall and part skin (injection mold wall) were compared. First, the comparison of samples taken from parts manufactured at different melting temperature. The structure in three different areas: skin layer, middle of the sample and layer contacting water channel is shown in Figure 4.37 (a) for parts of lower melt temperature (Tm=190°C) and in Figure 4.37 (b) for parts obtained at higher melting temperature (Tm=220°C). In parts of Tm=190°C exhibited a degree of crystallinity than parts of Tm=220°C. This is due to the fact that increase the melt temperature decreases the cooling rate of the materials during the cooling process. On the other, to make a comparison of the crysallinity of parts molded by different in step of water dalay time, Figure 4.38 (a) for parts of water delay time at 1 second and Figure 4.38 (b) for parts of water delay time at 3 second. In parts of water delay time 1 second exhibited a degree of crystallinity lower than in parts of water delay time 3 second. This is due to the fact that increases the water delay time increase the cooling time. Molded parts thus exhibited a degree of crystallinity.

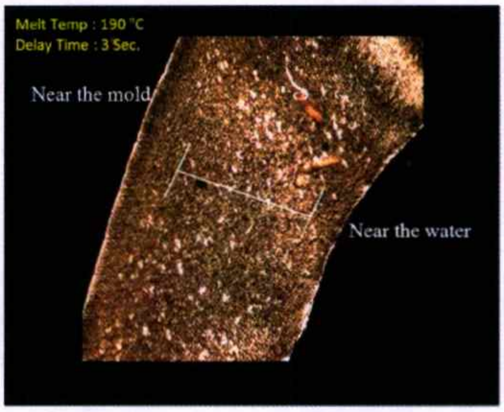

(a)

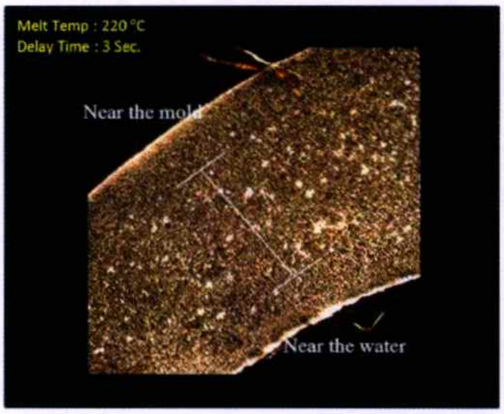

(b)

Figure 4.37 Cross-section of sample obtained at (a) the melting temperature Tm=175°C and (b) the melting temperature Tm=220°C

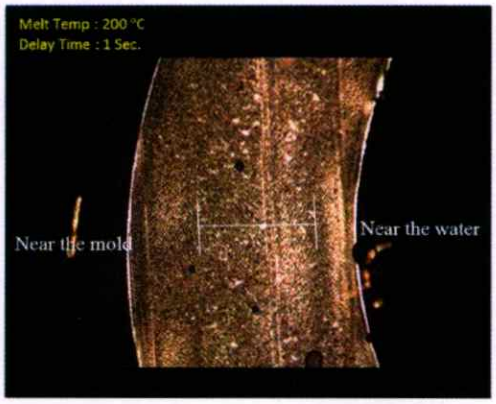

(a)

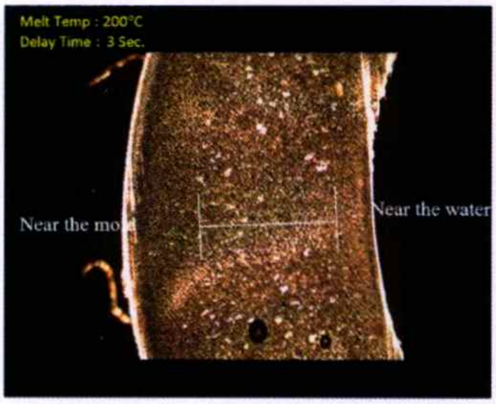

(b)

Figure 4.38 Cross-section of sample obtained at (a) the water delay time 1 Sec. and (b) the water delay time 3 Sec.

CHAPTER 5

CONCLUSIONS AND SUGGESTIONS

5.1 Conclusions

The residual wall thickness distribution in water-assisted injection molded tube with difference corner angles were investigated in this work.

As the effect of sharp corners curve, the residual wall thickness in curved sections is usually not axial-symmetrical. The inner residual wall thickness is thinner than outer residual wall thickness. When water penetrated the melt, it sought the path of least resistance and tended to penetrate into the core of the melt near the inner side of the molded parts, and the RWT difference increased at the curve corner angle increase, the maximum RWT difference occurred at the curve corner angle molded part at 90 degrees as the higher shear thinning viscosity behaviour and the highest velocity gradient (shear rate) at the inner sharp corner. On the other hand, the hollow core ratios were obviously increased for the shape corner angle at 0 degree to 45 degrees respectively. It then gradually increased from the angle 45 degrees to the shape corner angle 90 degrees.

As for the influence of the melt flow property, the inner residual wall thickness decreased at the lower melt viscosity, whereas the outer residual wall thickness increased at the higher melt flow. The maximum difference percentage occurred at the lower viscosity and the hollow core ratio of the lower viscosity showed the opposite result.

As for the influence by the processing parameters of the water assisted injection molding. The melt temperature, the water delay time and the water pressure are the most dominant factor for the inner and outer residual wall thickness. The difference percentage of residual wall thickness increased at the shape corner angle from 45 degree with increased the melt temperature. Additionally, the water injection delay time was the principal parameter affecting the hollowed behaviour of molded parts. Moreover, water injection delay time also was the principal parameter affecting the outside surface quality.

As for the fluid-side surface roughness, water assisted injection molding can provide the smoother inner part surface and can be used for automotive water-cooling pipe in the engine compartment with minimize pressure loss in fluid-transport applications.

As for the compressive stiffness of molded tubes depends on the average thickness and degree of crystallinity depends on the rate of cooling.

5.2 Recommendation

Although this work was finished, it was only the first step of the water assisted injection molding. There are some suggestions to this work to improve some point as follow:

5.2.1 There are other factors related with the water assisted injection molding such as water temperature and injection pressure that can be affected to the quality of the finished part. Therefore it should be studied to find out the effect of those left factors.

5.2.2 As this research testing only 1 plastic types. however, there are a lot of plastic types that can be used in the water-assisted injection molding. therefore it should be studied other plastics to find the residual wall thickness distribution.

5.2.3 In this research, the molding orientation at the upstream flow, might be study the effect of downstream flow.

REFERENCES

[1] R. Stauber and L. Vollrath.,**Plastic in Automotime Engineering**, Hanser Publishers, 2007,p.112

[2] Knights M.,**Water injection molding makes hollow parts faster. Lighter**, PlastTechnol 2002; p.42

[3] S.J. Liu and Y.C. Wu., **Dynamic Visualization of Cavity Filling Process in Fluid- assisted Injection Molding - Gas vs. Water**, Polymer Testing, 26, 232-242 (2007)

[4] W. Michaeli, T. Juntgen, A. Brunswick., **WIT-an route to series production: first industrial application of water injection technique**, Kunststoffplast. Euroupe 91 (2001) 37.

[5] S.J. Liu and Y.S. Chen., **Water assisted injection molding of thermoplastic material: effect of processing parameter**, Polym. Eng. Sci. 43 (2003) 1806.

[6] **"Water Injection Molding Makes Hollow Parts Faster, Lighter"**[Online]. Available:http://www.ptonline.com/articles/water-injection-molding-makes-hollow-parts-faster-lighter

[7] **"Water Assisted Injection Moulding(WAIM)"**[Online]. Available: http://www.polyeng.com/fluidassist/WAIM/waim.htm

[8] Liu S. J. and Hsieh, M. H.,**Residual Wall Thickness Distribution at Transition and Curve Section of Water-Assisted Injection Molded tubes**, Inter Polym Process, 22:82-89(2007).

[9] Liu S. J. and Lin S. P.,**An Experimental study of water-assisted injection molding of plastic tubes with dimensional transitions**. Journal of reinforced plastics and composites, 26: 1441-1453 (2007)

[10] G.Potsch and W. Michaeli.,**Injection Molding: An Introduction**, HanserPublishers ,NewYork, NY. (1995), p. 21

[11] Patcharaphun. S.,**Characterization and simulation of material distribution and fiber orientation in sandwich injection molded parts**, ISBN 3-939382-04-3(2006)

[12] W. Michaeli and T. Juntgen., **The water injection technique (WIT) - opportunities and challenges**, Injection Molding 2002; 73

[13] W. Michaeli, **Water injection technique (WIT)**, : M. Kamal, A. Isayev, S.J. Liu (Eds.),Injection Molding: Technology and Fundamentals and Applications, Hanser Publishers 2009.

REFERENCES (CONT.)

[14] Lin K. Y., Chang F. A. and Liu S. J., **Using differential mold temperatures to improve the residual wall thickness uniformity around curved sections of fluid assisted injection molded tubes**, IntCommun Heat Mass 36(5):491-497 (2009)

[15] AHMADZAI A. Z. and BEHRAVESH A. H., **An experimental investigation on water penetration in the process of water assisted injection molding of polypropylene**, POLIMERY 2009:564-572

[16] Erik Lokensgard, **Industrial Plastics: Theory and Applications**. (5^{th} Edition) (2010), pp168

[17] S.J. Liu, Y.S. Chen,**The manufacturing of thermoplastic composite parts by water-assisted injection-molding technology**, Composites A, Vol. 35, pp. 171–180, 2004.

[18] G. Potsch and W.Michaeli,**Injection Molding: An Introduction**, HanserPublishers 2008.

[19] Liu X.H and Huang H.X., **Flow patterns and water penetration in water-assisted melt filling using an emulated mold**.SPE ANTEC Tech. Papers 2007,p. 672.

[20] W. Michaeli, A. Brunswick and M. Gruber., **Step on the gas with water injection**. KunstoffePlast Europe (1999) 89,pp 84-86

[21] W. Michaeli, A. Brunswick and C. Kujat., **Reducing cooling time with water-assisted injection moulding - Advantages over gas-assisted injection**.KunstoffePlast Europe (2000) 90, p.67

[22] Liu S. J., Lin S. P and Wu Y. H., **An experimental study of the water-assisted injection molding of glass fiber filled poly-butylene-terephthalate (PBT) composites**, Compos SciTechnol 67 (2007):1415-1424

[23] Avery J., **Gas-assist injection molding: Principles and applications**. Munich: Hanser; 2000.

[24] T Juntgen, W Michaeli., **The Water Injection Technique (WIT) as an Attractive Alternative and supplement to Gas-Assisted Injection Molding**.SPE ANTEC Technical paper (2002) ,pp679-683

[25] **"Water-Assist Injection Molding (WAIM)"**[Online]. Available: http://www.ides.com/articles/processing/2007/fleck_waterassist.asp

[26] **"Aquamould®"**[Online]. Available: http://www.battenfeld-imt.com/en/maschinen/wasserinjektionstechnik/aquamould.html

[27] Joachim Kragl, **"Watermelt"**, Technical information paper (2002)[Online]. Available: http://www.eurotecsls.com/Acrobat%20Files/Advanced%20Processes/Watermelt%2005-2302.pdf

REFERENCES (CONT.)

[28] ZHANG Zengmeng, Zhou Hua., **Analysis of Load Characteristics and Control of Water Hydraulic System for WAIM**, Proceedings of the 7th JFPS International Symposium on Fluid Power, Toyama, Japan, 2008: Vol. 3 685-690

[29] Zhou Hua, Chen Yinglong, Zhang Zengmeng and RyuShohei, **Simulation and experiment research on the proportional pressure control of water assisted injection molding**, Proceedings of the 7th JFPS International Symposium on Fluid Power, Lanzhou, China, 2010: pp 5-10

[30] A. Z. Ahmadzal. and A. H. Behravesh.,**Effect of processing parameters on water penetration in water assisted injection molding of ABS**:POLIMERY 2011, 56,nr3 pp.232

[31] Liu S. J. and Lin S. P., **Study of 'fingering' in water assisted injection molded composites**., Composite: Part A 36 (2005) 1507-1517

[32] Liu , S.J. and Shih , C.C., **An Experimental Study of the Water-Assisted Injection Molding of PA-6 Composites**., Journal of Reinforced Plastics and Composites, vol. 27, issue 9, pp. 985-999

[33] Jong W-R., Huang J-S., and Chang Y-S., **Experiment studies of design guidelines for gas-assisted injection molding process**. SPE ANTEC Tech Paper 1996: 668-673

APPENDIX A

Injection molding specification

Table A.1 The specification of conventional injection molding machine

Parameter	Unit	Value
Injection		
Shot Weight (PS)	oz	10.9
	g	310
Swept Volume	cm^3	341
Screw Diameter	mm	46
Injection Pressure (Max)	kgf/cm^2	2543
Screw Stroke	mm	205
Screw Speed Range	rpm (max)	207
Plasticizing Capacity	kg/h	90
Injection Rate	cm^3/s	176
Hopper Capacity	liter	45
Screw L/D Ratio	mm/mm	20
Nozzle Control Force	t	6.2
Nozzle Stroke	mm	330
Clamping Unit		
Mold Clamping Force	t	228
Opening Stroke	mm	490
Space Between Tie Bar (H x V)	mm	520 x 520
Mold Thickness (Min-Max)	mm	200-550
Maximum Daylight	mm	1040
Hydraulic Ejector Force (Max)	T	5.5
Hydraulic Ejector Stroke	mm	150
Mold Register Hole (H7)	mm	120
Power / Heating Unit		
Pump Motor	kW (HP)	22 (30)
System Pressure	kgf/cm^2	175
Heating Capacity	kW	15.5
Temperature Control Zones		3+1
Others		
Dry Cycle Time	s	2.4
Machine Dimensions (LxWxH	m x m x m	5.56 x 1.42 x 1.95
Oil Tank Capacity	liter	465
Machine Weight (Dry)	t	6.5

APPENDIX B

Mold geometry

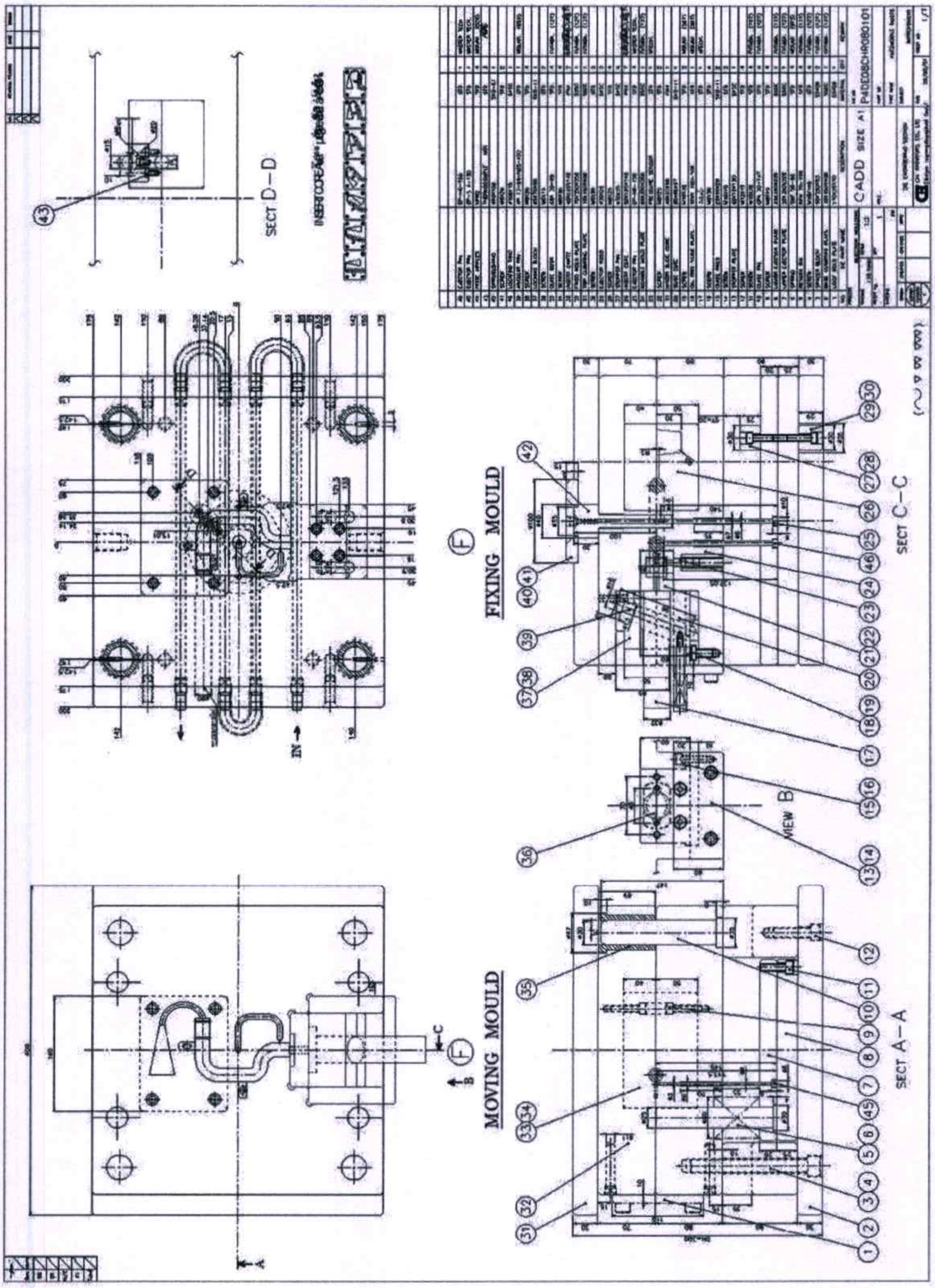

Figure B.1 Mold geometry

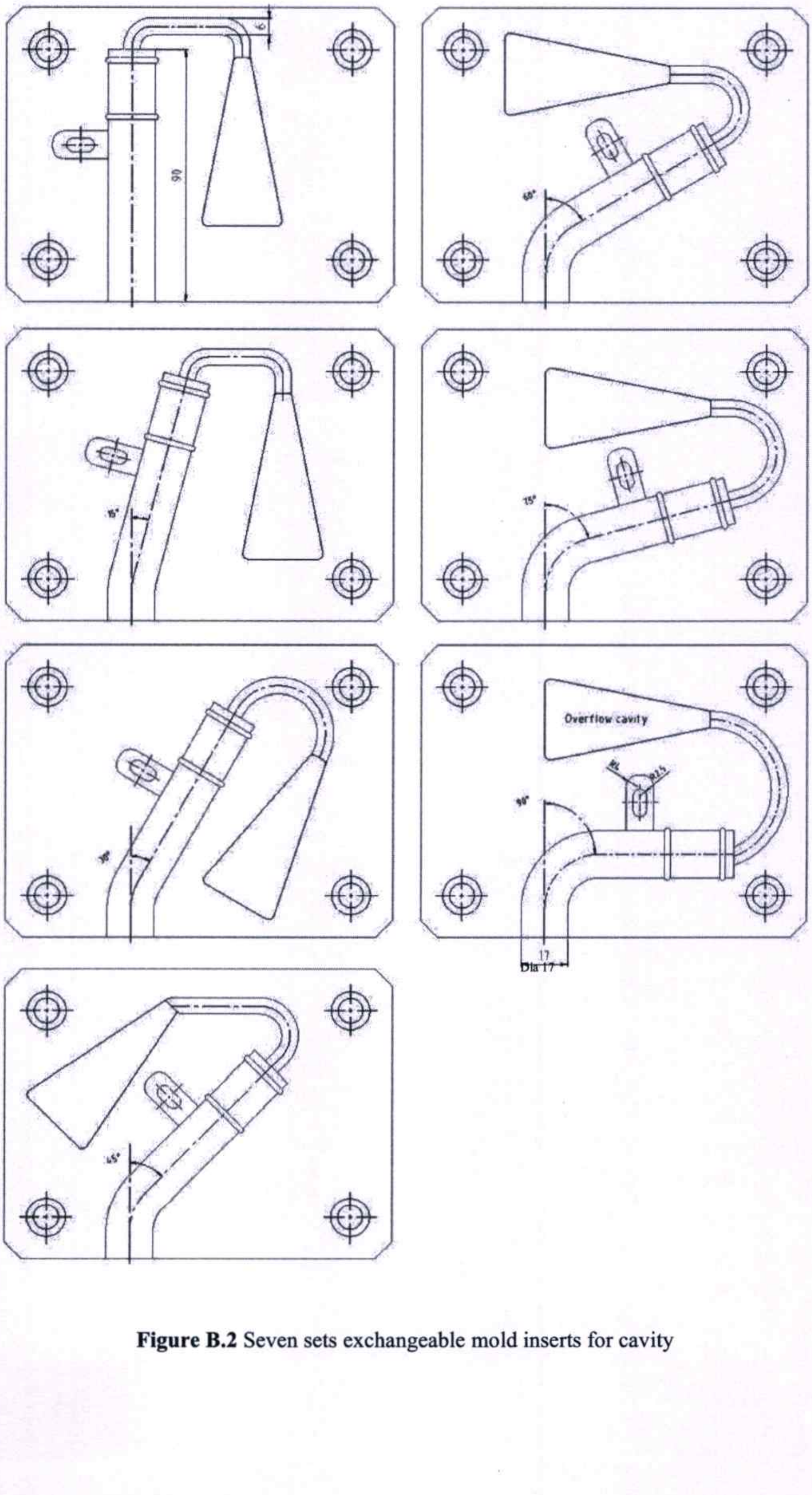

Figure B.2 Seven sets exchangeable mold inserts for cavity

APPENDIX C

Material properties of three grade PP

Table C.1 Material properties of polypropylene homopolymer; Moplen HP400K

HMC POLYMERS
COMPANY LIMITED

Moplen HP400K

General Purpose Polypropylene Homopolymer Resin

Features :

- Good processability
- Low odor and taste transfer
- Excellent chemical resistance
- Low yellowness
- Good tensile strength

Typical Applications :

- Slit tape
- Straw
- Monofilaments
- Rope, twine
- Housewares
- Furniture

Resin properties (a)	Moplen HP400K	ASTM METHOD(b)
Melt flow rate, dg/min.	4	D 1238
Density, g/cm^3	0.90	D 792B
Tensile strength at yield, MPa	33	D 638
Elongation at yield, %	11	D 638
Flexural modulus, MPa	1400	D 790A
Notched Izod Impact strength at 23°C, J/m	32	D 256A
Deflection temperature, at 455 kPa, °C	93	D 648

(a) Values shown are averages and are not to be considered as specifications.
(b) ASTM test methods are the latest under Society' s current procedures. All molded specimens are prepared by injection.

Table C.2 Material properties of polypropylene homopolymer; Moplen HP400M

HMC POLYMERS
COMPANY LIMITED

Moplen HP400M

General Purpose Polypropylene Homopolymer Resin

Features :

- Good Processability
- Low odor and taste transfer
- Excellent resistance to environmental stress - cracking

Typical Applications :

- Housewares
- Toys
- Containers
- Closures

Resin properties (a)	Moplen HP400M	ASTM METHOD(b)
Melt flow rate, dg/min.	7.5	D 1238
Density, g/cm^3	0.90	D 792B
Tensile strength at yield, MPa	34	D 638
Elongation at yield, %	10	D 638
Flexural modulus, MPa	1450	D 790A
Notched Izod impact strength at 23°C, J/m	27	D 256A
Deflection temperature, at 455 kPa, °C	96	D 648

(a) Values shown are averages and are not to be considered as specifications.
(b) ASTM test methods are the latest under Society' s current procedures. All molded specimens are prepared by injection.

Table C.3 Material properties of polypropylene homopolymer; Moplen HP550R

HMC POLYMERS
COMPANY LIMITED

Moplen HP550R

High Flow Polypropylene Homopolymer Resin

Features :

- Improved processability
- Low odor and taste transfer
- Excellent resistance to environmental stress-cracking

Typical Applications :

- Staple & multifilament fiber
- Thin wall injection molding
- Food containers
- Hospital and institutional wares

Resin properties (a)	Moplen HP550R	ASTM METHOD(b)
Melt flow rate, dg/min.	22	D 1238
Density, g/cm^3	0.90	D 792B
Tensile strength at yield, MPa	34	D 638
Elongation at yield, %	9	D 638
Flexural modulus, MPa	1480	D 790A
Notched izod impact strength a t23°C,J/m	22	D 256A
Deflection temperature, at 455 kPa, °C	97	D 648

(a) Values shown are averages and are not to be considered as specifications.
(b) ASTM test methods are the latest under Society' s current procedures. All molded specimens are prepared by injection.

APPENDIX D

Processing parameter

Table D.1 Molding condition molded tube

Rang of varying parameter

Sharp corner angle (°)	0	15	30	45	60	75	90
Melt flow index (g/10 min)	**4**	7.5	22				
Melt Temperature (°C)	190	**200**	210	220			
Mold Temperature (°C)	40	**50**	60	70			
Water delay time (sec)	1	**3**	5	7			
Water pressure (Mpa)	120	**150**	180	200			
Water holding time (sec)	**10**	15	20	25			

Reference condition for molding

Number of	Sharp corner angle (°)	Melt flow index (g/10 min)	Melt Temperature (°C)	Mold Temperature (°C)	Water Delay Time (Sec)	Water Pressure (bar)	Water Holding Time
1	0	4	190	50	3	150	10
2	0	4	200	50	3	150	10
3	0	4	210	50	3	150	10
4	0	4	220	50	3	150	10
5	0	4	200	40	3	150	10
6	0	4	200	60	3	150	10
7	0	4	200	70	3	150	10
8	0	4	200	50	1	150	10
9	0	4	200	50	5	150	10
10	0	4	200	50	7	150	10
11	0	4	200	50	3	120	10
12	0	4	200	50	3	180	10
13	0	4	200	50	3	200	10
14	0	4	200	50	3	150	15
15	0	4	200	50	3	150	20
16	0	4	200	50	3	150	25
17	15	4	190	50	3	150	10
18	15	4	200	50	3	150	10
19	15	4	210	50	3	150	10
20	15	4	220	50	3	150	10

Table D.1 (Cont.) Molding condition molded tube.

Reference condition for molding							
Number of	Sharp corner angle (°)	Melt flow index (g/10 min)	Melt Temperature (°C)	Mold Temperature (°C)	Water Delay Time (Sec)	Water Pressure (bar)	Water Holding Time
21	15	4	200	40	3	150	10
22	15	4	200	60	3	150	10
23	15	4	200	70	3	150	10
24	15	4	200	50	1	150	10
25	15	4	200	50	5	150	10
26	15	4	200	50	7	150	10
27	15	4	200	50	3	120	10
28	15	4	200	50	3	180	10
29	15	4	200	50	3	200	10
30	15	4	200	50	3	150	15
31	15	4	200	50	3	150	20
32	15	4	200	50	3	150	25
33	30	4	190	50	3	150	10
34	30	4	200	50	3	150	10
35	30	4	210	50	3	150	10
36	30	4	220	50	3	150	10
37	30	4	200	40	3	150	10
38	30	4	200	60	3	150	10
39	30	4	200	70	3	150	10
40	30	4	200	50	1	150	10
41	30	4	200	50	5	150	10
42	30	4	200	50	7	150	10
43	30	4	200	50	3	120	10
44	30	4	200	50	3	180	10
45	30	4	200	50	3	200	10
46	30	4	200	50	3	150	15
47	30	4	200	50	3	150	20
48	30	4	200	50	3	150	25
49	45	4	190	50	3	150	10
50	45	4	200	50	3	150	10

Table D.1 (Cont.) Molding condition molded tube.

Reference condition for molding

Number of	Sharp corner angle (°)	Melt flow index (g/10 min)	Melt Temperature (°C)	Mold Temperature (°C)	Water Delay Time (Sec)	Water Pressure (bar)	Water Holding Time
51	45	4	210	50	3	150	10
52	45	4	220	50	3	150	10
53	45	4	200	40	3	150	10
54	45	4	200	60	3	150	10
55	45	4	200	70	3	150	10
56	45	4	200	50	1	150	10
57	45	4	200	50	5	150	10
58	45	4	200	50	7	150	10
59	45	4	200	50	3	120	10
60	45	4	200	50	3	180	10
61	45	4	200	50	3	200	10
62	45	4	200	50	3	150	15
63	45	4	200	50	3	150	20
64	45	4	200	50	3	150	25
65	45	7.5	200	50	3	150	10
66	45	22	200	50	3	150	10
67	60	4	190	50	3	150	10
68	60	4	200	50	3	150	10
69	60	4	210	50	3	150	10
70	60	4	220	50	3	150	10
71	60	4	200	40	3	150	10
72	60	4	200	60	3	150	10
73	60	4	200	70	3	150	10
74	60	4	200	50	1	150	10
75	60	4	200	50	5	150	10
76	60	4	200	50	7	150	10
77	60	4	200	50	3	120	10
78	60	4	200	50	3	180	10
79	60	4	200	50	3	200	10
80	60	4	200	50	3	150	15

Table D.1 (Cont.) Molding condition molded tube.

Reference condition for molding							
Number of	Sharp corner angle (°)	Melt flow index (g/10 min)	Melt Temperature (°C)	Mold Temperature (°C)	Water Delay Time (Sec)	Water Pressure (bar)	Water Holding Time
81	60	4	200	50	3	150	20
82	60	4	200	50	3	150	25
83	75	4	190	50	3	150	10
84	75	4	200	50	3	150	10
85	75	4	210	50	3	150	10
86	75	4	220	50	3	150	10
87	75	4	200	40	3	150	10
88	75	4	200	60	3	150	10
89	75	4	200	70	3	150	10
90	75	4	200	50	1	150	10
91	75	4	200	50	5	150	10
92	75	4	200	50	7	150	10
93	75	4	200	50	3	120	10
94	75	4	200	50	3	180	10
95	75	4	200	50	3	200	10
96	75	4	200	50	3	150	15
97	75	4	200	50	3	150	20
98	75	4	200	50	3	150	25
99	90	4	190	50	3	150	10
100	90	4	200	50	3	150	10
101	90	4	210	50	3	150	10
102	90	4	220	50	3	150	10
103	90	4	200	40	3	150	10
104	90	4	200	60	3	150	10
105	90	4	200	70	3	150	10
106	90	4	200	50	1	150	10
107	90	4	200	50	5	150	10
108	90	4	200	50	7	150	10
109	90	4	200	50	3	120	10
110	90	4	200	50	3	180	10

Table D.1 (Cont.) Molding condition molded tube

Reference condition for molding							
Number of	Sharp corner angle (°)	Melt flow index (g/10 min)	Melt Temperature (°C)	Mold Temperature (°C)	Water Delay Time (Sec)	Water Pressure (bar)	Water Holding Time
111	90	4	200	50	3	200	10
112	90	4	200	50	3	150	15
113	90	4	200	50	3	150	20
114	90	4	200	50	3	150	25

APPENDIX E

Experimental results

Table E.1 Experimental results

Condition No.	Residual Wall Thickness (mm)																RWT Difference (%)	Hollow Core Ratio (%)
	Sample No.1				Sample No.2				Sample No.3				Average					
	Inner	Outer	Top	Bottom	Inner	Outer	Top	Bottom	Inner	Outer	Top	Bottom	Inner	Outer	Top	Bottom		
1	2.34	2.64	2.62	2.68	2.28	2.44	2.44	2.66	2.32	2.51	2.55	2.68	2.31	2.53	2.54	2.67	8.58	48.55
2	2.35	2.60	2.50	2.55	2.36	2.60	2.67	2.65	2.36	2.60	2.67	2.65	2.36	2.60	2.61	2.62	9.56	47.99
3	2.41	2.68	2.59	2.65	2.50	2.70	2.53	2.71	2.53	2.76	2.56	2.72	2.48	2.71	2.56	2.69	8.94	46.91
4	2.58	2.77	2.58	2.63	2.56	2.74	2.59	2.61	2.55	2.85	2.69	2.63	2.56	2.79	2.62	2.62	8.42	46.30
5	2.35	2.59	2.58	2.60	2.34	2.56	2.50	2.83	2.38	2.62	2.58	2.70	2.36	2.59	2.55	2.71	9.14	47.89
6	2.32	2.49	2.58	2.82	2.28	2.50	2.63	2.79	2.30	2.57	2.62	2.77	2.30	2.52	2.61	2.79	8.60	47.83
7	2.31	2.52	2.59	2.65	2.32	2.55	2.57	2.55	2.37	2.49	2.55	2.61	2.33	2.52	2.57	2.60	7.45	48.66
8	2.08	2.31	2.64	2.47	2.14	2.30	2.37	2.56	2.04	2.29	2.46	2.44	2.09	2.30	2.49	2.49	9.12	51.47
9	2.46	2.62	2.61	2.69	2.41	2.51	2.66	2.69	2.46	2.57	2.61	2.73	2.44	2.57	2.63	2.70	4.77	47.35
10	2.49	2.60	2.85	2.66	2.45	3.15	2.89	2.74	2.56	2.64	2.70	2.83	2.50	2.80	2.81	2.74	10.69	45.25
11	2.54	2.73	2.68	2.73	2.46	2.72	2.58	2.88	2.47	2.70	2.62	2.77	2.49	2.72	2.63	2.79	8.53	46.16
12	2.36	2.53	2.62	2.63	2.37	2.53	2.48	2.43	2.29	2.53	2.40	2.54	2.34	2.53	2.50	2.53	7.69	49.18
13	2.21	2.41	2.52	2.61	2.18	2.36	2.48	2.59	2.30	2.47	2.61	2.62	2.23	2.41	2.54	2.61	7.50	49.67
14	2.28	2.42	2.60	2.67	2.16	2.44	2.35	2.57	2.26	2.56	2.57	2.49	2.23	2.47	2.51	2.58	9.84	49.66
15	2.21	2.41	2.57	2.60	2.19	2.38	2.50	2.58	2.21	2.45	2.66	2.58	2.20	2.41	2.58	2.59	8.58	49.70
16	2.33	2.49	2.65	2.50	2.24	2.43	2.67	2.66	2.29	2.49	2.59	2.52	2.29	2.47	2.64	2.56	7.37	48.97
17	2.43	2.65	2.62	2.65	2.61	2.72	2.67	2.52	2.50	2.79	2.73	2.50	2.51	2.72	2.67	2.56	7.90	46.84
18	2.54	2.89	2.68	2.82	2.40	2.89	2.73	2.59	2.48	2.82	2.69	2.70	2.47	2.87	2.70	2.70	14.67	45.69
19	2.47	2.77	2.71	2.66	2.54	2.79	2.52	2.80	2.54	2.86	2.74	2.74	2.52	2.81	2.66	2.73	10.82	45.81
20	2.55	2.83	2.83	2.69	2.60	3.04	2.90	2.78	2.43	2.93	2.79	2.68	2.53	2.93	2.84	2.72	14.76	44.58
21	2.63	2.63	2.71	2.67	2.50	2.67	2.81	2.58	2.48	2.66	2.83	2.44	2.54	2.65	2.78	2.56	4.45	46.53
22	2.44	2.50	2.46	2.58	2.46	2.76	2.78	2.46	2.62	2.75	2.66	2.67	2.51	2.67	2.63	2.57	6.25	47.19
23	2.59	2.39	2.69	2.44	2.51	2.66	2.62	2.59	2.44	2.65	2.81	2.69	2.51	2.57	2.71	2.57	7.21	47.27
24	2.30	2.01	2.37	2.64	2.25	2.57	2.55	2.57	2.30	2.65	2.44	2.53	2.28	2.41	2.45	2.58	13.15	49.93
25	2.53	2.55	2.58	2.56	2.47	2.67	2.59	2.56	2.43	2.55	2.60	2.49	2.48	2.59	2.59	2.54	4.44	47.96
26	2.55	2.97	2.77	2.79	2.40	2.79	2.59	2.77	2.57	2.56	2.55	2.76	2.51	2.77	2.64	2.77	10.11	45.91
27	2.73	2.83	2.98	2.50	2.88	2.91	3.10	2.80	2.88	2.70	2.85	2.87	2.83	2.81	2.98	2.72	3.67	43.28
28	2.41	2.73	2.52	2.77	2.64	2.66	2.72	2.67	2.41	2.85	2.65	2.66	2.49	2.75	2.63	2.70	9.89	46.42
29	2.42	2.71	2.61	2.67	2.30	2.69	2.43	2.65	2.32	2.69	2.62	2.39	2.35	2.70	2.55	2.57	13.80	48.07
30	2.54	2.89	2.68	2.82	2.40	2.89	2.73	2.59	2.48	2.82	2.69	2.70	2.47	2.87	2.70	2.70	14.67	45.69

Table E.1 (Cont.) Experimental results

Condition No.	Residual Wall Thickness (mm)																RWT Difference (%)	Hollow Core Ratio (%)
	Sample No.1				Sample No.2				Sample No.3				Average					
	Inner	Outer	Top	Bottom	Inner	Outer	Top	Bottom	Inner	Outer	Top	Bottom	Inner	Outer	Top	Bottom		
31	2.23	2.71	2.37	2.71	2.42	2.65	2.50	2.62	2.44	2.71	2.73	2.63	2.36	2.69	2.53	2.65	12.82	47.77
32	2.33	2.78	2.70	2.66	2.29	2.53	2.37	2.59	2.30	2.62	2.29	2.67	2.31	2.64	2.45	2.64	13.32	48.59
33	2.00	3.17	2.53	2.47	2.25	3.00	2.76	2.40	2.44	2.83	2.73	2.76	2.23	3.00	2.67	2.54	29.78	46.91
34	2.37	2.79	2.68	2.47	2.46	3.03	2.82	2.60	2.43	2.85	2.88	2.50	2.42	2.89	2.79	2.52	17.65	46.17
35	2.37	3.27	2.69	2.62	2.31	3.09	2.65	2.69	2.46	3.12	2.74	2.90	2.38	3.16	2.69	2.74	28.49	44.77
36	2.39	3.25	2.73	2.73	2.40	3.10	2.83	3.61	2.44	3.16	2.76	2.88	2.41	3.17	2.77	3.07	26.69	42.95
37	2.34	2.87	3.06	2.50	2.36	3.07	2.66	2.42	2.34	2.40	2.82	2.55	2.35	2.78	2.85	2.49	16.36	46.84
38	2.28	2.96	2.63	2.66	2.23	2.93	2.58	2.55	2.40	3.12	2.58	2.83	2.30	3.00	2.60	2.68	26.46	46.35
39	2.38	2.88	2.69	2.48	2.45	2.89	2.77	2.50	2.22	2.99	2.56	2.69	2.35	2.92	2.67	2.56	21.74	46.68
40	2.19	3.08	2.73	2.61	2.22	2.99	2.65	2.57	2.21	2.34	2.26	2.40	2.21	2.80	2.55	2.53	22.91	48.45
41	2.06	2.95	2.51	2.54	2.46	3.03	2.82	2.60	2.70	3.04	2.88	2.50	2.41	3.01	2.74	2.55	22.84	45.90
42	2.33	3.03	2.88	2.75	2.23	3.03	2.85	2.61	2.24	3.01	2.61	2.56	2.27	3.02	2.78	2.64	28.30	45.83
43	2.52	3.37	3.15	2.66	2.55	2.92	2.78	2.54	2.43	3.03	2.76	2.58	2.50	3.11	2.90	2.59	21.67	44.27
44	2.25	2.55	2.85	2.58	2.09	2.81	2.77	2.99	2.13	2.76	2.71	2.46	2.16	2.71	2.78	2.68	21.27	47.45
45	2.02	2.67	2.51	2.31	2.33	3.01	2.82	2.52	2.14	3.05	2.58	2.59	2.16	2.91	2.64	2.47	29.31	48.02
46	2.23	2.69	2.55	2.57	2.20	2.64	2.44	2.38	2.26	2.45	2.37	2.40	2.23	2.59	2.45	2.45	14.85	49.93
47	2.06	2.63	2.36	2.50	2.07	2.74	2.60	2.50	2.13	2.69	2.45	2.43	2.09	2.69	2.47	2.48	24.67	49.96
48	2.20	2.80	2.51	2.46	2.29	2.86	2.54	2.61	2.25	3.05	2.68	2.44	2.25	2.90	2.58	2.50	25.64	47.81
49	2.48	2.88	2.98	2.56	2.39	2.96	2.86	2.70	2.21	2.76	2.63	2.41	2.36	2.87	2.82	2.56	19.19	46.26
50	2.31	3.12	2.82	2.78	2.20	3.24	2.79	2.55	2.45	2.98	3.01	2.55	2.32	3.11	2.87	2.63	29.08	44.92
51	1.92	3.24	2.80	2.54	2.04	3.21	2.84	2.53	1.90	3.31	2.83	2.52	1.95	3.25	2.82	2.53	49.25	46.44
52	2.05	3.34	2.72	2.61	2.09	3.46	2.87	2.78	1.93	3.55	2.76	2.51	2.02	3.45	2.78	2.63	52.45	45.09
53	2.54	2.97	2.50	2.69	2.40	2.96	2.78	2.64	2.37	2.94	2.73	2.57	2.44	2.96	2.67	2.63	19.45	45.88
54	2.46	2.99	3.15	2.41	2.27	2.99	2.84	2.50	2.23	3.14	2.77	2.54	2.32	3.04	2.92	2.48	26.84	45.61
55	2.36	3.09	2.84	2.69	2.28	3.05	2.75	2.59	2.35	3.08	2.91	2.53	2.33	3.07	2.83	2.60	27.44	45.29
56	2.24	2.82	2.91	2.25	2.15	2.82	2.72	2.49	2.25	2.91	2.88	2.39	2.21	2.85	2.84	2.38	24.78	47.61
57	2.31	3.23	2.88	2.74	2.52	3.27	3.11	2.67	2.28	3.37	3.03	2.58	2.37	3.29	3.01	2.66	32.54	43.33
58	2.35	3.25	3.14	2.72	2.39	3.26	3.01	2.59	2.56	3.19	2.98	2.81	2.43	3.23	3.04	2.71	28.06	42.98
59	2.15	3.51	3.05	2.62	2.24	3.33	2.79	2.73	2.08	3.42	2.53	2.97	2.16	3.42	2.79	2.77	45.35	44.08
60	2.19	3.03	2.72	2.66	2.28	3.07	2.80	2.53	2.30	3.11	2.76	2.65	2.26	3.07	2.76	2.61	30.41	45.86

Table E.1 (Cont.) Experimental results

Condition No.	Residual Wall Thickness (mm)																RWT Difference (%)	Hollow Core Ratio (%)
	Sample No.1				Sample No.2				Sample No.3				Average					
	Inner	Outer	Top	Bottom	Inner	Outer	Top	Bottom	Inner	Outer	Top	Bottom	Inner	Outer	Top	Bottom		
61	1.89	3.15	2.70	2.31	2.18	3.19	2.74	2.61	2.09	3.17	2.77	2.50	2.05	3.17	2.74	2.47	42.95	46.97
62	2.23	2.96	2.70	2.66	2.24	2.96	2.81	2.43	2.19	3.09	2.69	2.78	2.22	3.00	2.73	2.62	29.58	46.36
63	2.22	3.05	2.67	2.52	2.20	3.08	2.83	2.54	2.21	3.08	2.75	2.50	2.21	3.07	2.75	2.52	32.60	46.48
64	2.30	2.94	2.67	2.56	2.12	2.94	2.71	2.39	2.28	2.96	2.76	2.45	2.23	2.95	2.71	2.47	27.59	47.26
65	2.19	3.03	2.72	2.66	2.18	3.19	2.74	2.61	2.12	2.94	2.71	2.39	2.16	3.05	2.72	2.55	33.89	46.72
66	1.96	4.01	3.04	2.77	1.92	3.86	3.00	2.71	1.95	3.99	3.00	2.64	1.94	3.95	3.01	2.71	69.20	42.20
67	2.15	3.18	2.87	2.35	2.36	2.96	2.82	2.51	2.30	2.57	2.72	2.33	2.27	2.90	2.80	2.40	24.16	47.22
68	2.16	3.24	2.75	2.51	2.09	3.15	2.76	2.43	2.22	3.08	2.82	2.63	2.16	3.16	2.78	2.52	37.73	46.22
69	1.89	3.49	2.75	2.40	2.24	3.10	2.71	2.60	1.83	3.30	2.63	2.48	1.99	3.30	2.70	2.49	50.17	46.80
70	1.69	3.74	2.87	2.43	1.72	3.51	2.84	2.35	1.89	3.41	2.74	2.55	1.77	3.55	2.82	2.44	67.52	46.36
71	1.92	3.32	2.75	2.52	1.90	3.19	2.75	2.47	1.97	3.18	2.78	2.46	1.93	3.23	2.76	2.48	49.97	47.08
72	1.98	3.13	2.69	2.51	1.94	3.21	2.72	2.31	1.80	3.21	2.59	2.44	1.91	3.18	2.67	2.42	50.23	48.03
73	1.97	2.95	2.65	2.60	2.10	2.94	2.66	2.46	1.90	2.97	2.70	2.25	1.99	2.95	2.67	2.44	38.40	48.56
74	1.83	2.87	2.46	2.21	1.93	2.58	2.55	2.26	1.90	2.73	2.52	2.31	1.89	2.73	2.51	2.26	35.80	51.40
75	1.92	3.31	2.72	2.72	2.08	2.85	2.53	2.55	2.06	3.05	2.91	2.47	2.02	3.07	2.72	2.58	40.21	47.15
76	2.22	3.48	2.77	2.68	1.92	3.08	2.63	2.58	1.94	3.35	2.45	2.13	2.03	3.30	2.62	2.46	49.26	47.08
77	1.96	3.25	2.44	2.66	2.15	3.28	2.59	2.70	1.82	3.59	2.69	2.74	1.98	3.37	2.57	2.70	52.51	46.18
78	2.09	3.15	2.76	2.43	2.22	3.08	2.82	2.63	1.92	3.18	2.56	2.43	2.08	3.14	2.71	2.50	40.87	47.01
79	2.19	2.88	2.75	2.33	2.08	3.03	2.73	2.34	2.09	3.08	2.74	2.33	2.12	3.00	2.74	2.33	34.40	47.97
80	2.00	3.02	2.78	2.44	2.11	3.04	2.69	2.39	2.05	3.16	2.59	2.95	2.05	3.07	2.69	2.59	39.17	47.08
81	2.06	3.21	2.66	2.42	2.07	3.07	2.62	2.48	2.05	3.22	2.72	2.48	2.06	3.17	2.67	2.46	42.74	47.29
82	1.91	3.13	2.61	2.34	1.94	3.02	2.55	2.49	2.19	2.99	2.62	2.50	2.01	3.05	2.59	2.44	41.04	48.36
83	2.21	2.96	2.90	2.44	2.23	3.01	2.97	2.39	2.20	2.96	2.78	2.36	2.21	2.98	2.88	2.40	29.16	46.81
84	1.92	3.32	2.81	2.36	2.18	3.13	2.75	2.48	2.12	3.09	2.82	2.28	2.07	3.18	2.79	2.37	42.49	47.02
85	2.15	3.20	2.85	2.46	2.06	3.32	2.71	2.66	2.09	3.19	2.77	2.48	2.10	3.24	2.78	2.53	42.69	46.08
86	1.85	3.66	3.16	2.32	1.89	3.45	3.09	2.60	1.88	3.35	2.82	2.55	1.87	3.49	3.02	2.49	59.31	45.16
87	2.06	3.25	2.84	2.50	2.08	3.72	2.90	2.44	2.12	3.09	2.74	2.45	2.09	3.35	2.83	2.46	46.96	45.75
88	2.31	3.05	2.63	2.54	1.99	3.27	2.91	2.73	2.11	3.05	2.60	2.58	2.14	3.12	2.71	2.62	37.15	46.32
89	1.80	3.20	2.72	2.24	2.19	3.15	2.73	2.47	2.03	3.15	2.96	2.42	2.01	3.17	2.80	2.38	45.03	47.30
90	1.74	3.13	2.58	2.28	1.87	3.03	2.52	2.31	1.73	2.92	2.57	2.44	1.78	3.03	2.56	2.34	51.37	50.01

Table E.1 (Cont.) Experimental results

Condition No.	Residual Wall Thickness (mm)																RWT Difference (%)	Hollow Core Ratio (%)
	Sample No.1				Sample No.2				Sample No.3				Average					
	Inner	Outer	Top	Bottom	Inner	Outer	Top	Bottom	Inner	Outer	Top	Bottom	Inner	Outer	Top	Bottom		
91	2.11	3.30	3.16	2.48	2.15	3.14	3.05	2.60	2.19	3.08	2.92	2.65	2.15	3.17	3.04	2.58	37.37	44.88
92	2.16	3.13	2.69	2.42	2.18	3.06	2.75	2.42	2.18	3.08	2.72	2.53	2.17	3.09	2.72	2.46	35.12	46.93
93	2.31	3.26	3.02	2.48	2.18	3.31	2.78	2.56	2.24	3.30	2.71	2.56	2.24	3.29	2.84	2.53	38.43	45.04
94	2.08	3.49	2.68	2.63	2.00	3.16	2.67	2.53	2.10	3.03	2.60	2.60	2.06	3.23	2.65	2.59	44.21	46.59
95	1.97	3.25	2.81	2.38	1.91	3.05	2.62	2.32	1.90	3.27	2.80	2.34	1.93	3.19	2.74	2.35	49.47	47.91
96	2.07	2.97	2.84	2.48	2.17	3.01	2.73	2.43	2.10	3.07	2.61	2.60	2.11	3.02	2.73	2.50	34.87	47.26
97	2.10	3.19	2.87	2.46	2.04	3.37	2.62	2.44	1.99	3.30	2.44	2.22	2.04	3.29	2.64	2.37	48.18	47.33
98	2.01	3.09	2.65	2.45	2.08	3.06	2.80	2.24	2.06	3.25	2.76	2.34	2.05	3.13	2.74	2.34	42.20	47.67
99	2.12	2.88	2.69	2.35	2.15	2.92	2.71	2.53	2.03	2.86	2.55	2.43	2.10	2.89	2.65	2.44	31.26	48.46
100	2.01	3.06	2.73	2.37	1.85	2.97	2.62	2.43	1.97	3.03	2.70	2.37	1.94	3.02	2.68	2.39	42.93	48.62
101	1.92	3.25	2.65	2.36	1.88	3.29	2.73	2.29	1.88	3.24	2.54	2.50	1.89	3.26	2.64	2.38	53.72	48.03
102	1.87	3.28	2.73	2.46	1.88	3.45	2.77	2.46	1.85	3.21	2.74	2.52	1.87	3.31	2.75	2.48	55.58	47.07
103	1.83	3.05	2.52	2.21	1.80	2.81	2.53	2.24	1.82	2.90	2.38	2.25	1.82	2.92	2.48	2.23	46.68	51.13
104	1.92	3.02	2.64	2.34	1.88	3.06	2.65	2.32	1.89	3.00	2.63	2.27	1.90	3.03	2.64	2.31	45.78	49.30
105	1.92	3.00	2.65	2.24	1.95	3.09	2.77	2.34	2.00	2.97	2.67	2.31	1.96	3.02	2.70	2.30	42.65	48.90
106	1.75	2.54	2.32	2.17	1.73	2.54	2.37	2.12	1.81	2.56	2.42	2.15	1.76	2.55	2.37	2.15	35.51	53.84
107	1.89	3.08	2.58	2.54	1.90	3.12	2.68	2.47	2.07	3.07	2.73	2.46	1.95	3.09	2.66	2.49	44.63	47.94
108	2.05	3.31	2.87	2.51	2.12	3.45	3.00	2.63	1.93	3.41	2.74	2.60	2.03	3.39	2.87	2.58	49.95	45.16
109	1.90	3.22	2.77	2.24	1.92	3.26	2.72	2.40	1.90	3.20	2.66	2.38	1.91	3.23	2.72	2.34	51.81	47.97
110	1.94	2.96	2.58	2.47	1.92	2.93	2.56	2.45	1.93	3.00	2.61	2.46	1.93	2.96	2.58	2.46	41.59	49.04
111	1.73	2.95	2.57	2.31	1.80	2.84	2.55	2.36	1.87	2.95	2.70	2.40	1.80	2.91	2.61	2.36	46.05	50.14
112	1.89	2.87	2.69	2.25	1.92	3.13	2.75	2.31	1.84	3.04	2.54	2.28	1.88	3.01	2.66	2.28	45.92	49.46
113	1.92	2.93	2.58	2.25	1.93	2.98	2.61	2.29	1.95	2.94	2.62	2.35	1.93	2.95	2.60	2.30	41.57	49.69
114	1.83	2.97	2.58	2.18	1.88	3.00	2.59	2.35	1.83	2.95	2.60	2.34	1.85	2.97	2.59	2.29	46.47	50.04

APPENDIX F

Cross section images of molded parts

Table F.1 Section images of corner angle parts at 45 degree affected by varied melt flow index

Melt Flow Index (g/10min)	Shape corner angle 45 degree		
	Sample#1	Sample#2	Sample#3
4		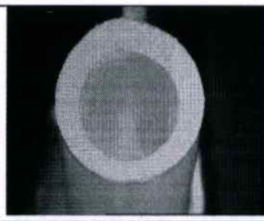	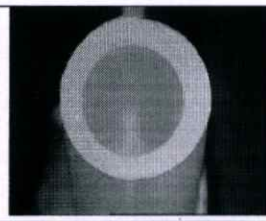
7.5			
22		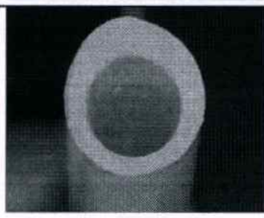	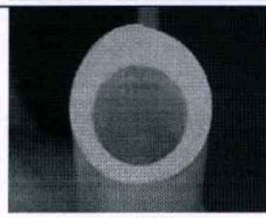

Table F.2 Section images of corner angle parts at 0 degree affected by varied melt temperature

Melt Temperature (Degree Celsius)	Shape corner angle 0 degree		
	Sample#1	Sample#2	Sample#3
190	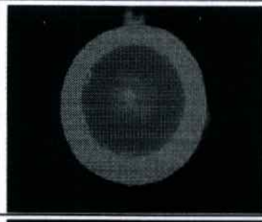	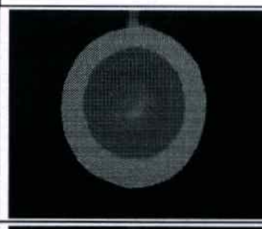	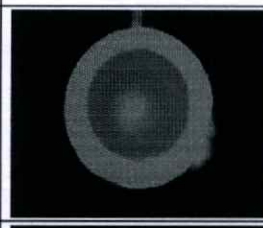
200	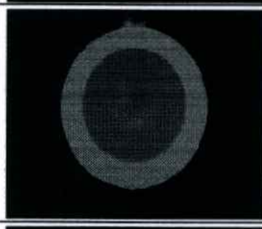	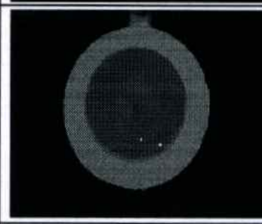	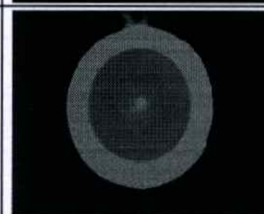
210	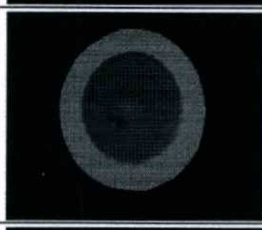	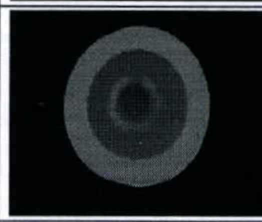	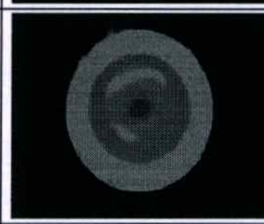
220	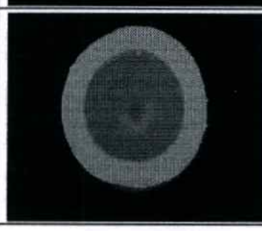	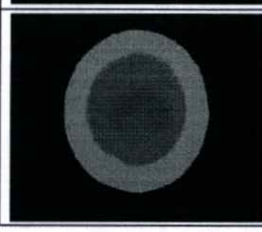	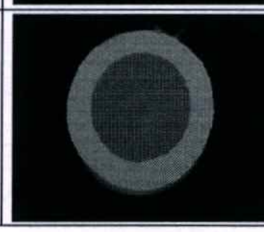

Table F.3 Section images of corner angle parts at 15 degree affected by varied melt temperature

Melt Temperature (Degree Celsius)	**Shape corner angle 15 degree**		
	Sample#1	**Sample#2**	**Sample#3**
190	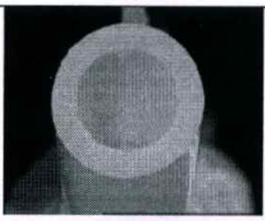	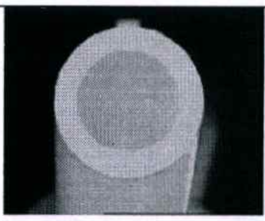	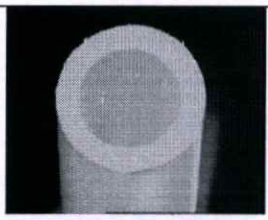
200		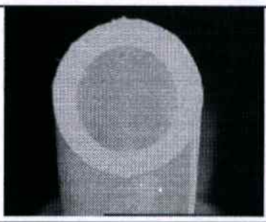	
210			
220			

Table F.4 Section images of corner angle parts at 30 degree affected by varied melt temperature

Melt Temperature (Degree Celsius)	Shape corner angle 30 degree		
	Sample#1	Sample#2	Sample#3
190			
200	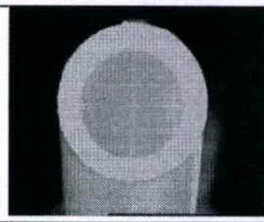	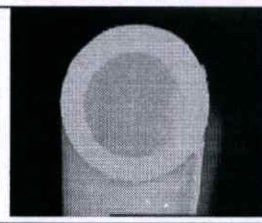	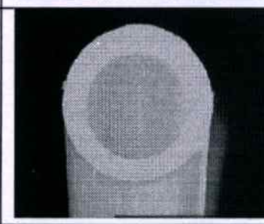
210		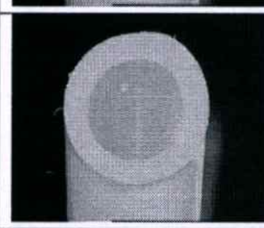	
220	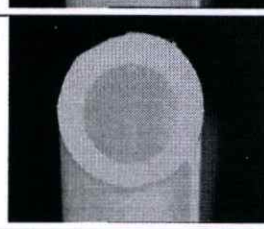	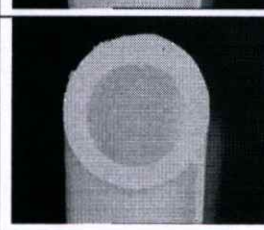	

Table F.5 Section images of corner angle parts at 45 degree affected by varied melt temperature

Melt Temperature (Degree Celsius)	**Shape corner angle 45 degree**		
	Sample#1	**Sample#2**	**Sample#3**
190		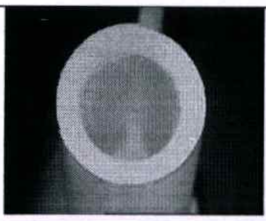	
200			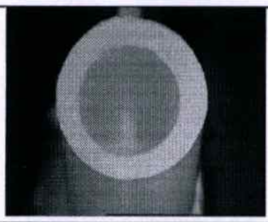
210			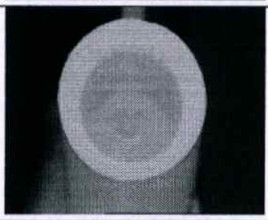
220		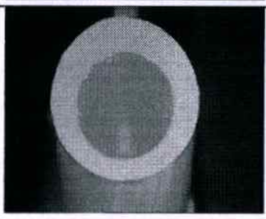	

Table F.6 Section images of corner angle parts at 60 degree affected by varied melt temperature

Melt Temperature (Degree Celsius)	**Shape corner angle 60 degree**		
	Sample#1	**Sample#2**	**Sample#3**
190		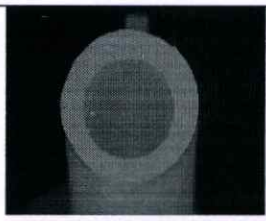	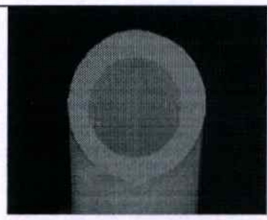
200		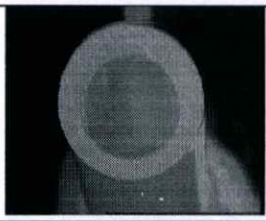	
210			
220	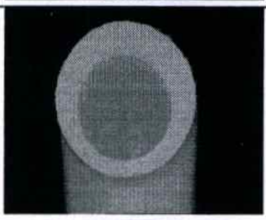		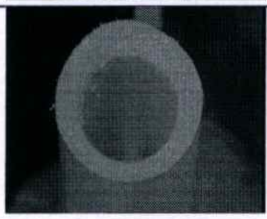

Table F.7 Section images of corner angle parts at 75 degree affected by varied melt temperature

Melt Temperature (Degree Celsius)	**Shape corner angle 75 degree**		
	Sample#1	**Sample#2**	**Sample#3**
190	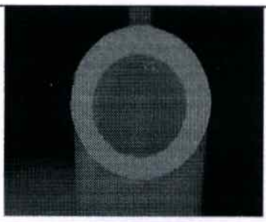	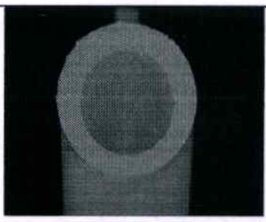	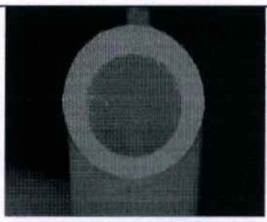
200			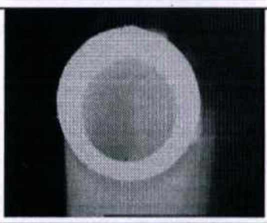
210			
220	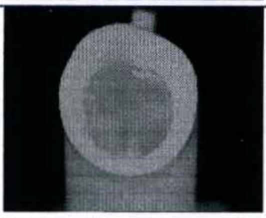		

Table F.8 Section images of corner angle parts at 90 degree affected by varied melt temperature

Melt Temperature (Degree Celsius)	Shape corner angle 90 degree		
	Sample#1	Sample#2	Sample#3
190	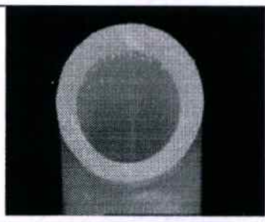		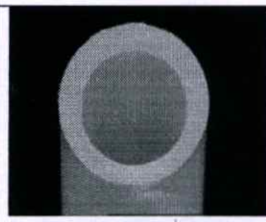
200	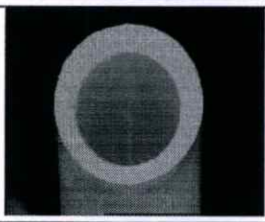	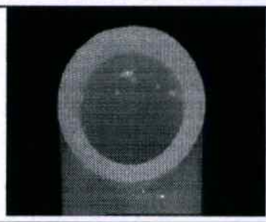	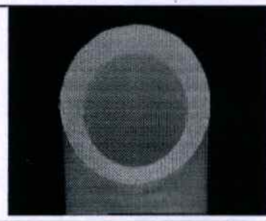
210	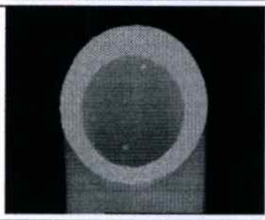		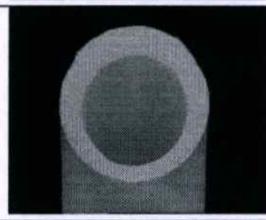
220	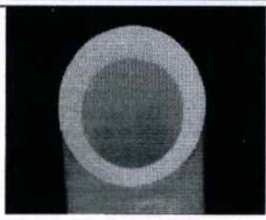		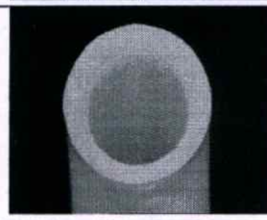

Table F.9 Section images of corner angle parts at 0 degree affected by varied mold temperature

Mold Temperature (Degree Celsius)	Shape corner angle 0 degree		
	Sample#1	Sample#2	Sample#3
40		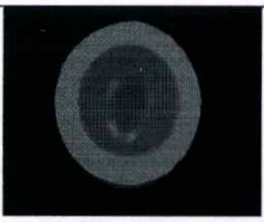	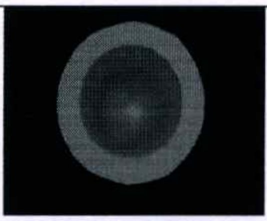
50	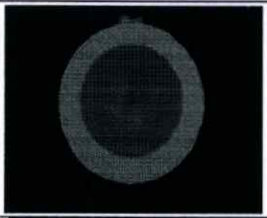	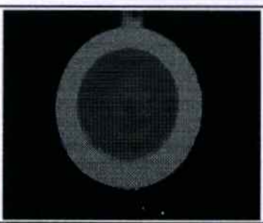	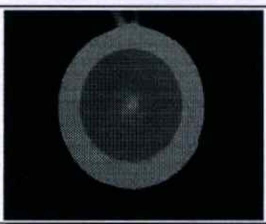
60	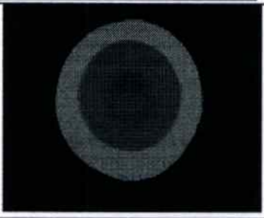	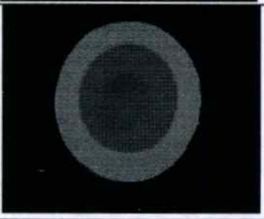	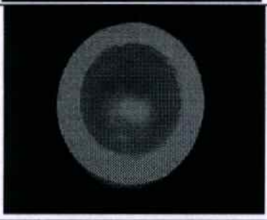
70	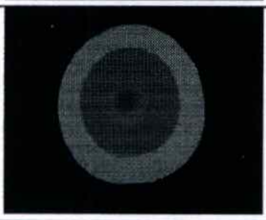	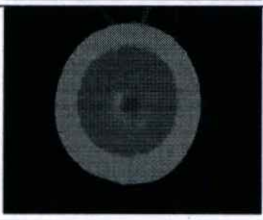	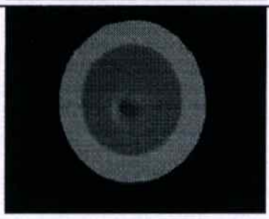

Table F.10 Section images of corner angle parts at 15 degree affected by varied mold temperature

Mold Temperature (Degree Celsius)	Shape corner angle 15 degree		
	Sample#1	**Sample#2**	**Sample#3**
40	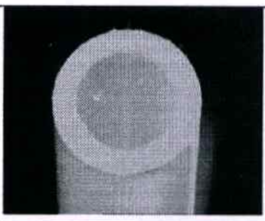	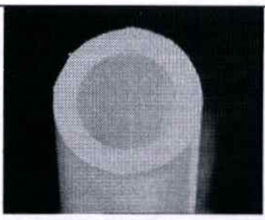	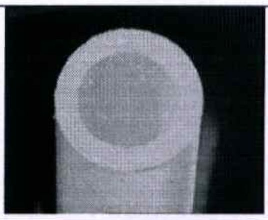
50	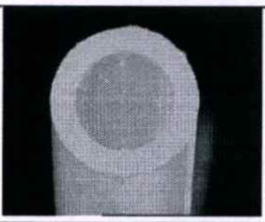	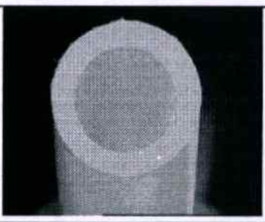	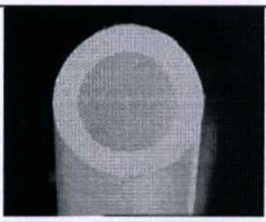
60	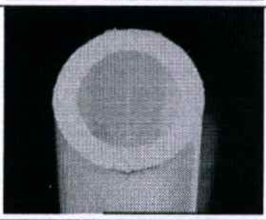	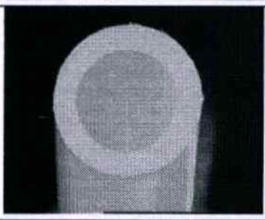	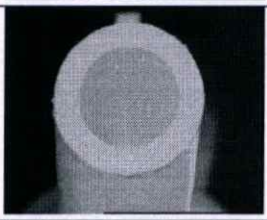
70			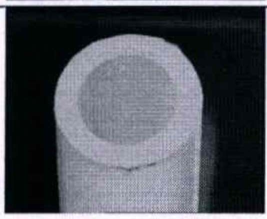

Table F.11 Section images of corner angle parts at 30 degree affected by varied mold temperature

Mold Temperature (Degree Celsius)	**Shape corner angle 30 degree**		
	Sample#1	**Sample#2**	**Sample#3**
40	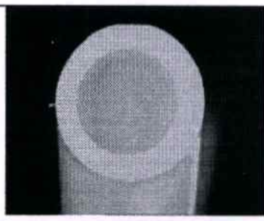		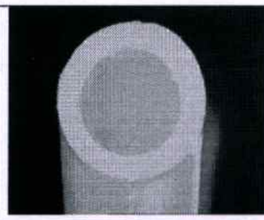
50	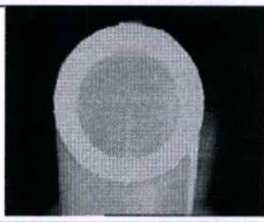		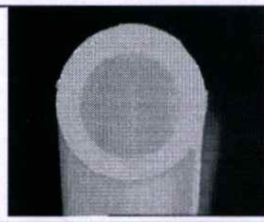
60	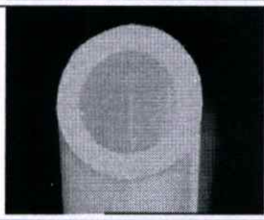	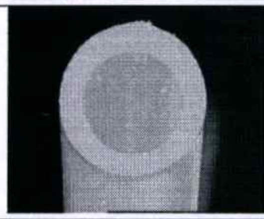	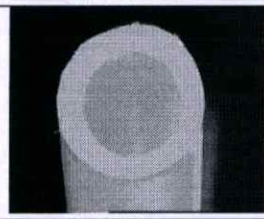
70		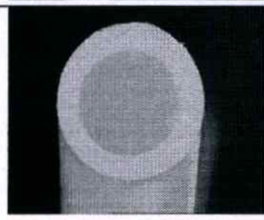	

Table F.12 Section images of corner angle parts at 45 degree affected by varied mold temperature

Mold Temperature (Degree Celsius)	Shape corner angle 45 degree		
	Sample#1	**Sample#2**	**Sample#3**
40	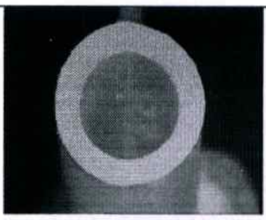	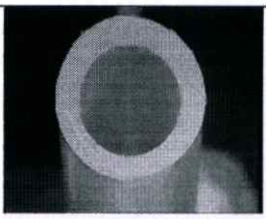	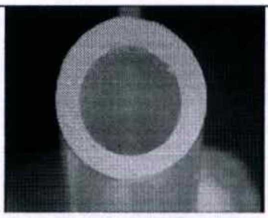
50	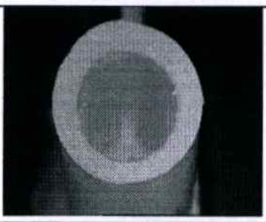		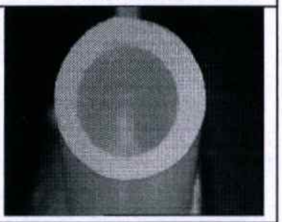
60	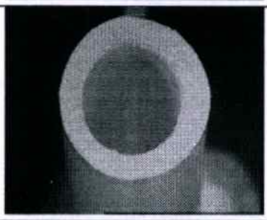		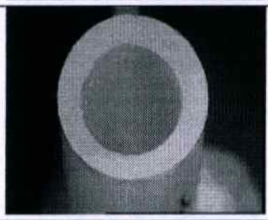
70		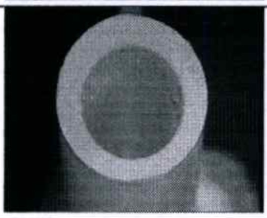	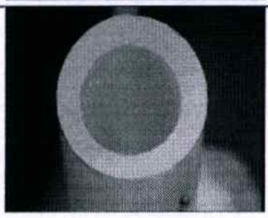

Table F.13 Section images of corner angle parts at 60 degree affected by varied mold temperature

Mold Temperature (Degree Celsius)	Shape corner angle 60 degree		
	Sample#1	Sample#2	Sample#3
40			
50			
60	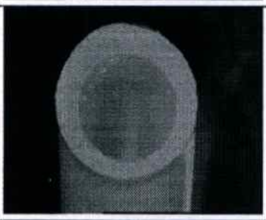		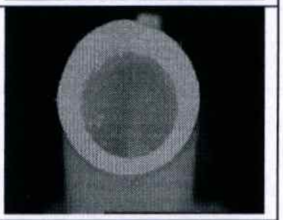
70	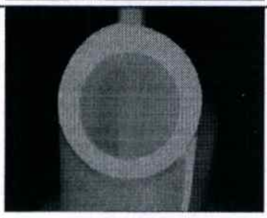	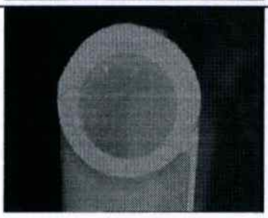	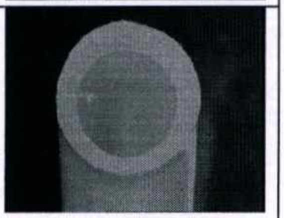

Table F.14 Section images of corner angle parts at 75 degree affected by varied mold temperature

Mold Temperature (Degree Celsius)	**Shape corner angle 75 degree**		
	Sample#1	**Sample#2**	**Sample#3**
40	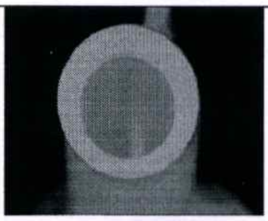	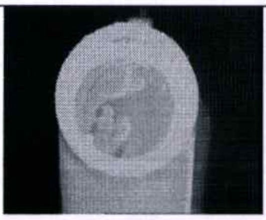	
50			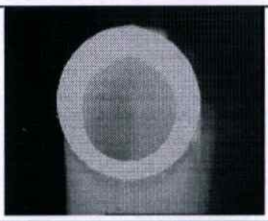
60	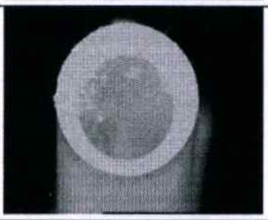		
70			

Table F.15 Section images of corner angle parts at 90 degree affected by varied mold temperature

Mold Temperature (Degree Celsius)	Shape corner angle 90 degree		
	Sample#1	**Sample#2**	**Sample#3**
40	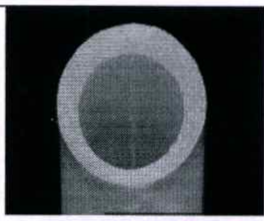	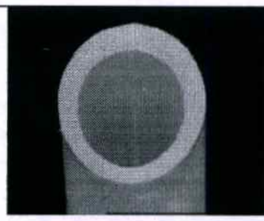	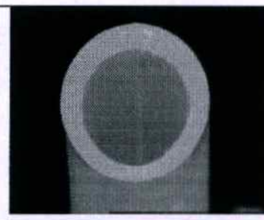
50	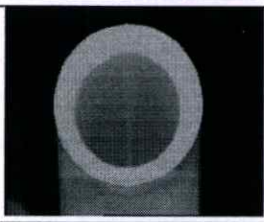	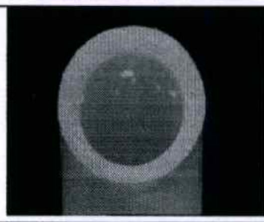	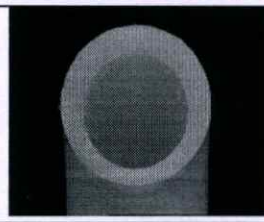
60	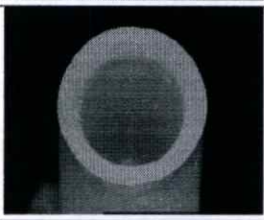	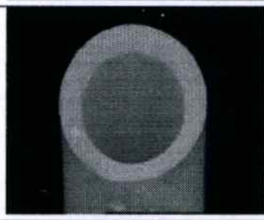	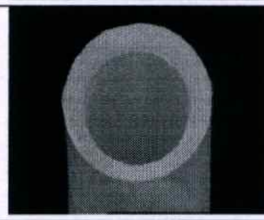
70	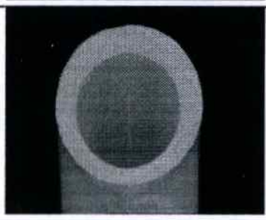		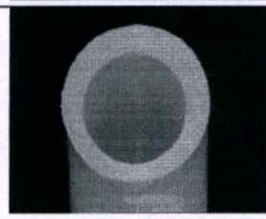

Table F.16 Section images of corner angle parts at 0 degree affected by varied water delay time

Water delay time (sec.)	Shape corner angle 0 degree		
	Sample#1	Sample#2	Sample#3
1	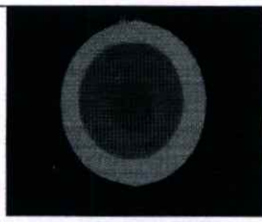	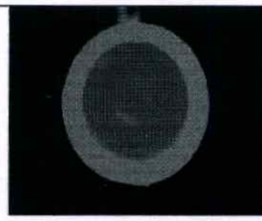	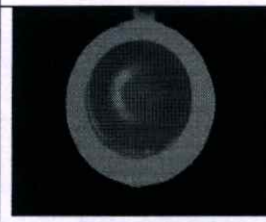
3		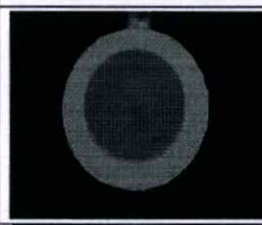	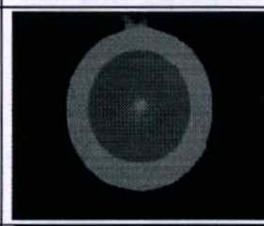
5	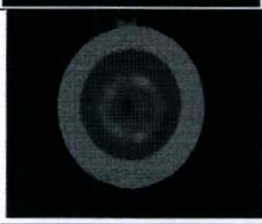	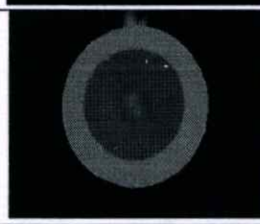	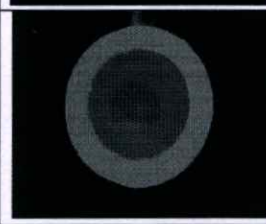
7	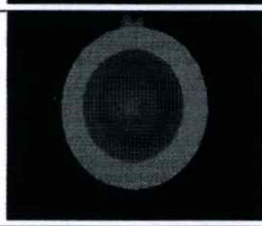	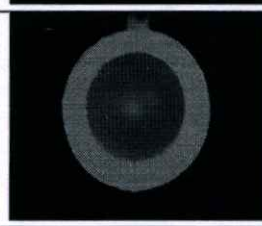	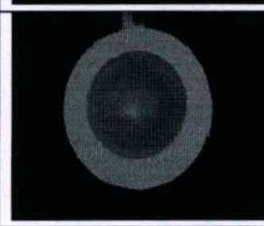

Table F.17 Section images of corner angle parts at 15 degree affected by varied water delay time

Water delay time (sec.)	**Shape corner angle 15 degree**		
	Sample#1	**Sample#2**	**Sample#3**
1	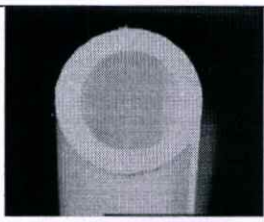	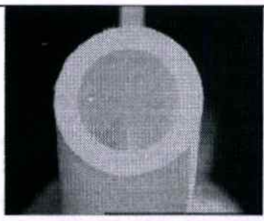	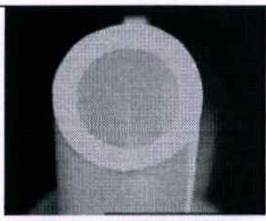
3		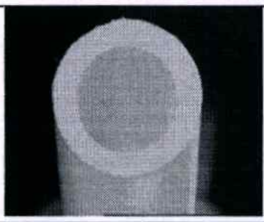	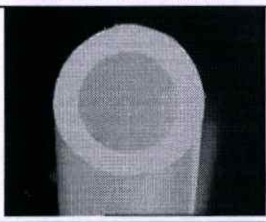
5		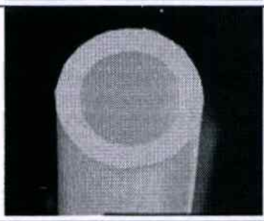	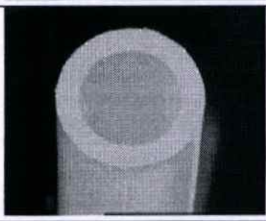
7		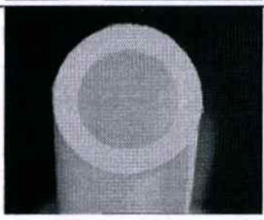	

Table F.18 Section images of corner angle parts at 30 degree affected by varied water delay time

Water delay time (sec.)	Shape corner angle 30 degree		
	Sample#1	Sample#2	Sample#3
1	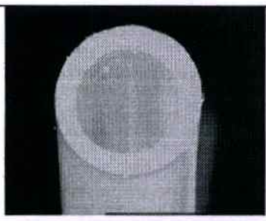		
3	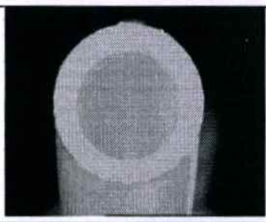		
5	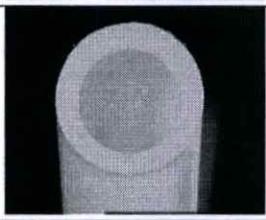	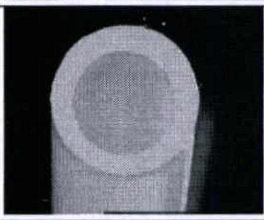	
7			

Table F.19 Section images of corner angle parts at 45 degree affected by varied water delay time

Water delay time (sec.)	**Shape corner angle 45 degree**		
	Sample#1	**Sample#2**	**Sample#3**
1	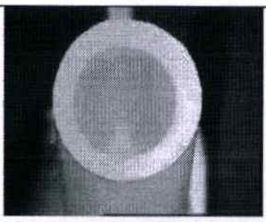	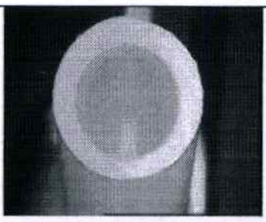	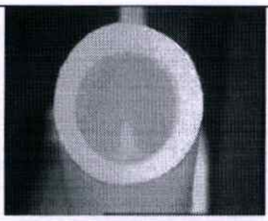
3		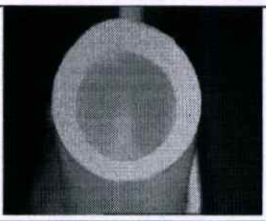	
5			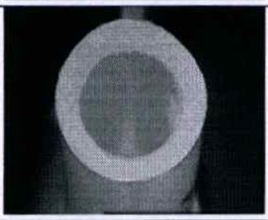
7	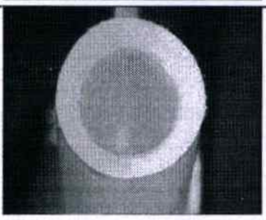	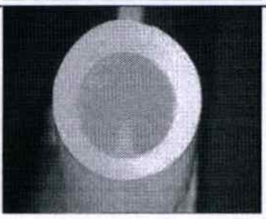	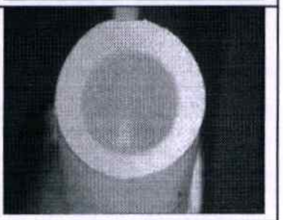

Table F.20 Section images of corner angle parts at 60 degree affected by varied water delay time

Water delay time (sec.)	**Shape corner angle 60 degree**		
	Sample#1	**Sample#2**	**Sample#3**
1	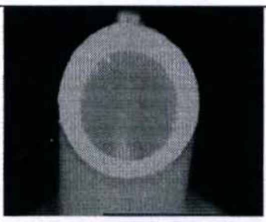		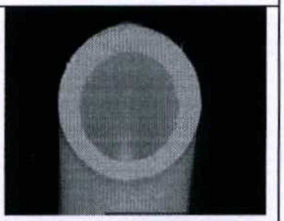
3			
5	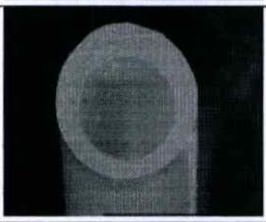		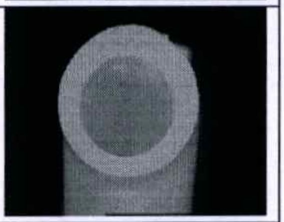
7		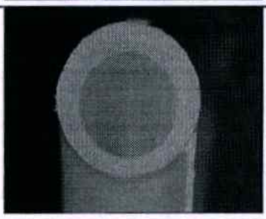	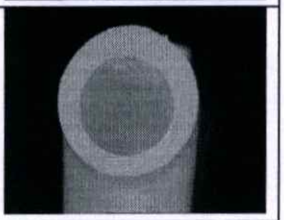

Table F.21 Section images of corner angle parts at 75 degree affected by varied water delay time

Water delay time (sec.)	Shape corner angle 75 degree		
	Sample#1	**Sample#2**	**Sample#3**
1		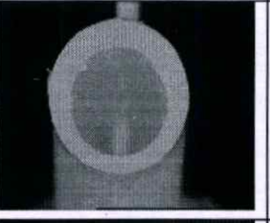	
3	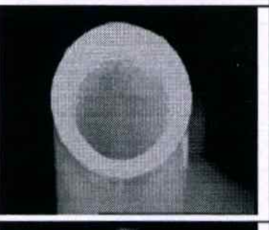		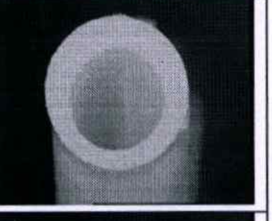
5	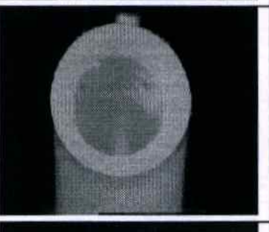		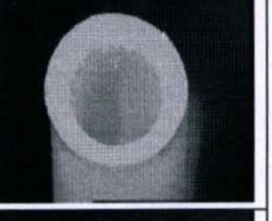
7		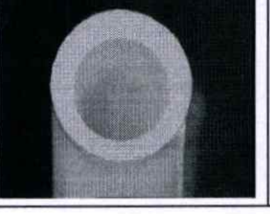	

Table F.22 Section images of corner angle parts at 90 degree affected by varied water delay time

Water delay time (sec.)	**Shape corner angle 90 degree**		
	Sample#1	**Sample#2**	**Sample#3**
1	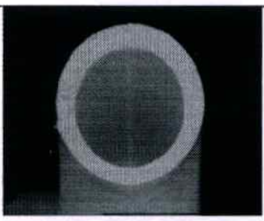	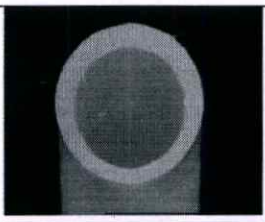	
3	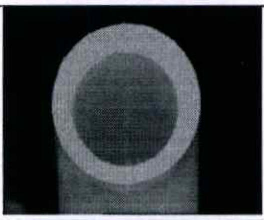	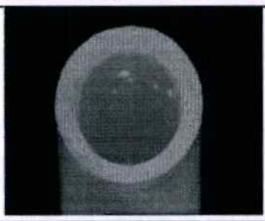	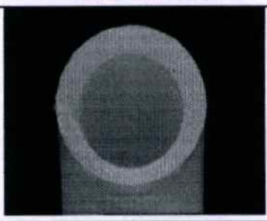
5		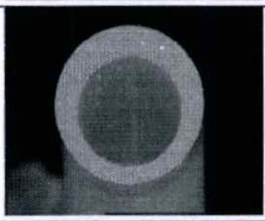	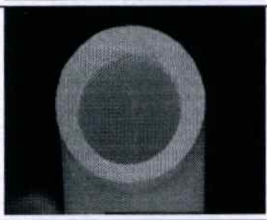
7		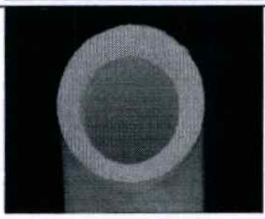	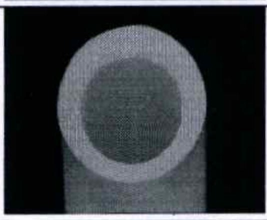

Table F.23 Section images of corner angle parts at 0 degree affected by varied water pressure

Water pressure (bar)	Shape corner angle 0 degree		
	Sample#1	Sample#2	Sample#3
120	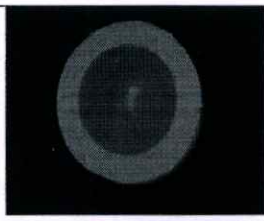	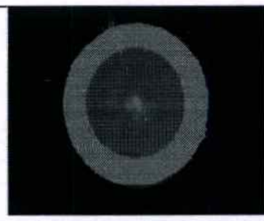	
150	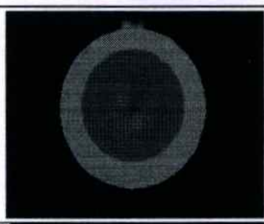	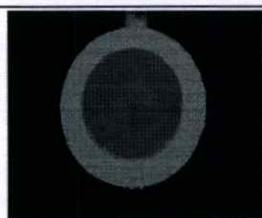	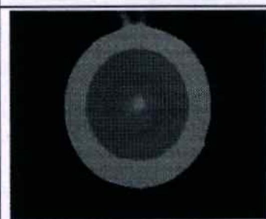
180		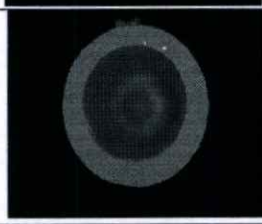	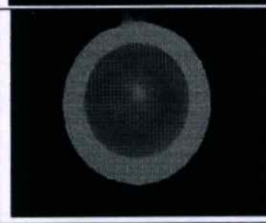
210	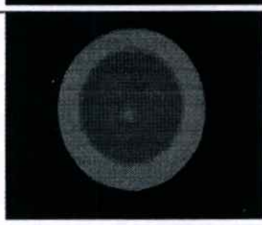	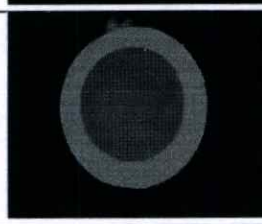	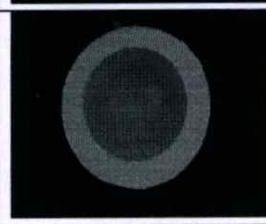

Table F.24 Section images of corner angle parts at 15 degree affected by varied water pressure

Water pressure (bar)	**Shape corner angle 15 degree**		
	Sample#1	**Sample#2**	**Sample#3**
120	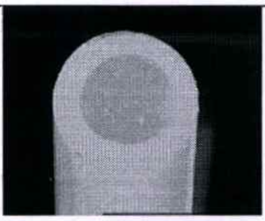	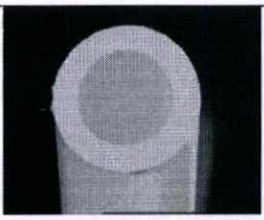	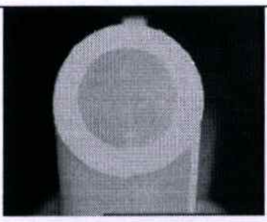
150	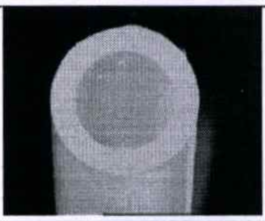	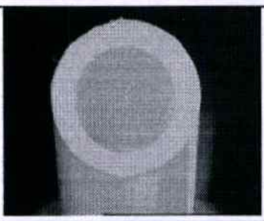	
180	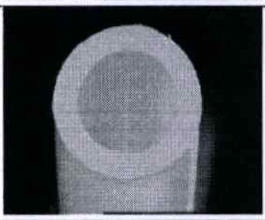		
210	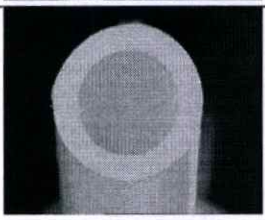	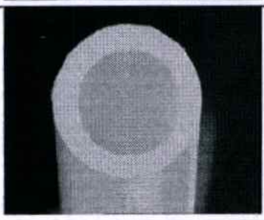	

Table F.25 Section images of corner angle parts at 30 degree affected by varied water pressure

Water pressure (bar)	**Shape corner angle 30 degree**		
	Sample#1	**Sample#2**	**Sample#3**
120	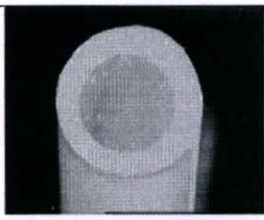	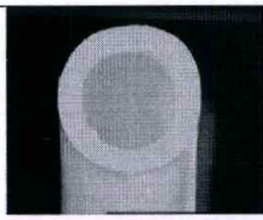	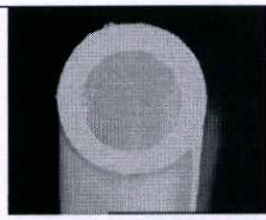
150	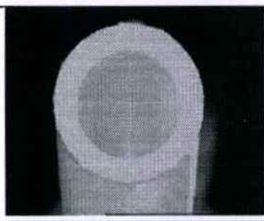	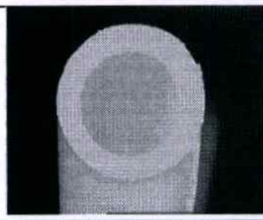	
180			
210			

Table F.26 Section images of corner angle parts at 45 degree affected by varied water pressure

Water pressure (bar)	**Shape corner angle 45 degree**		
	Sample#1	**Sample#2**	**Sample#3**
120			
150	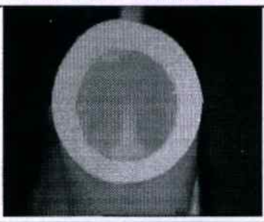	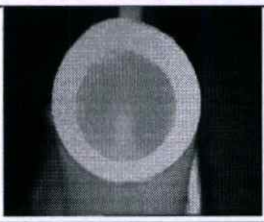	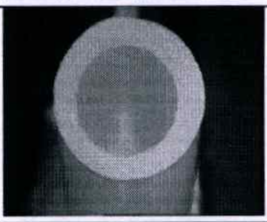
180			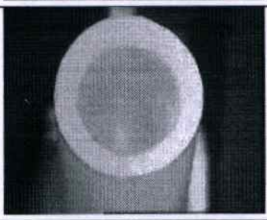
210			

Table F.27 Section images of corner angle parts at 60 degree affected by varied water pressure

Water pressure (bar)	**Shape corner angle 60 degree**		
	Sample#1	**Sample#2**	**Sample#3**
120	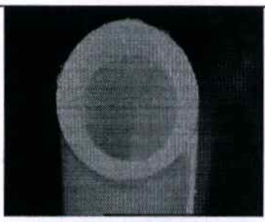	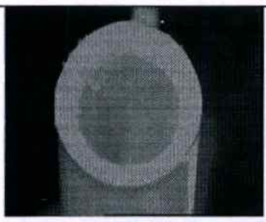	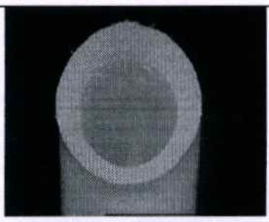
150		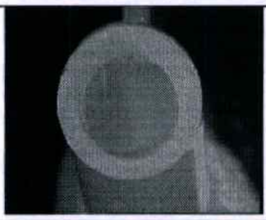	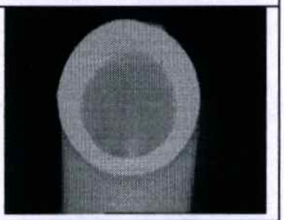
180	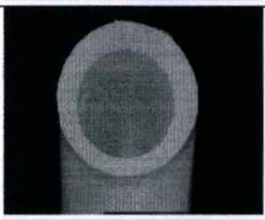		
210			

Table F.28 Section images of corner angle parts at 75 degree affected by varied water pressure

Water pressure (bar)	Shape corner angle 75 degree		
	Sample#1	Sample#2	Sample#3
120	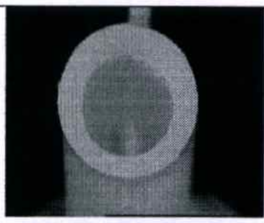	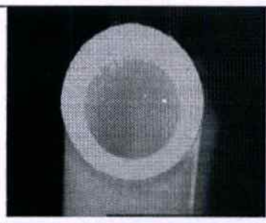	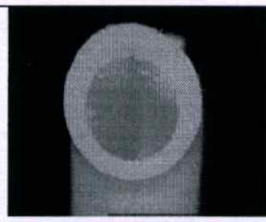
150			
180		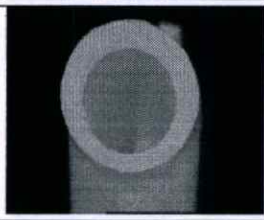	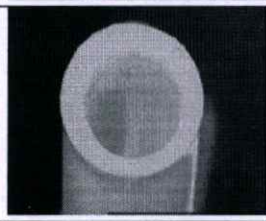
210	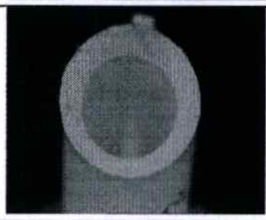	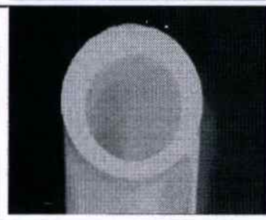	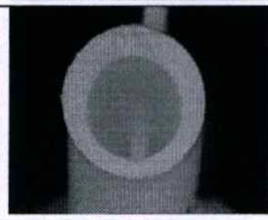

Table F.29 Section images of corner angle parts at 90 degree affected by varied water pressure

Water pressure (bar)	**Shape corner angle 90 degree**		
	Sample#1	**Sample#2**	**Sample#3**
120	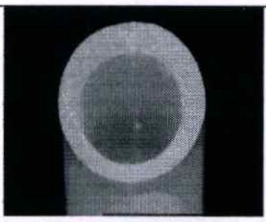	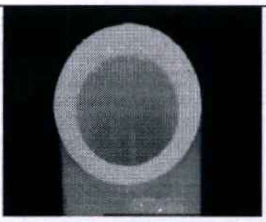	
150	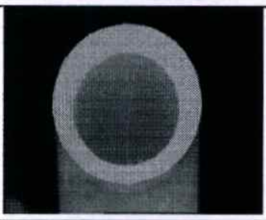	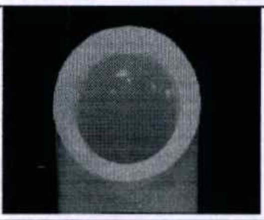	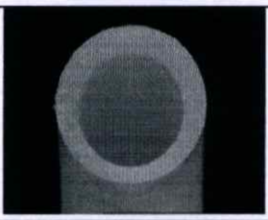
180	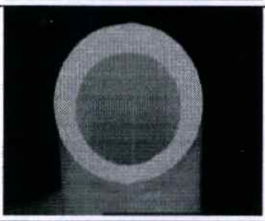		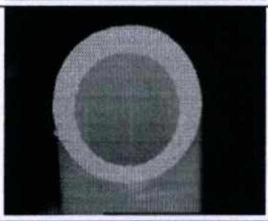
210		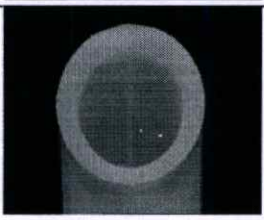	

Table F.30 Section images of corner angle parts at 0 degree affected by varied water holding time

Water holding time (sec)	Shape corner angle 0 degree		
	Sample#1	Sample#2	Sample#3
10	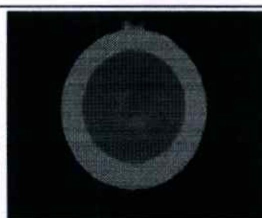	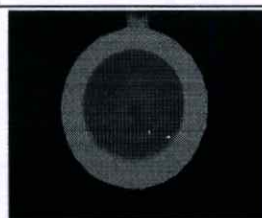	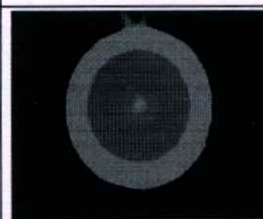
15	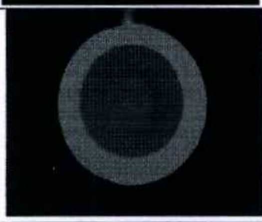	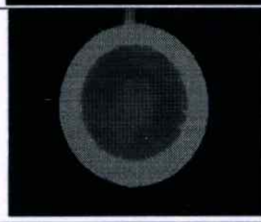	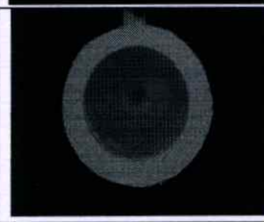
20	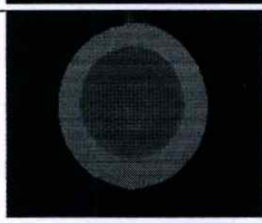	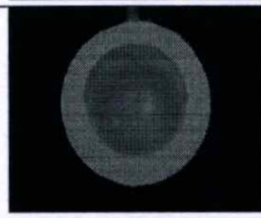	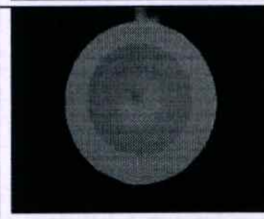
25	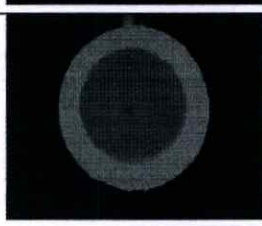	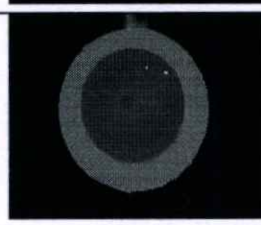	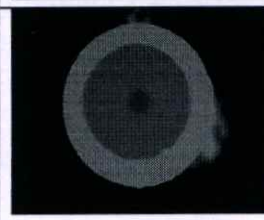

Table F.32 Section images of corner angle parts at 30 degree affected by varied water holding time

Water holding time (sec)	Shape corner angle 30 degree		
	Sample#1	**Sample#2**	**Sample#3**
10	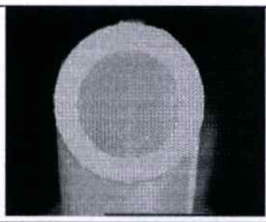		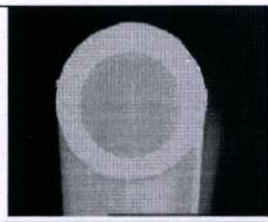
15			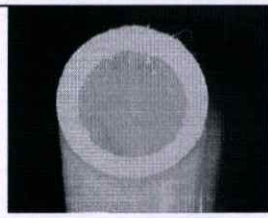
20	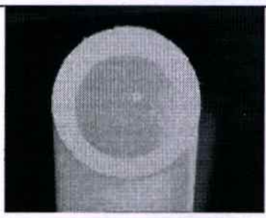	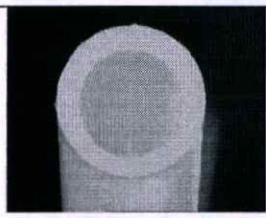	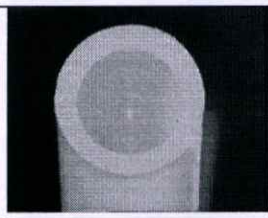
25	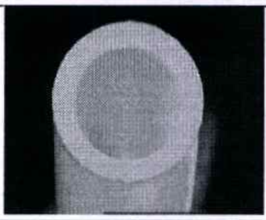		

Table F.31 Section images of corner angle parts at 15 degree affected by varied water holding time

Water holding time (sec)	Shape corner angle 15 degree		
	Sample#1	Sample#2	Sample#3
10		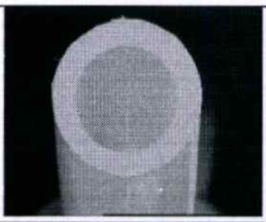	
15			
20	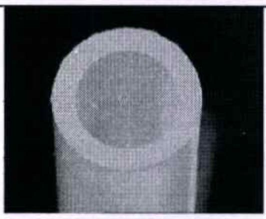	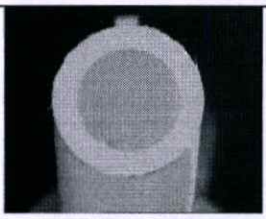	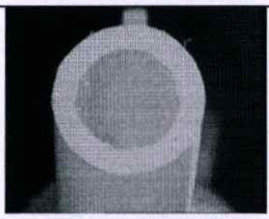
25	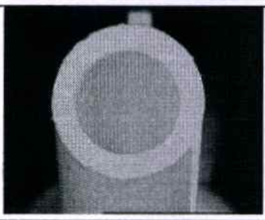	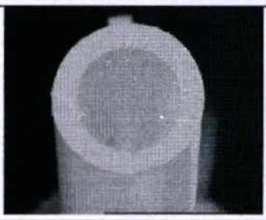	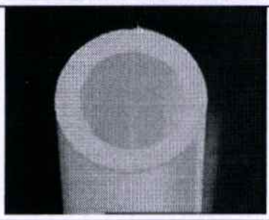

Table F.33 Section images of corner angle parts at 45 degree affected by varied water holding time

Water holding time (sec)	Shape corner angle 45 degree		
	Sample#1	**Sample#2**	**Sample#3**
10		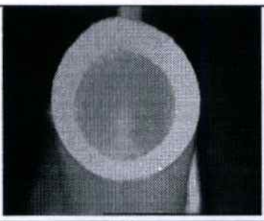	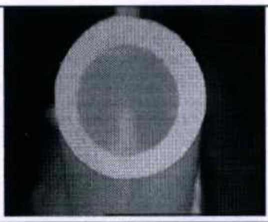
15	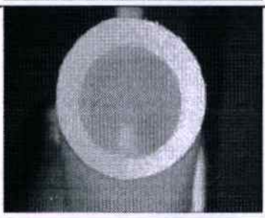	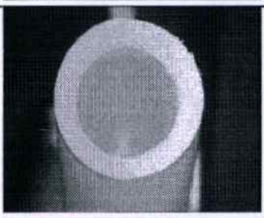	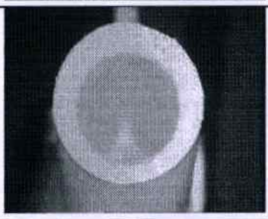
20	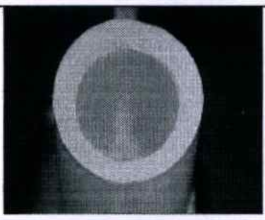		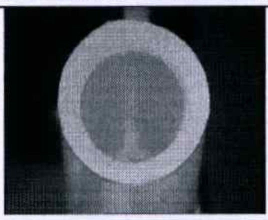
25			

Table F.34 Section images of corner angle parts at 60 degree affected by varied water holding time

Water holding time (sec)	**Shape corner angle 60 degree**		
	Sample#1	**Sample#2**	**Sample#3**
10	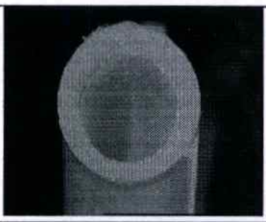		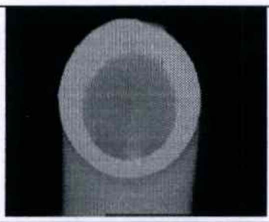
15	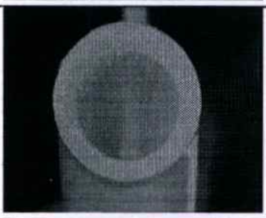		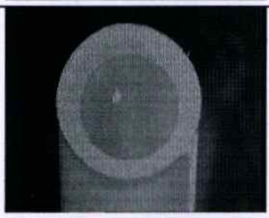
20		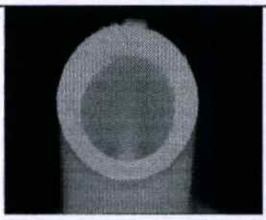	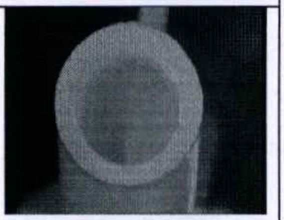
25		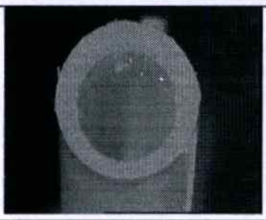	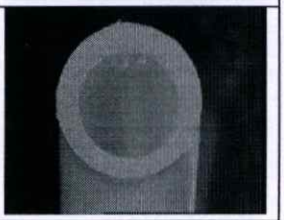

Table F.35 Section images of corner angle parts at 75 degree affected by varied water holding time

Water holding time (sec)	**Shape corner angle 75 degree**		
	Sample#1	**Sample#2**	**Sample#3**
10		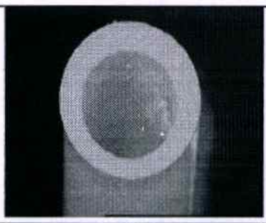	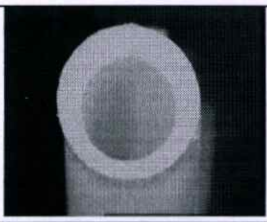
15			
20	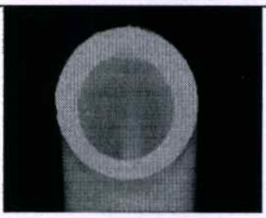	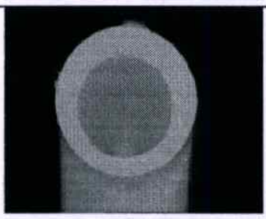	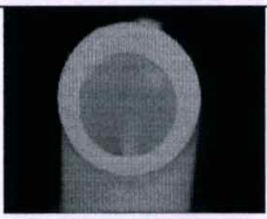
25	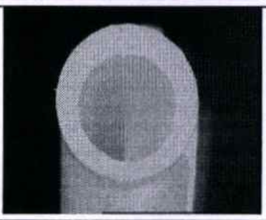	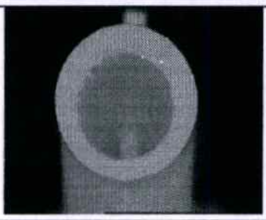	

Table F.36 Section images of corner angle parts at 90 degree affected by varied water holding time

Water holding time (sec)	Shape corner angle 90 degree		
	Sample#1	Sample#2	Sample#3
10	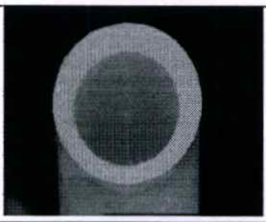	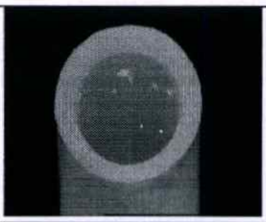	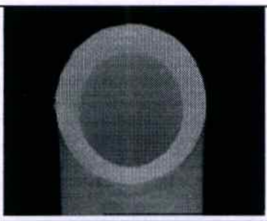
15	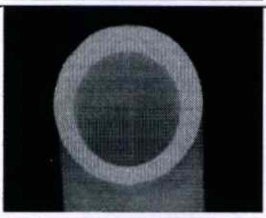		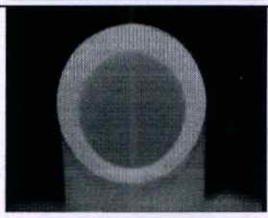
20	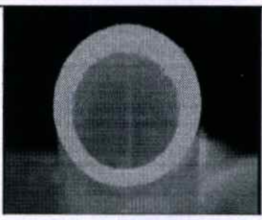	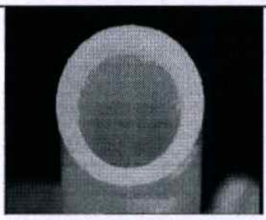	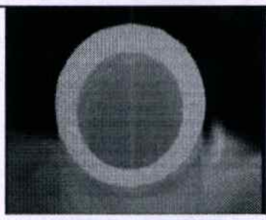
25		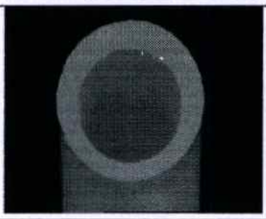	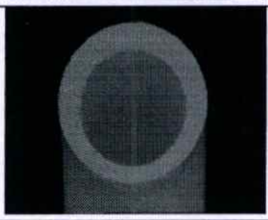

APPENDIX G

Shear rate simulation result

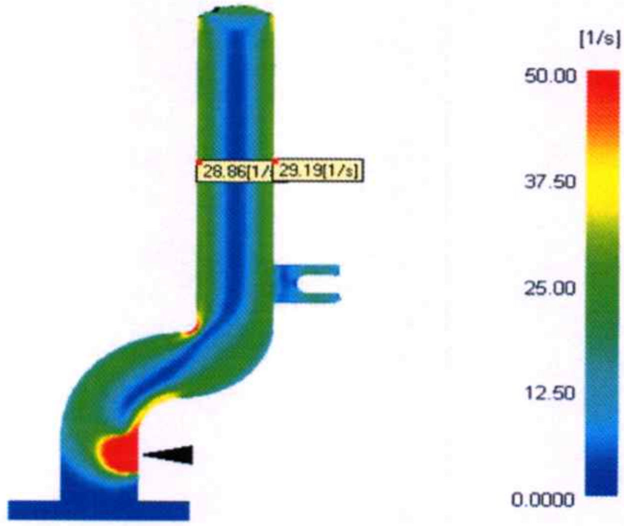

Figure G.1 Shear rate simulation result of corner angle at 0 degree

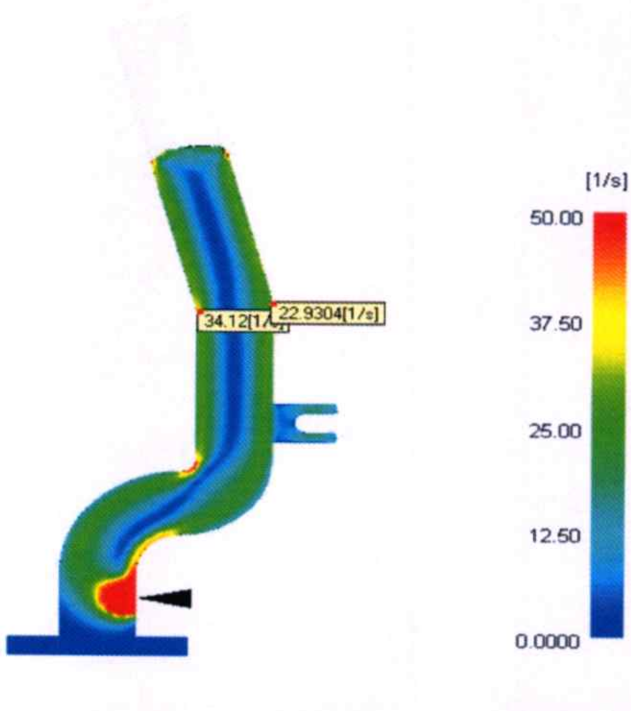

Figure G.2 Shear rate simulation result of corner angle at 15 degree

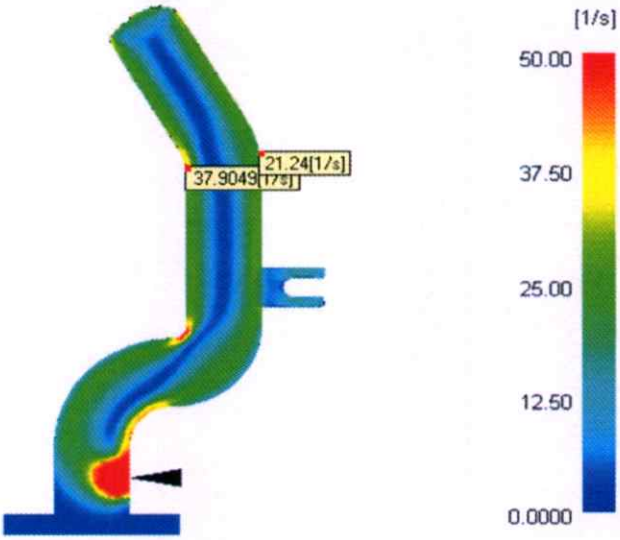

Figure G.3 Shear rate simulation result of corner angle at 30 degree

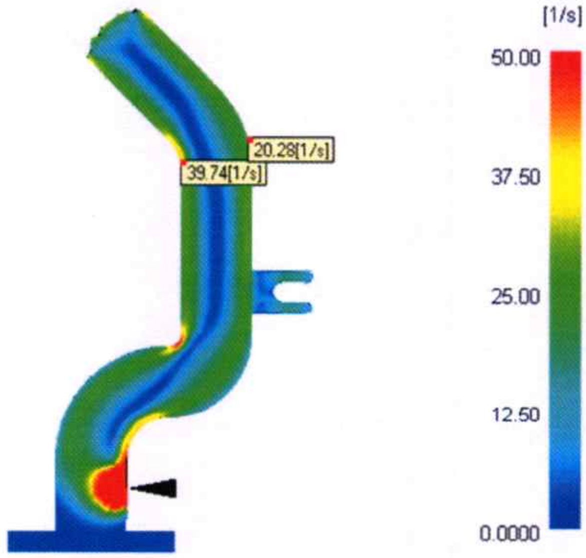

Figure G.4 Shear rate simulation result of corner angle at 15 degree

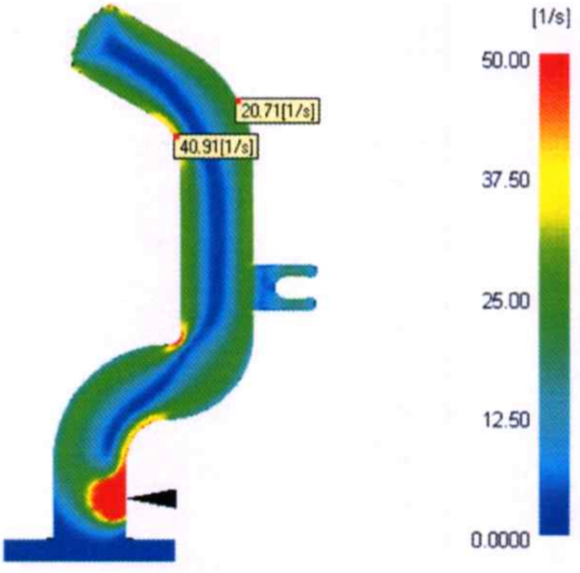

Figure G.5 Shear rate simulation result of corner angle at 0 degree

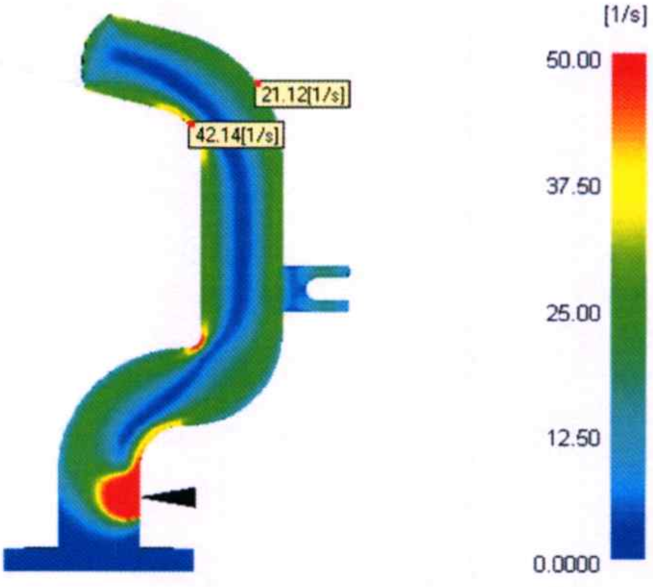

Figure G.6 Shear rate simulation result of corner angle at 15 degree

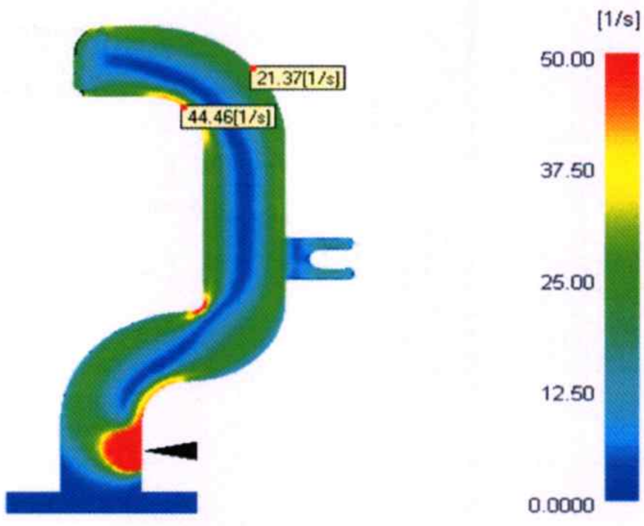

Figure G.7 Shear rate simulation result of corner angle at 90 degree

BIOGRAPHY

Name:	Mr.Tiwagorn Pudpong
Date of Birth:	September 24, 1977
Place of Birth:	Chachoengsao, Thailand
Education:	
1998-2000	B.Technical Education in Department of Electrical Power., Pathumwan Institute of Technology.
Scholarships:	
2007-2009	Full scholarship for study in the master degree from National Science and Technology Development Agency (NSTDA)
Work experience:	
2005-2011	CH.Radiators Co., Ltd
2003-2004	Sony Device Technology (Thailand)
2001-2003	Sony Magnetic Products (Thailand)